PLA AND CELLULOSE BASED DEGRADABLE POLYMER COMPOSITES

A Dissertation
Presented to
The Academic Faculty

by

Mihir Anil Oka

In Partial Fulfillment
of the Requirements for the Degree
Doctor of Philosophy in the
School of Polymer, Textile and Fiber Engineering

Georgia Institute of Technology
May, 2010

PLA AND CELLULOSE BASED DEGRADABLE POLYMER COMPOSITES

Approved by:

Dr. Yonathan Thio, Advisor
School of Polymer, Textile and Fiber Engineering
Georgia Institute of Technology

Dr. Yulin Deng
School of Chemical and Biomolecular Engineering
Georgia Institute of Technology

Dr. Anselm Griffin
School of Polymer, Textile and Fiber Engineering
Georgia Institute of Technology

Dr. Kenneth Gall
School of Materials Science and Engineering
Georgia Institute of Technology

Dr. Meisha Shofner
School of Polymer, Textile and Fiber Engineering
Georgia Institute of Technology

Date Approved: March 16, 2010

I dedicate this thesis to my parents Mrs. Vidya Anil Oka and Mr. Anil Gopal Oka and to my teachers whose tireless efforts helped me get here.

ACKNOWLEDGEMENTS

First and foremost, I would like to express my gratitude and thank my advisor, Dr. Yonathan Thio, whose constant encouragement, support and patience helped me during the course of this work. He gave me the freedom to define the project and always encouraged creative thinking. His questions and comments brought out the best in me and made me a better researcher.

I would like to thank my committee members including Dr. Anselm Griffin, Dr. Meisha Shofner, Dr. Yulin Deng and Dr. Ken Gall for their helpful suggestions and time. I especially thank Dr. Haskell Beckham and his research group for allowing me to use his laboratory equipments. Thanks to Dr. Dongang Yao and his research group for letting me use their carver press for compression molding.

I am thankful to my friends/colleagues at Georgia Tech Sungwon Ma, Jasmeet Kaur, Sarang Deodhar, Dr. Shamal Mhetre, Ashish Pande, Rama K.R.T, Ryan Kincer, Dr. Sudhakar Jagannathan, Dr. Asif Rasheed, Dr. Marcus Foston, Eric Crawford Sr., Sandeep Prabhakara, Shubham Saxena, Nitin Changlani for their helpful suggestions and for their constructive criticism.

My friends from Clemson University also deserve to be thanked, Dr. Santosh Rahane, Dr. Amol Janorkar, Dr. Sourabh Pansare, Sameer Vaidya, Amit Sidhaye, Dr. Shamik Sharma for their help, understanding and encouragement.

Last but not the least; I would like to thank the staff in the School of Polymer, Textile & Fiber Engineering Angie Abbott, Hope Payne, Linda Roberson, Mike Boyett for their willingness to help which made PhD life that much simpler and I

am grateful to the School of Polymer, Textile & Fiber Engineering for providing funding for this research.

TABLE OF CONTENTS

LIST OF TABLES

LIST OF FIGURES

SUMMARY

At present there is significant interest for the development of environmentally friendly polymers and polymer based composites from renewable resources. Concerns about greenhouse gas emissions produced by using fossil fuel combined with low degradability of polymers derived from fossil fuel has led to increase in research to develop degradable polymers and composites. Polylactic acid, PLA, and cellulose are two such examples of degradable polymers that come from renewable resources.

In this study, we have investigated the process-structure-property relationship in PLA-cellulose composites. The effects of particle size, filler-matrix compatibility and the processing technique used on the composites mechanical, thermal properties and degradation behavior were studied. Cellulose in the form of microcrystalline cellulose particles and cellulose whiskers derived by hydrolyzing microcrystalline cellulose particles was used for reinforcing PLA.

A brief background on PLA and cellulose including synthesis techniques and applications is given in chapter 2. This chapter also summarizes the different surface modification techniques employed and the theories associated with surface modification. Relevant micromechanical theory as developed for fiber reinforced composite is also reviewed.

Chapter 3 provides detailed procedures used for hydrolyzing microcrystalline cellulose, surface modification of cellulose particles and degradation of neat PLA and PLA-cellulose composites. Description of instruments used for

characterizing samples in terms of model, method and experimental conditions employed are also given.

In chapter 4 we investigated both the influence of unmodified microcrystalline cellulose particles as reinforcement in PLA and the influence of processing technique on the composite properties. The use of unmodified particles resulted in increased Young's modulus and storage modulus but decrease in toughness of PLA-cellulose composite. Processing PLA by melt mixing resulted in some thermal degradation and reduced the polymer chain length. The decreased chain length increased crystallization rate and resulted in the melt processed samples having higher crystallinity compared to solution processed samples. The higher crystallinity translated into melt processed samples having higher stiffness.

In chapters 5 and 6, the effect of surface modification of microcrystalline cellulose particles, both un-hydrolyzed and hydrolyzed, on composites mechanical and thermal properties was studied. Surface modification by grafting small length lactic acid chains or larger length polylactic acid chains resulted in increased filler-matrix compatibility. The improved compatibility resulted in relative increase in static and dynamic mechanical properties of the composite at lower cellulose content. The cellulose particles also acted as nucleating agents and increased the crystallization rate of the PLA matrix chains. The particles size and surface chemical composition were found to influence its nucleation efficiency.

In chapter 7, the degradation of neat PLA and PLA-cellulose composites are studied. Under the degradation conditions employed and the sample size studied,

the degradation was found to occur via surface erosion mechanism. The rate of degradation was found to depend on the initial sample crystallinity, concentration of the alkaline medium employed. The addition of cellulose particles increased the degradation rate of PLA. For all samples the degradation occurred preferentially in the amorphous regions as indicated by the increase in crystalline fraction of degraded samples.

This work provides detailed structure-property analysis of PLA-cellulose composite system. Broad variations in the properties were achieved through appropriate choice of processing technique and by manipulating the PLA-cellulose interfacial interactions. A simple and effective method to modify surface of cellulose particles by grafting lactic acid or polylactic acid chains that required no catalyst was successfully demonstrated. Reinforcing PLA with modified cellulose particles improved the overall mechanical properties and increased the degradability of PLA matrix under alkaline conditions.

CHAPTER 1

INTRODUCTION

1.1 Objectives

Developing environmentally friendly polymer composites that are reliable and economical offering all the advantages of petroleum-based plastics was the driving force behind this work. The objective of this work was to prepare degradable composites based on polylactic acid, PLA and cellulose. Both PLA and cellulose are available from renewable resources and the properties of PLA are comparable to properties of polystyrene and polypropylene. Another advantage of PLA from point of commercialization is its processing similarity to polyolefins. This particular property allows the use of existing technology to process PLA. This has made PLA a potential replacement material in applications utilizing polystyrene and polypropylene for example. At present PLA is used in variety of applications including those in biomedical, automotive and packaging fields. The main factors that have prevented PLA from realizing its full potential is its low toughness and low thermal stability.

The system we have considered here is PLA-Cellulose composite system wherein cellulose particles are used as reinforcement for improving mechanical and thermal properties of PLA. We had four different objectives that required synthesizing four different types of composites, described below, for understanding the reinforcement mechanism in PLA-cellulose composites and factors influencing composite properties.

1.1.1 Objective I

To understand the influence of processing technique employed on properties of neat PLA and PLA cellulose composites and the effect of cellulose particle addition on composite properties. For this a composite system of type (i) PLA + unmodified microcrystalline cellulose particles - was synthesized using melt and solution processing techniques and containing up to 20 % by weight of cellulose.

1.1.2 Objective II

To investigate the influence of interfacial interactions via filler surface modification. The cellulose particle surface was modified by grafting lactic acid (grafting from) and polylactic acid chains (grafting to). PLA was reinforced with lactic acid grafted and polylactic acid grafted cellulose particles separately. This gave samples of type (ii), which are PLA + lactic acid-g-microcrystalline cellulose and PLA + polylactic acid–g-microcrystalline cellulose particles. Samples were synthesized via solution processing.

1.1.3 Objective III

To study the influence of filler size and filler surface area on composite properties. The size of cellulose particles was altered via acid hydrolysis which changed the surface area and the particles morphology. The composite of type (iii) PLA + hydrolyzed microcrystalline cellulose - were made by solution processing.

1.1.4 Objective IV

To obtain a correlation between filler particle size and surface modification via surface grafting in terms of the mechanical reinforcement provided by the filler. The surface of hydrolyzed cellulose particles was modified by grafting lactic acid and polylactic acid.

This resulted in type (iv), which are PLA + lactic acid-g-hydrolyzed microcrystalline cellulose and PLA + polylactic acid–g- hydrolyzed microcrystalline cellulose particles - composite samples.

These four composite systems enabled us to study a variety of parameters. By comparing samples within type (i) the influence of processing technique on properties was studied. Studying samples types (i) and (ii) allowed us to study the effect of filler surface modification while the influence of filler size or the filler surface area was understood from comparison of samples types (i) and (iii). Finally comparison of types (iii) with type (iv) provided understanding of relative influence of filler surface area and filler-matrix compatibility on composite properties.

The significance of interfacial interactions and a simple method for modifying the extent of these interactions is demonstrated in this work. By understanding factors that influenced composite properties the utility of cellulose as an effective reinforcement of PLA has been demonstrated.

CHAPTER 2

LITERATURE REVIEW

More recently, due to large quantities of plastic waste being generated and increasing price of oil, attention has being given to development of environmentally benign composites from renewable resources. Polymers which can bio-degrade or whose degradation products are non-toxic are desirable. Polylactic acid, PLA is a degradable polymer that has properties comparable to those of commodity plastics like polystyrene and can be processed in similar way as polypropylene [1, 2]. Compared to polypropylene, PLA possesses good stiffness and strength but has poor impact strength and is a slowly crystallizing polymer [3]. Blending of PLA or synthesizing PLA composites by incorporation of inorganic/organic micro or nanoparticles in the PLA matrix is one way of improving the properties of PLA.

2.1 Polylactic acid (PLA)

PLA consists of lactic acid as the basic constitutional unit. It is manufactured by carbohydrate fermentation or chemical synthesis [4]. Lactic acid (2-hydroxy propionic acid) is a hydroxyl acid with an asymmetric carbon atom and exists in two optically active configurations, the L (+) and D(-) isomers. In general, lactic acid can be manufactured from petroleum based sources or from a renewable source such as glucose and maltose from corn or potato, sucrose from cane or beat sugar etc. Chemical structure of PLA is shown in Figure 1.

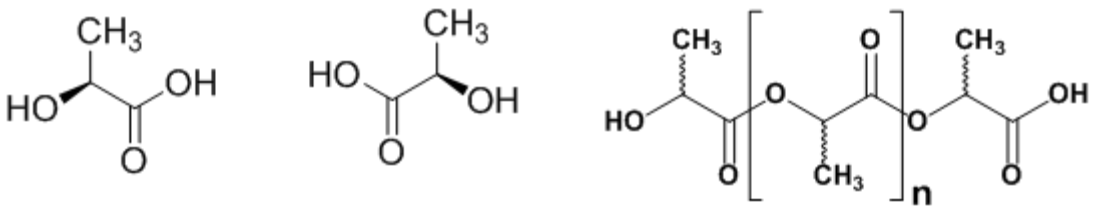

(a) **(b)**

Figure 1. Chemical structure of (a) L-lactic acid, D-lactic acid and (b) polylactic acid (PLA) [4]

In addition to its biodegradable character, other advantages of PLA polymer are biocompatibility, availability from renewable resource, non-toxic byproducts, metabolization or mineralization of biodegradable byproducts and chance to cover large range of properties through copolymerization or blending [5, 6].

2.2 PLA polymerization routes

It is possible to produce lactic acid based polymers from various monomers via different routes.

2.2.1 By step-growth polymerization of lactic acid with other hydroxy acids

This polymerization method (of mixtures of L- and D-lactic acid) reportedly leads to a random distribution of the L and D units. Since the step-growth polymerization is an equilibrium reaction, the presence of even trace amount of water in the late stages of polymerization can limit the ability to form high molecular weight polymer. Other drawback of direct synthesis of PLA by polycondensation of lactic acid is that high molecular weight can be achieved only above 99% conversion also monofunctional impurities such as ethanol or acetic acid from fermentation can limit the molecular weight. Due to these limitations, it is difficult to obtain high molecular weight polymer

with condensation polymerization [7]. However there is at least one company, Mitsui Toatsu Chemicals, which employ condensation polymerization to obtain high molecular weight PLA [8].

2.2.2 By chain-growth polymerization of the dimer lactide

Three stereoisomer of lactic acid exists namely, i) L-lactide, ii) D-lactide and iii) meso-lactide. The stereochemical composition of the resulting polymer is therefore determined by the make-up of the lactide monomer stream. The three chemical structures are shown below in Figure 2.

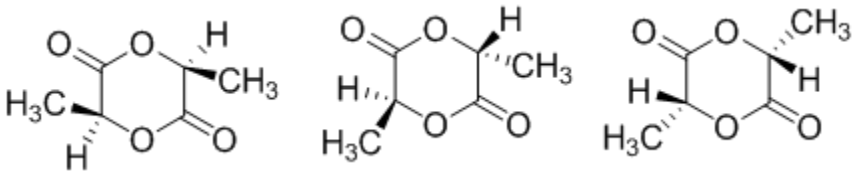

Figure 2. Chemical Structures of LL-, meso- and DD-lactides [4]

Lactide, structure shown in Figure 2, is composed of two lactic acid units linked by two ester bonds to form a dimeric cyclic monomer. The cyclic dimer bears two asymmetric carbon atoms. High molecular weight polymer can be obtained via ring opening polymerization of lactide containing feeds in organic solution or in the bulk at different temperatures. The chain-growth polymerization can proceed by different mechanism, e.g., cationic, anionic etc. [5] Jan Nieuwenhuis [9] has discussed the various polymerization routes of lactides, namely melt, bulk, suspension and solution polymerization in details.

Depending on the synthesis route and the chiral monomer(s) used, the resulting distribution of chiral repeating units can be very different. The use of cyclic dimer (lactide) together with controlled residence time, temperature and catalyst type used, makes it possible to control the ratio and sequencing of D- and L-lactic acid units in the final polymer [6]. The optical composition of the polymer significantly affects crystallization kinetics and the ultimate extent of crystallinity. PLA derived from greater than 93% L-or D-lactic acid can be semi-crystalline whereas PLA containing greater than 7% of second isomer is found to be amorphous [4]. This second isomer acts as an impurity leading to introduction of twists in the otherwise regular polymer molecular architecture. The molecular imperfections result in decrease in both the rate and extend of PLA crystallization. Ikada et al. [10] have reported that the glass transition temperature, T_g, is determined by the proportion of different lactides present, which results in PLA polymers with wide range of stiffness and hardness values. Table 1 gives the physical properties of PLA (98% L-lactide), PLA (94% L-lactide), polystyrene (PS) and polyethylene terephthalate (PET).

Table 1. Physical properties of PLA (98% L-lactide), PLA (94% L-lactide), PS and PET. Reproduced from ref. [17]

Sample	**PLA (98% L-lactide)**	**PLA (94% L-lactide)**	**PS (atactic)**	**PET**
T_g (ºC)	71	66	100	80
T_m (ºC)	160-170	140-150	-	240-245
Enthalpy of fusion (J. g^{-1})	37.5	21.9	-	47.7
% Crystallinity	40	25	-	38

In spite of PLA having similar T_g and T_m values as those of commodity plastics like PS and PET, PLA has its own drawbacks. PLA can be degraded by presence residual metals or catalyst [11]. The residual metal can catalyze chain transfer, transesterification and depolymerization reactions. PLA is hydrolyzed by trace amounts of water and this reaction is further catalyzed by the hydrolyzed monomer (lactic acid) which may result in zipper-like depolymerization. PLA chains can also undergo oxidative random chain scission and transesterification giving monomer and oligomeric esters [12].

Thermal history can induce changes in the crystallinity and thus affect the physical properties of PLLA. Properties such as tensile strength are reported to improve with increasing L-lactide content of the PLA sample [13]. Annealing PLLA increases the tensile and impact strength due to increase in crystallinity and the physical cross-linking effects of the crystalline domains. The mechanical properties of PLA are comparable to those of commodity polymers like PS. However the main advantage of PLA over these and other widely used olefinic polymers is its ability to undergo degradation producing water and carbon dioxide. Properties of PLA can be tuned by controlling the stereochemical structure of the polymer, blending of PLA with other polymer, e.g. cellulose or by addition of particles, e.g. clay nanoparticles to the PLA matrix.

All these observations afford us the possibility of preparing PLA composites with improved mechanical and thermal properties together with increased degradation rate of the matrix polymer.

2.3 Cellulose

Cellulose is a biopolymer, obtained from a renewable resource is one of the most abundant organic compounds found in nature. Cellulose is insoluble in water and common organic solvents, but is swellable in many polar protic and aprotic liquids. Lack of suitable solvent has been one of the main reasons for its limited exploitation. The food and Agriculture Association has estimated that about 3.2 billion m^3 of cellulose exists on the earth of which only about 1 percent is being utilized [14]. Cellulose can be obtained from various sources, such as trees, and is also synthesized by some algae, fungi, bacteria, and some animals. When the cellulose is dissolved in a solvent it is termed as regenerated cellulose. Compared to inorganic fillers, some of the advantages of using cellulose as a reinforcing phase in polymer matrix are its renewable nature, low density, relatively reactive surface due to presence of hydroxyl groups (making surface modification possible), and low cost [15].

Cellulose is a polydispersed linear polymer of β(1,4)-D-glucose and has a syndiotactic configuration. The β-D-glucose units exist in the $^4C_1$ chair configuration which is the lowest energy conformation. Figure 3 shows the structure of cellulose in its chair configuration [16].

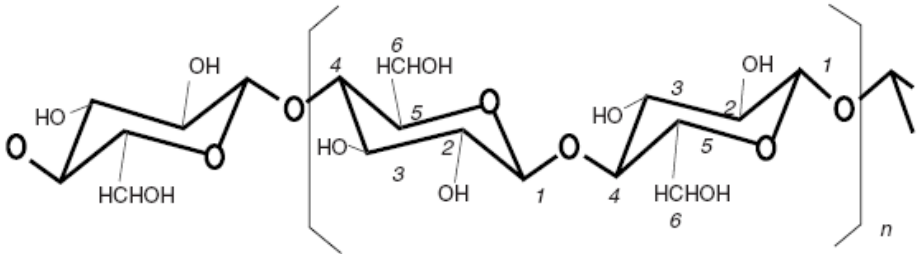

Figure 3. Structure of Cellulose. Reproduced from ref. [16]

Due to hydrogen bonding between hydroxyl groups of adjacent molecules, the cellulose chains aggregate to form a fibril. A fibril is a threadlike bundle of molecules stabilized laterally by hydrogen bonding between adjacent molecules. The molecular arrangement of these fibrillar bundles is called Microfibrils. One microfibril contains several elementary fibrils which are in turn composed of multiple cellulose chains. The arrangement of microfibrils is regular enough to exhibit a crystalline X-ray pattern [17]. The microfibrils are about 10 – 30 nm wide and can contain 2 – 30,000 cellulose molecules. As mentioned earlier, cellulose can be natural (native) or man made (regenerated). It is very difficult to find cellulose in pure state. When derived from plant source, cellulose is associated with other substances like lignin and hemicellulose. In addition to lignin and hemicellulose, a number of non structural components such as waxes, inorganic salts and nitrogenous substances are also present [18] . Figure 4 shows the schematic of hierarchical structure of wood [19].

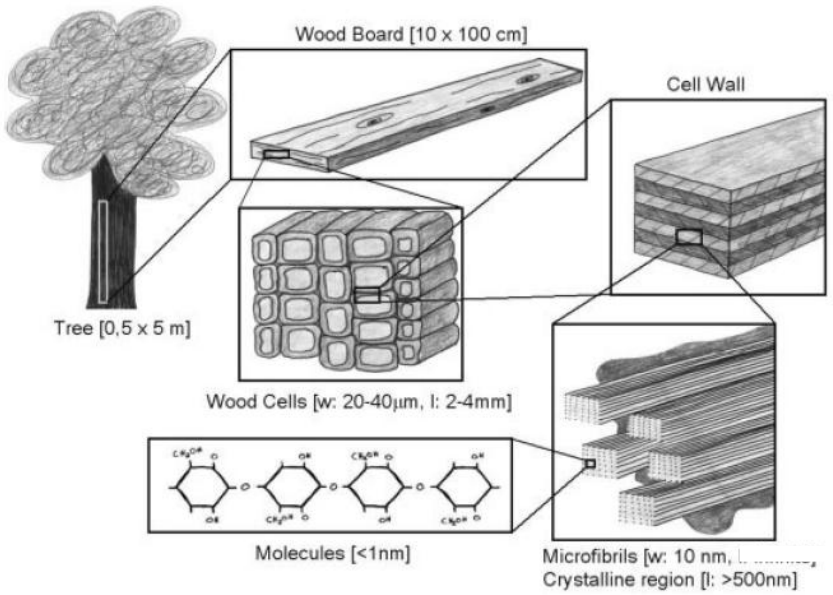

Figure 4. Schematic of hierarchical structure of wood from macro to nano. Reproduced from ref. [19]

Since the cell walls differ in their composition and in the orientation of the microfibrils, the mechanical properties of cellulose fibers depend on the cellulose content and the spiral angle of the fibril. The modulus of elasticity of the perfect crystal of native cellulose has been calculated by various authors and estimated to be between 130 to 250 GPa and the tensile strength is assessed to be approximately 0.8 to 10 GPa [20]. To utilize the excellent mechanical properties offered by these cellulose fibrils, attempts have been made to fragment cellulose fiber into smaller units. Two examples are microfibrillated cellulose (MFC), obtained through a mechanical homogenization process and microcrystalline cellulose (MCC) obtained via chemical treatment. Both involve either degradation or dissolution of the amorphous part leaving only the crystalline part behind.

2.3.1 Crystalline Structure of Cellulose

Cellulose chains are biosynthesized and self-assembled into microfibrils which consist of amorphous and crystalline domains. The biosynthesis mechanism is the same and is independent of origin, but crystal dimension and the degree of crystallinity are dependent on their origin. The nanocrystals obtained from different cellulose sources show a wide variation in length. For e.g. algal and tunicate cellulose microfibrils yield nanocrystals that are several micrometers in length whereas wood microfibrils yield much shorter nanocrystals of only a couple of hundred nanometers. All cellulose nanocrystals show a large distribution in length, independent of their origin. This may be due to acid hydrolysis conditions, non-selectivity of the hydrolysis conditions, packing structure of cellulose chains etc. The dimensions of the nanocrystals obtained after hydrolysis is

mainly dependent on the percentage crystallinity of the starting material or in other worlds on the percentage of amorphous regions in the starting material [21, 22].

It is known that hydrolysis of native cellulose with strong sulfuric acid or hydrochloric acid causes a rapid lowering of its degree of polymerization until level off degree of polymerization (LODP) is reached. Once LODP is reached, increasing hydrolysis time does not lower the molecular weight further. This LODP value depends on the source of cellulose. The cellulose microfibrils get longitudinally cleaved during hydrolysis into smaller crystalline objects called "whiskers". Whiskers have the same diameter as the initial microfibril, but the length depends on the origin and can vary from tenth of a nanometer to several micrometers. Whiskers are fully stretched cellulose chain segments that are arranged in a perfect crystalline arrangement [23].

Cellulose chains in the amorphous regions are randomly oriented resulting in a lower density in the amorphous regions. This makes the amorphous regions susceptible to attack by acids. Consequently, the hydronium ions are able to penetrate into these amorphous domains of the cellulose chains and promote the hydrolytic cleavage of the glycosidic bonds. This process results in separation of amorphous part from crystalline part and releasing of individual crystallites [22]. These individual crystallites (nanofibrils) have been calculated to have tensile strength of 10 GPa and modulus of 150 GPa [24]. The properties of nanocrystals are affected by the hydrolysis conditions and the acid used. Highly stable aqueous suspension of nanocrystals is obtained by employing sulfuric acid. The use of sulfuric acid results in esterification of the surface hydroxyl groups of cellulose nanocrystals producing charged sulfate groups [25, 26].

2.4 Particulate filled composites

Factors that influence the properties of particulate filled composites are the properties of individual components, composition and interaction between the components. Two kinds of interactions can occur in particulate filled composites

(i) Formation of an interphase- polymer adheres to surface of particles forming an interphase. The interphase layer can have properties different from that of the polymer matrix

(ii) Aggregation – particles aggregate due to interaction between particles

These two interactions are dependent on the forces of separation and adhesion between particles. Particle separation is influenced by the extent of shear forces exerted on the particles. Aggregation of the particles on the other hand is influenced by the particle size and surface tension of the particles.

Pukanszky [27] has given factors that affect particle-particle interactions: particle size, specific surface area and surface energetic. It has been shown for PP filled $CaCO_3$ composites [28] that particle aggregation increases with decreasing particle size. However increasing particle surface area by decreasing particle size, increases contact surface between filler and matrix and thus influences the filler matrix interactions.

Ess and Hornsby [29] have identified the adhesive forces that cause particle agglomeration and have listed them in order of increasing adhesive strength as mechanical interlocking, electrostatic forces, van der waals forces, liquid bridging and solid bridging.

Surface modification of filler particles is done to prevent or reduce particle-particle aggregation. Some surface treatments can result in decrease in surface tension of

particles. Decrease in surface tension results in decrease in interfacial tension and work of adhesion. The lowering of work of adhesion results in weaker particle-matrix interactions [30]. For some systems, e.g. using mica particles for reinforcement, matrix stretching around filler particles occurs and is promoted by debonding of the interface resulting in an increase in crack growth resistance and hence the toughness of the composite. Improvement of interfacial adhesion due to treating mica flakes with silane coupling agent resulted in lowering of matrix stretching and lowering the maximum crack growth resistance [31]. Thus good filler-matrix adhesion can alter the plastic deformation of the matrix and lower the composite toughness.

For PP/$CaCO_3$ composites, Jancar [32] has reported a much faster increase in composite modulus with increasing filler volume fraction for untreated $CaCO_3$ compared to surface treated $CaCO_3$. He has attributed this difference to a higher thermodynamic energy of adhesion of the untreated filler. Higher thermodynamic energy of adhesion resulted in greater filler-matrix interactions. The rate of increase of modulus is thus seen to depend on interfacial interactions. However, reduction in filler energy achieved by surface treatment of $CaCO_3$ was observed to improve dispersion of filler.

Therefore we have investigated surface modification of cellulose particles in order to reduce the interfacial tension between filler and matrix for avoiding particle-particle aggregation and improving filler-matrix interactions.

2.5 Effect of filler particles on matrix polymer conformation

The presence of filler particles can modify the conformations of the matrix polymer chains which in turn affects the properties of the polymer. Particles can restrict the conformation of polymer molecules in their vicinity. The polymer chain can expand

parallel to the surface of particles resulting in increase in effective molecular size in that particular direction. Depending on the polymer molecular weight and temperature employed, the polymer molecules can occupy large volumes. For small size particles, at high filler loadings, the inter-particle spacing may be smaller or similar size as particles. The polymer chains may then be forced to take up strained conformation resulting in alteration in polymer properties. The reduction in matrix chain mobility can cause an increase in macroscopic rigidity of matrix layer in contact with particles as compared to bulk matrix which is not influenced by the filler particles. This can result in increased modulus of the composite.

2.6 Effect of crystallinity

It has been reported that particulate fillers can affect the crystallinity of some polymers and hence influence the mechanical properties of the polymer [33]. Crystalline size and shape, orientation, percent crystallinity are some parameters that influence the properties. Since in thermoplastics the polymer chains have hindered motion, a high degree of super cooling may be required before crystallization [34], this makes the thermoplastic polymers prone to nucleating effects with addition of nucleating agents causing rapid nucleation. The nucleating agents in general affect the size and the number of crystallites formed.

Mitsuishi et al. [35] have reported for samples of $CaCO_3$ filled PP change in crystallization rate of the matrix polymer due to interactive motion of matrix chains at the particle surface. Decreasing particle size increases surface energy, which in turn increases activity of the particle surface. This resulted in increase in crystallization temperature with increasing volume fraction of filler at all particle sizes. The authors have also

reported decrease in impact strength with increasing nucleating effect of $CaCO_3$. Mathew et al. [19] have studied the crystallization behavior of PLA reinforced with microcrystalline cellulose, wood flour and cellulose fibers. They observed that the nucleating efficiency was more influenced by the surface topography than the chemical composition of the reinforcement. Garlotta [36] has shown that the mechanical properties of PLLA depend on the degree of crystallinity which in turn can be influenced by annealing. Ray et al. [37] have observed that dispersed organically modified clay particles, OMLS, act as nucleating agents in PLA and that the nature of OMLS influences the crystallization temperature.

2.7 PLA composites reinforced with microcrystalline cellulose particles

It is possible to develop degradable composites that have cellulose as the reinforcing material. Combination of cellulose with biodegradable polymer such as PLA results in formation of environmentally friendly composites. Microcrystalline cellulose, MCC, in which the amorphous part is removed by acid hydrolysis, is an example of a cellulose reinforcement material for polymeric composites. MCC is crystalline cellulose derived from cellulose source such as filter paper or high quality wood pulp that disintegrates into cellulose whiskers on complete hydrolysis. On acid hydrolysis, the microfibrils are believed to undergo transverse cleavage along the amorphous regions and release whiskers or crystalline cellulose [38].

MCC is also reported to have a high specific area compared to conventional cellulose fibers [39]. The high surface area of MCC (reinforcement) could lead to better interaction between the matrix and reinforcement, resulting in enhancement of mechanical properties and in thermal stability of the resulting composite. These cellulose based composites

have high stiffness and strength combined with biodegradability can be used in applications such as cardiac devices, blood bags etc. [40]

2.8 PLA composites reinforced with nano-sized cellulose whiskers

Cellulose whiskers derived from cellulose source such as microcrystalline cellulose is an example of a cellulose nano-reinforcement material for polymer nanocomposites. The microcrystalline cellulose particles disintegrate into cellulose whiskers after hydrolysis. Cellulose whiskers derived from cotton or microcrystalline cellulose is reported to have cross sections from 3-50 nm and lengths up to several hundred nanometers. These whiskers have a high aspect ratio, large interface area on account of their small size and possess high modulus. The modulus of cellulose whiskers is predicted to be to be around 150 GPa [41] with strength approximately equal to 10 GPa [42]. In addition, the cellulose reinforcements have low density and nonabrasive nature. The hydroxyl groups on the surface makes the cellulose reinforcements amenable for surface modification through grafting [15].

Uniform dispersion of the whiskers is crucial for preventing stress concentration that decreases the composite strength. If the whiskers agglomerate, then it will give rise to stress concentration from where it is easier to initiate cracks causing failure of the composite [43]. Hasegawa et al. [44] observed an increase in the strain-to-failure ratio for a polypropylene-clay system, when the clay was exfoliated in the polypropylene matrix and a decrease in the strain-to-failure ratio even for small amount of aggregation.

2.9 Comparison of micron and nano sized reinforcement

Winey and Vaia [45] have compared a microcomposite and a nanocomposite having same volume fraction of a spherical filler having volumes of 1 μm^3 and 1 nm^3 per particle, respectively. In the nanocomposite, mean particle–particle separation was found to be smaller by three orders of magnitude, the total internal interfacial area increased by six orders of magnitude and the number density of constituents was found to increase by nine orders of magnitude. At extremely small particle size, the volume of interface can be greater than the particle volume resulting in a majority of the volume fraction being occupied by the interfacial region. If this is the case, interface and particle-particle interaction dominate the macroscopic properties. Thus in an ideal polymer nanocomposite, the mean distance between the filler particles (nanoparticles), will be of the order of radius of gyration, R_g, of the matrix chains, which is the fundamental length scale characterizing the size of the matrix chains. The size of the filler is also of the order of R_g. The large aspect ratios observed with nanofillers can introduce orientational correlations between particles giving rise to low percolation thresholds [46]. Giannelis et al. [47] have observed the enhancements in mechanical and barrier properties of polymer nanocomposites to be a function of aspect ratio of the nanofiller.

In summary, the drastic improvements in material properties observed in nanocomposite systems at relatively low filler loadings can be related to [46]

1. short distances between particles
2. very high interfacial area per volume of particles
3. large number density of particle per particle volume
4. particle-particle interaction taking place at low volume fractions

5. comparable size scale among nanoparticles, distance between particles and the relaxation volume of polymer chains

2.10 Micromechanics

Huda et al. [48] observed that composites of PLA reinforced with wood pulp based cellulose fibers possess good thermal and mechanical properties. The modulus increased by three times from approximately 2.5 GPa to 6 GPa but the tensile strength did not show any improvement. They attributed the failure to get any significant improvement in tensile strength to lack of or low interaction between cellulose fibers and the PLA matrix caused by poor dispersion of fibers in the matrix. Absence of good adhesion prevents transfer of stress from the PLA matrix to the cellulose fibers. For short or discontinuous fiber reinforced composites the interfacial interaction between fiber and matrix is extremely important as tensile load is transferred via shear along the fiber surface.

For a given fiber diameter and fiber–matrix adhesion, the critical fiber length necessary for the fiber to develop maximum stress is calculated as

$$l_c = \frac{\sigma_{fu}}{2\tau_i} d_f \tag{1}$$

Where l_c = minimum fiber length required for the maximum fiber stress to be equal to the ultimate fiber strength at its midlength

d_f = fiber diameter

σ_{fu} = ultimate fiber strength

τ_i = interfacial shear strength of the interface or adjacent matrix

As seen from Equation 1, for a given fiber diameter and strength, the critical fiber length, l_c, can be controlled by increasing or decreasing τ_i. The interfacial modifications are observed to directly affect the composite performance as it influences the critical fiber length, l_c, required for stress transfer for a given fiber diameter, d_f [49]. This illustrates the importance of interface in controlling the mechanical properties of composite systems. As the aspect ratio of the filler increases, the filler length that carries the maximum load also increases resulting in improved mechanical properties.

2.11 Polymer filler interface

The interface in polymer composite systems is the surface between two mutually insoluble and chemically distinct phases which are at equilibrium with respect to each other. If there is no interaction between the phases, physical or chemical, then at larger strains the composite will respond as if the matrix contained holes of shape identical to the shape of the filler. In the case when there is interaction between the two phases, stress transfer can occur across the interface, resulting in filler carrying the load and thus reinforcing the matrix. However if the interface is too strong then properties such as impact strength may be adversely affected as energy dissipation becomes difficult.

In order to improve the interfacial strength it is necessary that the polymer wets the fiber (reinforcement) spontaneously during processing, wherein the adhesion energy between the polymer and fiber can overcome the cohesive energy of polymer [50]. Two methods are used for increasing the interfacial shear strength of the composite namely application of coupling/compatibilizing agent or chemical modification of the fiber surface. Examples of coupling agents employed are those which are capable of condensing

efficiently with surface hydroxyl groups present on the fiber surface such as, carboxylic anhydrides, isocynates, oxiranes and siloxanes. Improvement in mechanical properties, e.g., modulus and strength of thermoplastic composites reinforced with wood cellulose fiber have been reported after chemical modification of cellulose fiber surface [51-54]. It is crucial, that modification takes place on the surface of the fiber but the cellulose backbone is not modified.

Another important factor for achieving good interaction between matrix and fiber is the compatibility between their surface energies. Surface modification of cellulose fibers promotes adhesion by minimizing their interfacial energy with the non-polar polymer matrices. It is well established that the mechanical properties of the composite can be improved if chains (oligomer or polymer) grafted onto cellulose for surface modification can diffuse into and entangle with the matrix chains [50]. Chemical or physical modification of polymer is another approach for modifying the properties of the polymer to meet some specific requirements/applications.

Gandini et al. [55] have reviewed in detail the different procedures used for surface modification of cellulose fibers. Surface modification is necessary to increase the usefulness of cellulose as a reinforcing material to obtain new composites with desired properties. The surface of the cellulose whiskers can be chemically modified in order to improve dispersion in solvents such as water and organic solvents such as chloroform [56]. Heux et al [57] have described a method for obtaining stable dispersion of cellulose whiskers in nonpolar solvents using surfactants. In general, significant increase in the mechanical properties of composite are observed if uniform dispersion of reinforcement

in the matrix and good interfacial adhesion is achieved [58]. Surface modification is achieved through hydroxyl groups on the surface of cellulose particles.

2.11.1 Physical surface modification

Cellulose fiber surface can also be modified by cold plasma treatment or corona treatment. These techniques change the surface energy of the fiber by surface oxidation activation. The surface energy can be decreased or increased, reactive free radicals produced, surface crosslinking or other functional groups could be obtained by conveniently choosing the type and nature of gases that are used for these treatments [59, 60].

2.11.2 Surface modification via reactive processing

During synthesis of polymer composites by processing techniques like extrusion, injection molding, compounding etc. it is possible to modify the interface by addition of reactants that are activated at elevated processing temperature such as peroxides. The processing equipment acts as a reactor generating enough thermal energy to initiate reaction of peroxides which can lead to polymerization of monomer, grafting of polymer onto the fiber surface and/or compatibilization of fiber surface [61]. Sapieha et al. [62, 63] have shown that addition of small amount of peroxide to olefinic polymer-cellulose system during processing significantly improves the mechanical properties of composites, particularly the yield strength. The increase in mechanical properties was related to the peroxide initiated free radical reaction between polymer matrix and cellulose fibers resulting in better adhesion between the two components. The hydrogen abstraction from cellulose can occur from –OH, C-H of the cellulose backbone or from methylol group,

CH_2OH. The hydrogen abstraction can also occur from the tertiary carbon of the alpha olefin. The grafting of polymer to cellulose fibers depends on the available surface area of cellulose and on concentration of cellulose fibers in the composite [63]. The use of cellulose whiskers that have large surface area would be advantageous for grafting of polymer onto cellulose surface.

2.12 Surface grafting on cellulose

Dorgan et al. have modified cellulose surface using initiators that would polymerize lactide onto the cellulose surface during processing by extrusion [64]. Habibi et al [23] have used TEMPO mediated oxidation to convert surface hydroxyl groups to charged carboxyl group. Advantage of this method over hydrolysis by sulfuric acid is that the carboxyl groups are not as labile as the sulfate groups, which are readily removed under mild alkaline conditions.

Cellulose surface can be grafted with bi-functional molecules capable of polymerizing, one functional group can react with the surface hydroxyl group of cellulose and the other functional group can form a covalent bond with the polymer matrix. This approach is considered more suitable for polymer matrices that can be obtained by addition polymerization, for example, vinylic and acrylic polymers. One can also employ a planar stiff molecule that has two identical reactive groups, one capable of forming covalent bond with surface hydroxyl group of cellulose through condensation and the other with the matrix. This approach is more suitable with polymer matrices which are obtained by condensation polymerization, for example, polyesters, polyurethane and epoxies. This fact in particular is very useful for surface modification of cellulose using monomer such as lactic acid. Lactic acid monomer has two hydroxyl groups and under suitable

conditions it can modify the surface of cellulose. Controlled surface silylation of the cellulose whiskers has also been done for grafting hydrophobic chains on the whisker surface. This resulted in dispersion of whiskers in low polarity solvents like THF [65].

Surfactant type structures having long hydrophobic tails and having one or more polar end groups are capable of reacting with surface hydroxyl groups of cellulose. These surfactant type molecules can increase the compatibility of cellulose with non-polar polymer matrix. Heux et al. [57] have used surfactants as stabilizing agent for dispersing microcrystalline cellulose in toluene and cyclohexane. The surfactant can also provide a hydrophobic barrier and prevent water uptake by cellulose particles.

2.13 Model Fitting

Instron and DMA modulus data was fitted to three existing models, Rule of Mixture (ROM) series model, Halpin Tsai model and Paul model [66]. The DMA data were fitted at a temperature of 40 ˚C which was below Tg. The equations for volume fraction, ROM, Halpin-Tsai and Paul model are given below.

The volume fraction of filler was calculated using equation 2

$$V_f = \frac{\left(W_f / \rho_f\right)}{\left(W_f / \rho_f\right) + \left(W_m / \rho_m\right)} \qquad (2)$$

Where, W_f, W_m – weight of fiber and matrix, P_f,– density of fiber (1.4 g/cm^3) [67]

ρ_m – density of matrix (1.25g/cm^3) [68]

Modulus of composite with ROM series model was calculated using equation 3. It gives the modulus as the combination of the modulus of the fiber and the matrix by taking volume weighed average of the individual phase properties. This model assumes that the

reinforcement has uniform size and the applied load produces equal strains in both matrix and the reinforcement. The later assumption is similar to considering two phases in parallel. The rule of mixtures model best simulates an orthotropic material loaded uniaxially in the direction of reinforcement [49].

$$E = E_f V_f + E_m V_m \tag{3}$$

Where, V_f and V_m – volume fractions of fiber and matrix respectively

E_f and E_m – fiber and matrix modulus respectively

The Halpin Tsai equation is given below, this model has been proven to work well with different reinforcement geometries such as fibers, ribbons and flakes. The model was developed for predicting the modulus of unidirectional composite material as a function of aspect ratio of the reinforcement.

$$\frac{E}{E_m} = \frac{(1+\xi V_f)E_f + \xi(1-V_f)E_m}{(1-V_f)E_f + (\xi+V_f)E_m} \tag{4}$$

Where, $\xi = 2\ (l/d)$, is a measure of particle reinforcement geometry and this particular form of ξ is used for calculating the longitudinal modulus.

E_f = modulus of reinforcement in direction of applied load.

For continuous fiber composites, $\xi \rightarrow$ infinity the Halpin-Tsai equation reduces to the same form as the rule of mixtures.

The modulus with Paul model was fitted using equation 5. This model is best suited for irregular shaped reinforcement, e.g. microcrystalline cellulose particles or hydrolyzed microcrystalline cellulose particles

$$\frac{E}{E_m} = \frac{E_m + (E_d - E_m)V_d^{\,2/3}}{E_m + (E_d - E_m)V^{2/3}(1-V_d^{1/3})} \tag{5}$$

Where, E, E_m , E_d = modulus of composite, matrix and reinforcement respectively and

V_d = volume fraction of particulate reinforcement

Following assumptions were made when fitting data with any given model,

1) The cellulose particles are uniformly dispersed in the PLA matrix
2) Particles have uniform shape and size
3) Good interfacial interactions exists between PLA and cellulose particles
4) PLA matrix is free of voids
5) Initially there are no residual stresses in the PLA matrix
6) Both PLA matrix and the cellulose reinforcement behave as linearly elastic materials

2.14 Degradation of PLA-cellulose composites

Reinforcing PLA with cellulose particles either unmodified or surface modified resulted in respective improvement in modulus and the overall mechanical properties and will be discussed in details in chapters 4-6. One of the drawbacks of semi-crystalline PLA samples and composites in certain applications is their relatively slow rate of degradation [69]. The slow degradation results in long in vivo life time reported to be several years in some cases [70]. This may adversely affect the use of these materials in applications where both good mechanical properties and fast degradation is required.

The objective of using PLA-cellulose composite was to improve the mechanical properties of PLA and also to obtain a composite material based on renewable resource capable of undergoing degradation under controlled conditions. For this, it was important to study the degradation of neat PLA and PLA-cellulose composites.

A number of studies both in vitro and in vivo, dealing with neat PLA and PLA based micro/nanocomposite degradation under various conditions have been carried out [69,

71-81]. The pH of the degradation media is found to have a profound influence on both the rate and mechanism of degradation. Degradation under alkaline [73, 78] or acidic pH [82] resulted in increased degradation rate compared to degradation in phosphate-buffer solution [79] . Basic or acidic pH catalyzes the hydrolytic degradation of PLA and PLA based composites. Bulk erosion has been reported to occur in phosphate-buffer (pH- 7.4) and in acidic conditions (pH – 2). Surface erosion has been observed for degradation in alkaline media (pH > 10). The erosion mechanism is characterized by monitoring the sample mass loss as a function time and by comparing the peak position and peak area of the un-degraded and the degraded samples GPC curves. Surface erosion is characterized by a linear mass loss with no induction time and no relative shift of peak position in GPC. The bulk erosion on the other hand is characterized by an induction time before sample mass loss occurs and by a shift in the relative position of the GPC peak toward lower molecular weight side for degraded samples. Degradation by bulk and surface erosion is shown in figures 5.

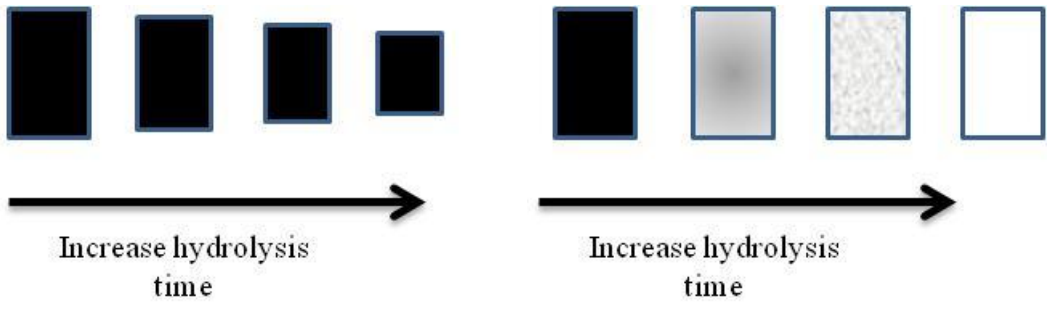

(a) **(b)**

Figure 5. Degradation by (a) surface erosion (heterogeneous degradation) and (b) bulk erosion (homogeneous degradation).

CHAPTER 3

MATERIALS AND METHODOLOGIES

In this chapter the detailed procedures and description is given for the materials used, processing techniques employed and instruments used for preparation and characterization of samples the results of which are reported in the subsequent chapters. The procedures used for cellulose hydrolysis, cellulose surface modification and degradation of PLA-cellulose samples are also given in this chapter.

3.1 Materials

Polylactic acid pellets were obtained from NatureWorks LLC and Avicel microcrystalline cellulose was obtained from FMC Biopolymers, Delaware. Monomer L-lactic acid (98%) was purchased from Sigma-Aldrich. Organic solvents chloroform, toluene and tetrahydrofuran were purchased from VWR and used as received.

3.2 Processing

3.2.1 Solution processing of PLA-Avicel composites

Solvent cast films were obtained by casting the solution, made by sonicating mixture of polymer and filler in chloroform, onto a glass Petri dish and drying under ambient conditions in air. Samples were then dried under vacuum at room temperature for one day and then annealed under vacuum for one day at 120 ˚C.

3.2.2 Melt processing of PLA-Avicel composites

Melt mixing was done in a Haake Minilab twin screw extruder followed by compression molding in a Carver hot press. Both the extrusion and compression molding temperatures were set at 180°C. After compression molding, samples are allowed to cool down to room temperature under pressure. External cooling was not employed. Total cooling time for samples in the compression mold was around 6 hours.

3.3 Hydrolysis of Avicel microcrystalline cellulose

Gray et al. [83] have reported the synthesis procedure for obtaining stable colloidal suspension of cellulose micro crystallites via acid hydrolysis of filter paper. Bondeson et al. [84] reported optimized hydrolysis conditions for isolation of cellulose nanocrystals from microcrystalline cellulose. We employed similar procedure as given in [84] and is reported below. Microcrystalline cellulose particles were added to a 63.5% sulfuric acid solution. The ratio of cellulose to acid used was 1:8.75 g/ml. The reaction was carried out for 130 min. at 45°C. The heating was then turned off and distilled water was added to the reaction mixture which was 10 times the volume of the reaction mixture. The reaction vessel was then left undisturbed for several hours. After acid hydrolysis the acid moieties were removed with centrifugation followed by addition of sodium hydroxide solution to neutralize remaining acid. The sodium sulfate salt formed as a consequence of adding base to acid was removed by further centrifugation. Finally the neutralized suspension that was salt free was freeze dried.

3.4 Grafting polylactic acid to cellulose

L-lactic acid or preformed PLA was grafted onto the surface of cellulose particles via condensation reaction of L-lactic acid and hydroxyl group on cellulose. No catalyst was employed for the grafting reaction. The hydroxyl groups on the surface of cellulose particles act as initiator for lactic acid resulting in a 'grafting from' type of reaction. In a typical preparation, 6 g L-lactic acid and 2 g of cellulose particles were mixed in toluene in a flame dried 3-neck round bottom flask. Reaction was carried out at 160°C (oil bath temperature) under nitrogen atmosphere with constant stirring. Water formed was removed by azeotropic dehydration with toluene using a Dean-Stark trap. Reaction was carried out for ~42 hours. The reaction product was recovered by centrifugation. The product was washed with excess amount of chloroform and filtered. Three wash-and-filter cycles were employed to remove any un-grafted lactic acid and PLA homopolymer that may be present in the solution. The washed and filtered product was dried in air for one day and then under vacuum for 24 hours at 60°C to remove residual chloroform. The procedure is analogues to the grafting procedure used by Chen et al. [85] for surface grafting of oligomeric lactic acid on silica nanoparticles.

3.5 Degradation of PLA and PLA-cellulose composites

The degradation experiments were carried out in 10 ml glass vials placed in a water bath at 37 °C. The bath temperature was maintained using a thermocouple attached to the water bath. All sample vials contained 4 ml of aqueous NaOH solution. After specified time in the hydrolysis medium, the hydrolyzed films remaining after hydrolysis were removed and washed with distilled water and then dried in air for one day followed by

drying in vacuum to constant weight. Dried samples were analyzed by GPC, DSC and for weight loss.

3.6 Characterization techniques

3.6.1 Mechanical properties

All samples were annealed under vacuum for 24 hours at ~120°C prior to testing. Tensile modulus, strength and maximum strain at break were measured on an Instron Corporation tensile testing machine 5566 with a 10KN load cell. All samples were tested at crosshead speed of 5mm/min. Dynamic mechanical analysis (DMA) was performed on the materials using TA Instruments model Q800 using a film tension clamp. All samples were heated at a rate of 2°C/min between 35°C and 130°C at a frequency of 2 Hz and 0.05% strain. A typical stress-strain curve obtained with tensile testing machine is shown in Figure 6.

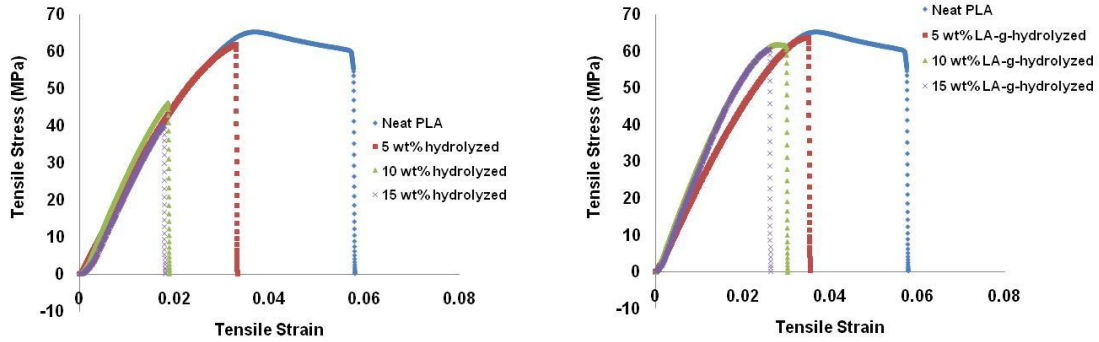

(a) (b)

Figure 6. Stress strain curves for PLA samples reinforced with (a) hydrolyzed microcrystalline cellulose particles and (b) lactic acid grafted hydrolyzed microcrystalline cellulose particles.

3.6.2 Scanning electron microscopy (SEM)

SEM characterization was done on 1530 Leo or Hitachi S-800 scanning electron microscope. Samples are sputter coated with gold to prevent charging. Images are obtained under an accelerating voltage of 10 KV. Using SEM, information about filler dispersion, filler orientation, presence of voids and composite homogeneity can be obtained.

3.6.3 Thermal properties

The thermal properties of samples were studied with differential scanning calorimetry, DSC, using a TA Instrument model Q200. Samples were heated from 0°C to 200°C at a rate of 10°C/min. A constant nitrogen flow of 50ml/min was maintained throughout the test. As the samples were annealed before analyzing with DSC, the 1st heating run was used to calculate the transition temperatures and sample crystallinity. To calculate the crystallinity of PLA, the heat of fusion of 100% crystalline PLA was taken as 93 J/g [86, 87]. For composite samples, the value of heat of fusion was normalized by the mass fraction of PLA in the composites for calculating crystallinity of PLA in composite.

For isothermal DSC experiments, the samples were heated from 0°C to 200°C at a rate of 10°C/min and held at this temperature for 5 min. The sample was then cooled rapidly at -100°C/min to the isothermal crystallization temperature of 120°C. Samples were held at the isothermal crystallization temperature for enough time to allow for their complete crystallization. The samples were then heated to 200°C at 10°C/min to observe the melting behavior of the isothermally crystallized samples.

Thermal stability studies were done with thermogravimetric analyzer, TGA on a TA Instrument model Q5000. Samples were heated under nitrogen from room temperature to 450°C at 10°C/min.

3.6.4 Spectroscopy

Transmission-FTIR experiments were performed using a Bruker IFS 66v/S FTIR spectrometer equipped with a MCT-A detector. A total of 128 scans were collected for the absorbance spectra at a resolution of 4 cm^{-1}. Spectra were obtained on pellet samples prepared by mixing sample with dry KBr powder.

WAXD studies were performed using a PANanalytical's X'Pert PRO Alpha-1 at an accelerating voltage of 45kV and a current of 40mA using monochromatized Cu Kα radiation. The diffraction pattern was collected over the 2θ range from 10-50° with a step size of 0.03° and scan rate of 1°/min.

Molecular weight was measured by gel permeation chromatography (GPC) Waters 2690. Calibration was performed with polystyrene standard. Samples were prepared in a 1wt% solution of tetrahydrofuran (THF) and filtered through a 0.2-µm nylon filter, with an eventual injection volume of 150µL. The molecular weight was calculated based on polystyrene taking the Mark-Houwink constants $K_{PS} = 1.1 \times 10^{-3}$ dl/g and $a_{PS} = 0.72$. [88] The K_{PLA} and a_{PLA} values were taken as 5.49×10^{-4} dl/g and 0.639 respectively. [4]

3.6.5 Model Fitting

The model fitting was done using least square difference method. For Halpin Tsai solution was obtained subject to the condition that the aspect ratio ξ be either ≥ 5 or ≤ 10. This condition was imposed based on our analysis of SEM micrographs of the Avicel

(microcrystalline cellulose) particles. The parameters were varied till the error was minimized.

CHAPTER 4

PLA-MICROCRYSTALLINE CELLULOSE COMPOSITES

4.1 Introduction

In this chapter PLA based composites reinforced with commercially available microcrystalline cellulose are studied. The goal was to understand effects of processing techniques and the influence of addition of cellulose particles on the thermal and mechanical properties of the composite. The reason for starting with microcrystalline cellulose particles was its ready availability and ability to be used without further processing. Such a composite will not significantly increase sample price and is a good material for understanding the reinforcement mechanism and the influence of filler on composite properties.

PLA consists of lactic acid as the basic constitutional unit. The monomer lactic acid can be manufactured from a glucose containing renewable resource such as corn, potato etc. [4, 6, 10]. PLA is a biodegradable polymer which is also biocompatible. It possesses high stiffness and good mechanical strength but has low toughness. Addition of plasticizer is reported to increase the toughness but decrease modulus and strength [89-92]. PLA can be hydrolyzed and this reaction could be further catalyzed by the hydrolyzed monomer [12].

Microcrystalline cellulose derived from cotton, reported to have a high specific area compared to conventional cellulose fibers [39] is a good cost effective reinforcement for making completely degradable polymer composites. The high surface area of microcrystalline cellulose typically leads to better interaction between the matrix and reinforcement, resulting in enhancement of mechanical properties and in thermal stability

of the resulting composite. Numerous researchers [19, 39, 93-95] have observed improvement in mechanical properties, mainly modulus, using microcrystalline cellulose as reinforcement. For example, Petersson et al. [94] prepared composites of PLA and microcrystalline cellulose, which was swollen in water, by solution processing. They observed improvement in the storage modulus and yield strength but no improvement in the tensile modulus. Mathew et al. [39] reinforced PLA with three different cellulose based materials microcrystalline cellulose, wood flour and wood pulp. Addition of microcrystalline cellulose resulted in samples with improved tensile modulus and dynamic modulus but having lower tensile strength. They attribute the improvement in mechanical properties to result form nucleating ability of microcrystalline cellulose. Wu et al. [95] prepared polyurethane based elastomeric composites with microcrystalline cellulose. They obtained higher values for modulus, strength, and strain to failure. The increase in strength and strain to failure were obtained due to strong interfacial interaction between the matrix and microcrystalline cellulose reinforcement.

Samples of PLA with microcrystalline cellulose were prepared by melt mixing and solution processing. The influence of the processing technique employed and the effect of microcrystalline cellulose particle addition on the thermal, static and dynamic mechanical properties of composites were studied. The dynamic mechanical analysis gives information about filler-matrix interaction and the ability of the filler to reinforce the matrix over wide temperature range. Room temperature static properties like tensile modulus, strength are useful indicators of composite behavior under relatively larger strains. In tension test, the stresses are uniform across the sample cross-section and the results represent the average property through the thickness.

4.2 Results and discussion

The mechanical and thermal properties of PLA- microcrystalline cellulose (Avicel) composites are discussed. The effect of adding cellulose particles is studied through addition of unmodified Avicel particles to PLA. Influence of processing method employed on the composite properties is studied by comparing samples made by solution and melt processing techniques.

4.2.1 Morphology of cellulose (Avicel) particles

The morphology of unmodified Avicel particles as observed in SEM is shown in Figure 7.

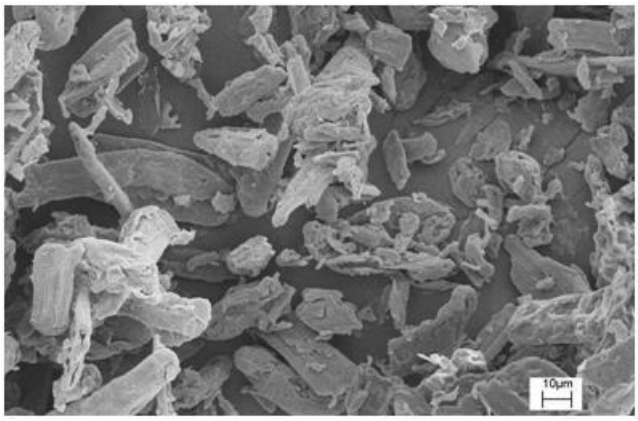

Figure 7. SEM micrographs of Avicel particles showing their size and broad size distribution.

The Avicel particles are observed to have a distribution of particle sizes with lengths from below 10µm up to 30µm. Bondeson [96] has reported that the Avicel particles are aggregates of individual crystallites. The SEM analysis shows that the particles have a wide size distribution and though the particles are neither rod shaped nor fiber like, most

particles have a non unity aspect ratio. The particles were also observed to have an irregular and rough surface.

4.2.2 Effect of processing method

4.2.3 Crystallinity

The molecular weight of melt processed samples was calculated to be around 120,000 g/mole while for solution processed samples it was calculated to be around 160,000 g/mole. The difference in molecular weight could have likely resulted in these samples having different crystallinity which lead to differences in mechanical properties. Figure 8 shows the influence of processing method on the resulting sample crystallinity. Since the samples were annealed prior to analysis, the first heating cycle in DSC was used for calculating the crystallinity. Tables 12 and 13 in Appendix A give the values for crystallinity of melt and solution processed samples.

For melt processed samples, addition of Avicel particles is observed to significantly increase sample crystallinity. In this case, Avicel particles are observed to act as nucleating agents and promote crystallization. This is consistent with the results by other authors [19, 97] who have observed that the microcrystalline cellulose acts as a nucleating agent and that the nucleation and growth occurs on the filler surface. A different behavior is observed in the solvent cast samples where adding Avicel particles did not lead to any significant increase in crystallinity. Petersson et al. [94] have also observed no increase in crystallinity for solvent cast composite films of PLA containing 5 wt% microcrystalline cellulose. In our case, the difference in crystallinity is likely due to the lower molecular weight of melt processed samples, which is due to thermal degradation even during the brief processing period and an often observed phenomenon

[72, 98, 99]. The higher molecular weight chains of solution processed samples require more time than smaller length chains of melt processed samples to rearrange to form crystallites. Celli et al. [12] have also observed higher crystallization values for lower molecular weight PLLA samples. Solution processing may have also resulted in the Avicel particles being less aligned and less well dispersed than in the case of melt processed samples [100] which could cause additional difference in crystallinity.

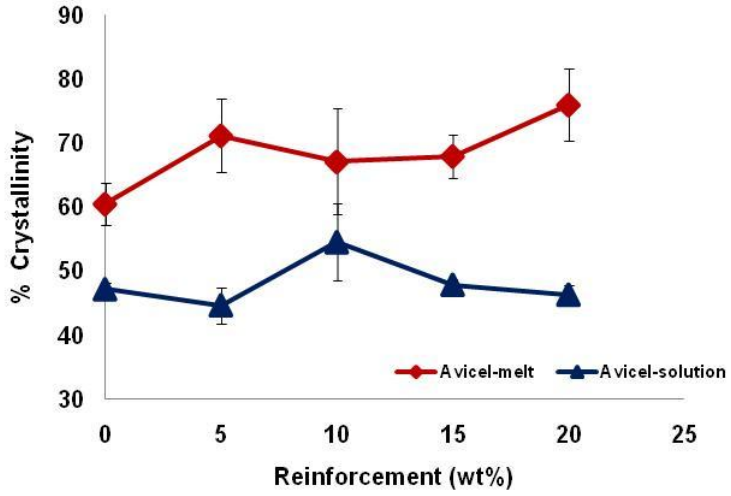

Figure 8. Effect of processing method on sample crystallinity.

To validate our hypothesis that melt processed samples having lower molecular weight can rearrange faster than solution processed samples increasing sample crystallinity, isothermal crystallization studies were done on melt and solution processed samples of neat PLA at 120°C. Samples were cooled rapidly (-100˚C min^{-1}) from melt to the crystallization temperature. The crystallization kinetics was analyzed using an Avrami type of fitting [101]:

$$\ln(1-x_t) = -(Kt)^n \quad (6)$$

where K = rate constant, n = Avrami exponent, and $x_t = X/X_{max}$, where X is the degree of crystallinity and X_{max} is the maximum crystallinity. The results are given in table 2.

Table 2. Avrami constants and half time of crystallization.

Sample	**K (min^{-1})**	**n**	**$t_{1/2}$ (min)**
PLA-melt	0.092 ± 0.001	2.42 ± 0.04	9.39 ± 0.5
PLA-solution	0.051 ± 0.007	1.88 ± 0.25	16.6 ± 1.8

The values of K and n were obtained by plotting a graph of $\ln(-\ln(1-X_t))$ against ln(time). The half time for crystallization was taken as time required for 50% transformation. The melt processed samples are observed to have a higher crystallizing rate and lower crystallization half time than solution processed samples.

4.2.4 Tensile properties

Figure 9 shows a comparison of tensile modulus and strength of PLA samples reinforced with unmodified Avicel made by melt and solution processing. For each property, "relative" indicates values normalized by those of the neat PLA.

For samples prepared using melt mixing, Figure 9(a), the modulus is observed to increase after the addition of 10 wt% of Avicel particles. For solution processed samples even 15 wt% Avicel addition does not lead to modulus improvement. Petersson et al. [102] observed no change in tensile modulus for solution cast samples of PLA reinforced with 5wt% microcrystalline cellulose that was swollen in water.

In our case, difference in the crystallinity between the melt and solution processed samples is likely to be responsible for this difference in modulus. Fambri et al. [103] have also observed increasing crystallinity to result in higher modulus for melt-spun PLA fibers. For 20 wt% particle loading the reinforcement is similar although the absolute values for the modulus are different which were 2.7 GPa for melt and 2.0 GPa for solution processed samples.

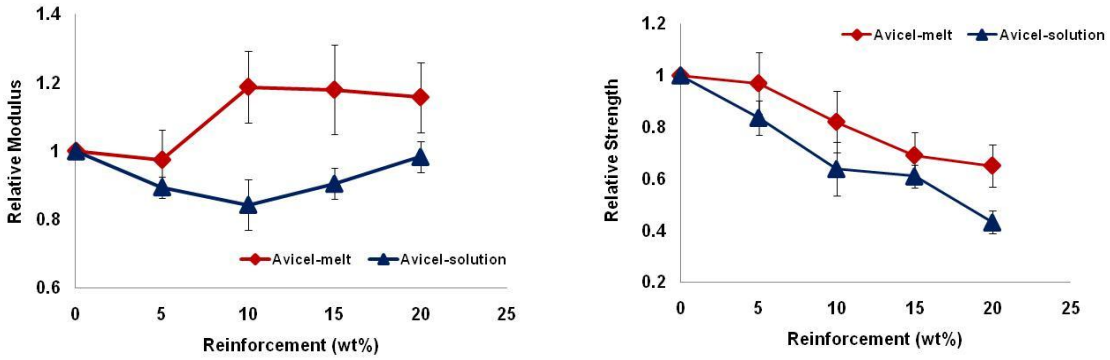

(a) (b)

Figure 9. Comparison of (a) modulus and (b) strength of PLA samples reinforced with unmodified Avicel and processed using melt and solution processing techniques.

With both melt and solution processing the sample strength is observed to decrease with increasing Avicel content as shown in Figure 9(b). The decrease in strength implies either a lack of or very low level of interaction between the matrix and the filler particles, which in turn results in a weak interface being formed affecting the transfer of stress from matrix to filler. The decrease in strength is thus the result of the filler not carrying the load to reinforce the matrix. [49]. Huda et al. have observed similar property variations for PLA reinforced with recycled cellulose fibers [104].

4.2.5 Model fitting to tensile modulus data for unmodified reinforcement

The modulus values obtained by tensile testing were compared to the values predicted by three different models, ROM, Halpin-Tsai and Paul model. The equations for the model are given in chapter 2. The models are fitted in a way that minimized the rms error between the experimental values and model values. Figure 10 shows the comparison of the three models when fitted to the experimental data. The model predicted modulus values are given in tables 3 and 4. These modulus values are similar to values of ~5 GPa obtained by Mathew et al. [39] using the ROM model.

Table 3. Fitted modulus values for unmodified Avicel particles of melt processed composite samples

Modulus of reinforcement - unmodified Avicel particles (MPa), melt processed			
	ROM model	Halpin-Tsai model	Paul model
Tensile Testing	4927	5165	5369
DMA (E' at 40˚C)	6966	7345	7792

Table 4. Fitted modulus values for unmodified Avicel particles of solution processed composite samples

Modulus of reinforcement - unmodified Avicel particles (MPa), solution processed			
	ROM model	Halpin-Tsai model	Paul model
Tensile Testing	N/A	N/A	N/A
DMA (E' at 40˚C)	3834	4049	3918

For solution processed samples characterized by tensile testing, fitted modulus values are not reported because it required assigning an unrealistic (negative) modulus value to the reinforcement. This is likely due to poor filler matrix interactions for PLA composite

samples reinforced with Avicel particles. A close fit between experimental and model values could be obtained for melt processed samples as shown in Figure 9(a). This is due to the higher crystallinity values of melt processed samples which resulted in these samples having greater modulus than solution processed samples.

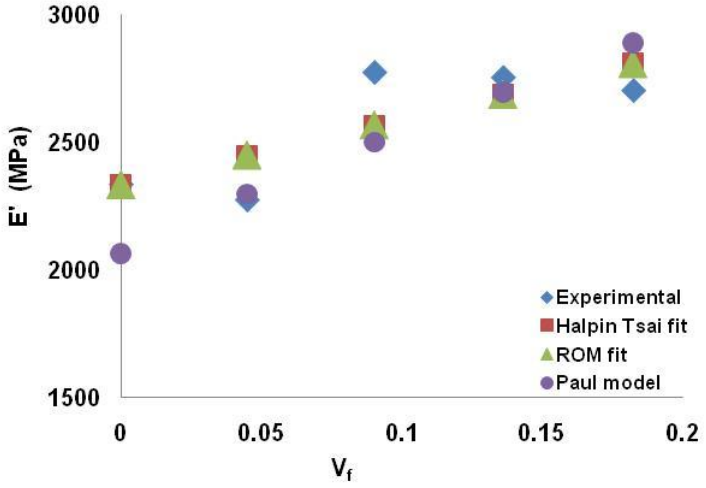

Figure 10. Model fitting of tensile modulus data for samples reinforced with unmodified Avicel particles and processed with melt processing technique.

The Halpin-Tsai model which takes into account the aspect ratio of reinforcement, the Paul model that assumes an irregular shape for the reinforcement and the ROM model which only considers volume fraction of constituents - predict similar values for modulus. This signifies that for composites samples reinforced with micron sized un-modified particles, the composite modulus was more dependent on the amount of filler added than on its shape or aspect ratio which was no greater than 10.

4.2.6 Dynamic mechanical properties of melt and solution processed PLA samples reinforced with unmodified microcrystalline cellulose particles

We now consider the influence of processing method used on the dynamic mechanical properties of the unmodified Avicel reinforced PLA composite samples. The relative storage modulus is plotted as a function of temperature (Figure 11). Data were obtained at a frequency of 2 Hz, heating from 35°C to 130°C at 2°C/min and 0.05% strain. No significant difference in Tg values was observed between neat and composite samples: all Tg values were between ± 2˚C of 82˚C. For melt processed samples (Figure 11a), below Tg, maximum increase in storage modulus is observed with 10 wt% addition of Avicel particles. Above the Tg, increasing the amount of Avicel particles is observed to increase the storage modulus of the composite samples with 100% increase in storage modulus obtained for samples containing 20 wt% Avicel particles.

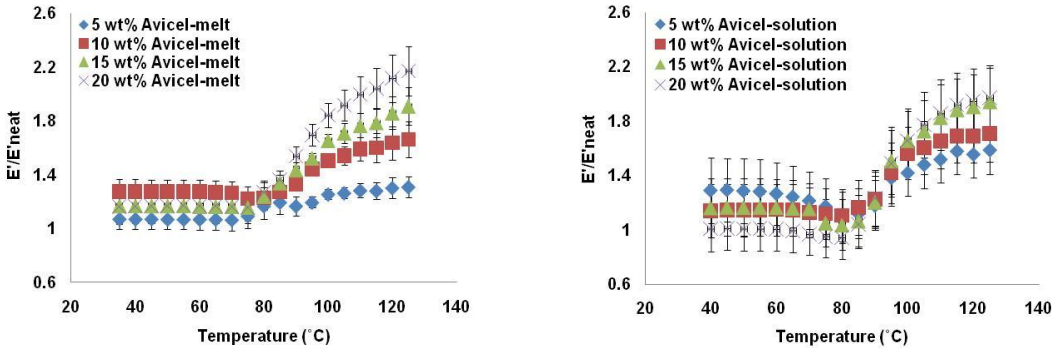

(a) (b)

Figure 11. Normalized storage modulus of unmodified Avicel reinforced PLA composites prepared by (a) melt and (b) solution processing.

For solution processed composites samples reinforced with unmodified Avicel particles Figure 11(b), above Tg, addition of 20 wt% filler particles does not result in any significant increase in composite modulus when compared to samples made with 15 wt% Avicel particles. The level of reinforcement obtained with the highest filler content of unmodified Avicel particles is similar for both melt and solution processed samples. The 5 wt% solution processed samples gave the highest while 20 wt% solution processed samples gave the lowest reinforcement below Tg. This may be the result of better dispersion at lower (5 wt%) filler loadings. Since it is the effective fraction of the high modulus filler that influences room temperature modulus [105], poor dispersion may lead to an increase in modulus below expected value based on the nominal volume fraction of reinforcement. The improvement in reinforcement above Tg for melt and solution processed samples can be attributed to the stiffness of the filler particles and the increase in the potential for chain mobility above polymer Tg.

In Figures 12 relative loss modulus of composite samples are plotted as function of temperature. The y-axis is normalized by taking the loss modulus peak value, Tg as reference and the x-axis is normalized by taking the loss modulus peak temperature as reference.

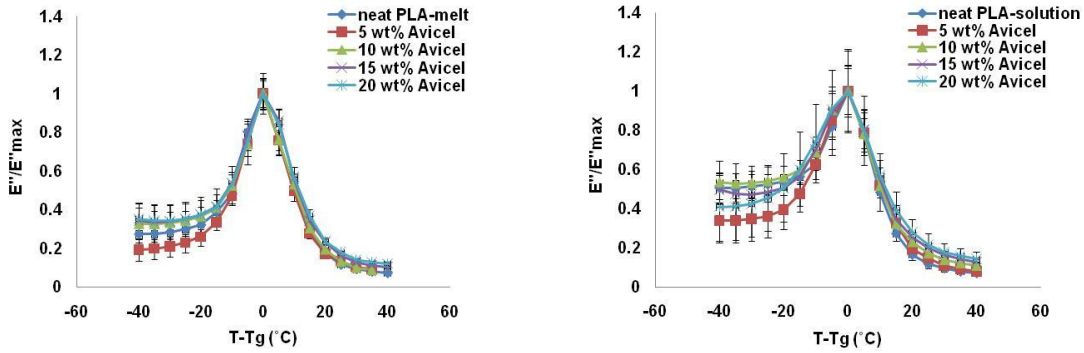

(a) (b)

Figure 12. Normalized loss modulus data for Avicel particles reinforced PLA samples prepared by (a) melt mixing and (b) solution processing.

The most significant difference of loss modulus behavior is observed below Tg. In the melt processed samples, Figure 12(a), below Tg, the relative loss modulus for composite samples is higher than that for neat PLA. For solution processed samples, Figure 12(b), the relative loss modulus for composite samples is lower than that for neat PLA. This difference in the loss modulus behavior is due to the melt processed samples having higher crystallinity. Above Tg in all cases, the relative loss modulus of composite samples is only slightly higher as a result of increased friction between matrix chains and the filler particles affecting matrix chain relaxation.

4.2.7 Model fitting to storage modulus data for unmodified reinforcement

For solution processed samples, the storage modulus data at 40˚C were fitted to existing models described earlier. At 40˚C (below Tg), the experimental E' values are higher than model predicted values. At highest filler loading the model predicted modulus are higher

than experimentally obtained values. This suggests deterioration in filler dispersion at the highest filler loading. The observed difference may also be on account of the difference between model assumptions: equal strains in matrix and filler, unidirectional orientation and experimental conditions: random filler orientation etc. The values are given in table 4.

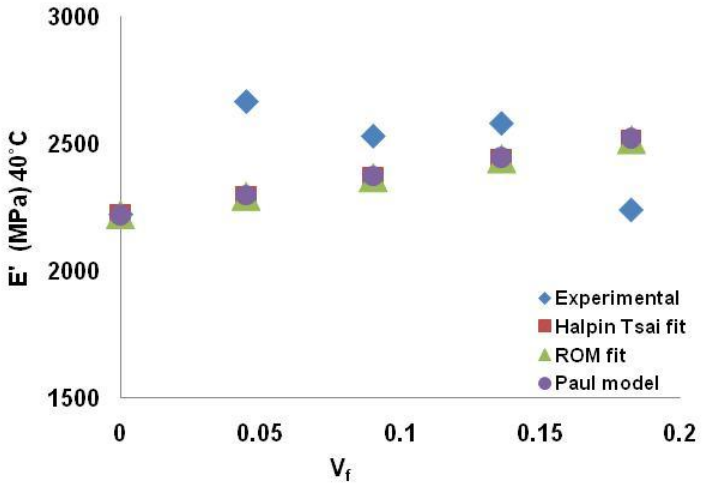

Figure 13. Model fitting to storage modulus data at 40˚C.

4.3 Summary

Composites of PLA with microcrystalline cellulose as reinforcement were prepared using both melt and solution processing techniques. The processing method employed influenced the molecular weight of samples which had a direct effect on the polymer's ability to crystallize. Samples having higher crystallinity were stiffer and had lower strength and toughness. Addition of unmodified microcrystalline cellulose only increased the modulus. The strength and strain at break values decreased with increasing particle

content. Below Tg, sample crystallinity was observed to influence composites loss modulus behavior. Samples having higher crystallinity had lower loss modulus.

CHAPTER 5

PLA-SURFACE MODIFIED MICROCRYSTALLINE CELLULOSE COMPOSITES

5.1 Introduction

A drawback with microcrystalline cellulose is its tendency to agglomerate by forming inter and intramolecular hydrogen bonds. Sanchez-Garcia et al. [106] have observed agglomeration of micro-cellulose fibers in PLA above 5 wt% loading. To overcome this drawback several researchers have tried surface modification of these microcrystalline cellulose particles. Habibi et al. [23] have used TEMPO mediated oxidation to convert surface hydroxyl groups to charged carboxyl group. Dorgan et al. [64] have modified cellulose surface using initiators that would polymerize lactide onto the cellulose surface during processing by extrusion. Braun et al. [107] have reactively compatibilized cellulose microfibers with lactide in presence of preformed high molecular weight PLA using surface hydroxyl groups of cellulose as initiator and observed improved fiber dispersion and interface adhesion which increased the shear modulus of the composite samples. These works on chain grafting have used a catalyst, co-catalyst or a transesterification agent in order to achieve high molecular weight of the grafted chains. Complete catalyst removal is necessary as presence of residual catalyst has been shown to accelerate the degradation of PLA [98]. Recently a one step hydrolysis and esterification procedure for isolation and surface modification of cellulose whiskers has been reported by Braun and Dorgan [108] using a mixed acid system of hydrochloric acid and an organic acid. Although this method can isolate the whiskers or modify the cellulose functionality, a subsequent step would be necessary for grafting longer chains.

We have carried out a more straightforward surface modification of microcrystalline cellulose particles by grafting the cellulose particles with polylactic acid via esterification reaction between hydroxyl group of cellulose and carboxyl of lactic acid without using any external catalyst. Simple washing steps were sufficient to remove any side reaction products or impurities. Lactic acid grafting of cellulose particles enhanced filler-matrix interactions and improved the dispersion of cellulose particles in PLA.

5.2 Effect of surface modification of Avicel particles

Lactic acid was surface grafted onto Avicel particles to help prevent agglomeration of Avicel particles and improve the dispersion of Avicel particles in PLA. The effect of grafting lactic acid on Avicel particles is now considered.

5.2.1 Surface grafting

L-lactic acid is grafted onto the surface of Avicel via condensation reaction of L-lactic acid and hydroxyl group on cellulose. No catalyst is employed for the grafting reaction. The hydroxyl groups on the surface of Avicel particles act as initiator for polylactic acid resulting in a 'grafting from' product. Some free oligomers or polymer may also be formed which may subsequently react with hydroxyl groups on Avicel giving a 'grafting to' reaction. These three reactions may be occurring simultaneously in the reaction mixture but purification of the product allowed us to isolate the grafted particles from the side products.

The grafting reaction is characterized using IR spectroscopy. A representative FTIR spectrum of Avicel particles grafted with lactic acid called LA-g-Avicel is shown (Figure

14). The FTIR spectrum of an unmodified Avicel sample is included for comparison. Spectra are shifted vertically for clarity.

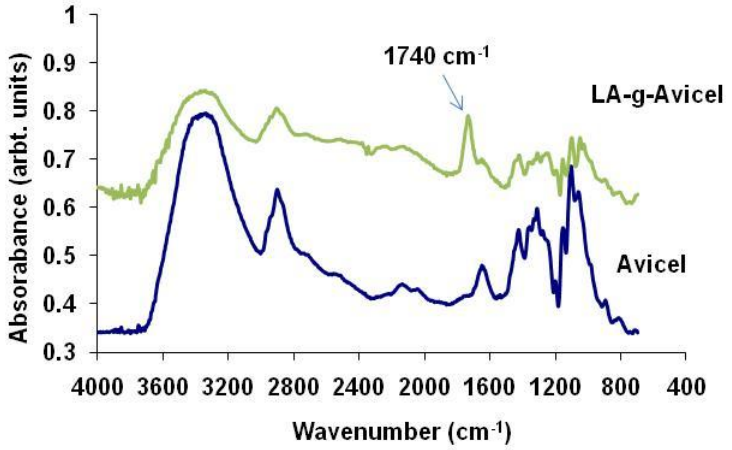

Figure 14. FTIR spectra of surface modified and unmodified microcrystalline cellulose particles.

The main difference between the two spectra is a peak observed for LA-g-Avicel sample at ~1740 cm^{-1} which is attributed to the carbonyl group (C = O) of lactic acid or PLA. The presence of this carbonyl peak in the grafted sample is taken as confirmation of the grafting of L-lactic acid (monomeric or oligomeric) on the surface of Avicel particles. All other peaks appearing in the spectra of unmodified sample are also seen in the grafted sample with the peak at 1630 cm^{-1} appearing as a shoulder in FTIR spectra of LA-g-Avicel.

Further, we verified whether heating cellulose under conditions similar to those employed during grafting could give rise to carbonyl peak in the FTIR spectra. Avicel particles were heated in toluene for 50 hrs in absence of monomer. After the product was

recovered by centrifugation, it was subjected to same washing and drying steps. Finally, an FTIR spectra was collected on the dried sample. The carbonyl peak at 1740 cm^{-1} was not seen in Avicel sample or in sample of Avicel subjected to identical reaction conditions as those used during grafting reaction. We also verified whether the lactic acid is simply physically adsorbed on the Avicel. For this, 3 g of PLA pellets were dissolved in toluene by heating and stirring. The solution was allowed to cool down to room temperature and then a gram of Avicel particles were added to the mixture. The mixture was stirred for 48 hours at room temperature. Sample was recovered by centrifugation. FTIR done after subjecting the sample to three washing and filtering cycles in chloroform did not show formation of carbonyl peak or any additional peaks. These observations support the assertion that the C=O peak at 1740 cm^{-1} appearing in the grafted samples is the carbonyl peak of lactic acid grafted onto Avicel particles.

5.2.2 Grafting efficiency

The efficiency of grafting with "grafting from" and "grafting to" approach (discussed later) was estimated with DSC following procedure reported by Labet et al. [109] who used it to determine the weight fractions of grafted polymers on starch nanocrystals. The weight fraction of Avicel in the surface modified sample was obtained by dividing the heat of melting of surface modified particles by the corresponding heat of melting of unmodified Avicel particles. Table 5 gives the values of melting enthalpies and weight fractions of cellulose and lactic acid in lactic acid grafted samples. Higher grafting levels achieved for LA-g-Avicel sample is because of relatively higher number of cellulose hydroxyl groups being accessible for reaction with the "grafting from' approach.

Table 5. Heat of melting (ΔH_m) and weight fractions of cellulose and lactic acid grafts in lactic acid and polylactic acid grafted Avicel particles

Sample	Degradation temperature from TGA (˚C)	ΔH_m (J/g)	% lactic acid (wt%)
Unmodified Avicel	340	422	0
LA-g-Avicel	360	357	14.2 ± 0.06
PLA-g-Avicel	360	371	12 ± 0.07

The corresponding dsc thermograms for unmodified and surface modified cellulose samples are shown in Figure 15.

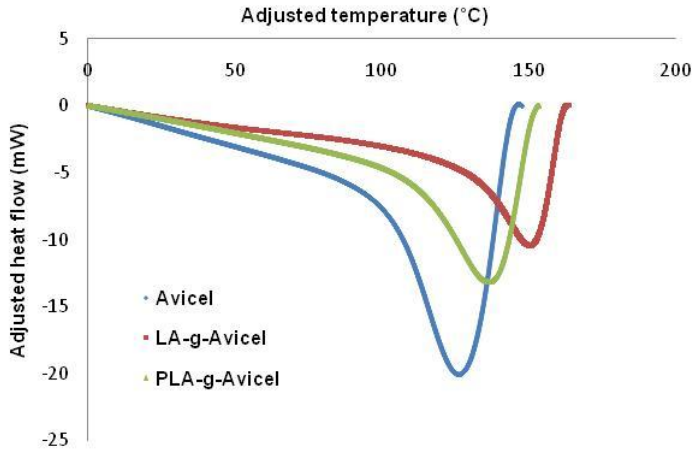

Figure 15. DSC thermogram of Avicel particles, lactic acid grafted Avicel particles and polylactic acid grafted Avicel particles.

5.2.3 Wide angle X-ray diffraction

WAXD studies were carried out to analyze the effect of grafting on the crystal structure of the Avicel particles and the corresponding plot is given in Figure 16. The data are normalized by value of intensity at 2 theta = 50. Sharp peaks are observed at 2θ = 22.5 and 34.5. In addition a shoulder is observed around the region 2θ= 14 to 17. These peaks correspond to the cellulose I structure [39]. No relative shift in peak position observed on surface modification of the Avicel particles confirmed that there was no change in crystal structure of Avicel particles.

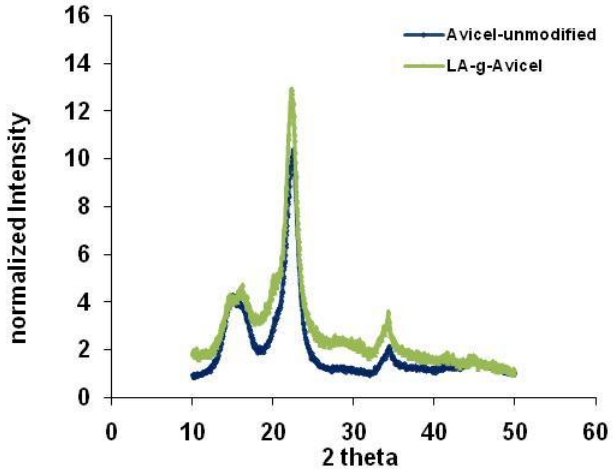

Figure 16. WAXD pattern of unmodified Avicel particles and lactic acid grafted Avicel powder.

5.2.4 Thermal stability of unmodified and surface modified particles

The effect of grafting on the thermal stability of the Avicel particles was studied using TGA and is shown in Figure 17. For comparison of thermal stability, the temperature of maximum weight loss rate was taken as reference. TGA was performed on powder samples of Avicel and surface modified Avicel particles. Surface grafting was observed to improve the stability of Avicel particles.

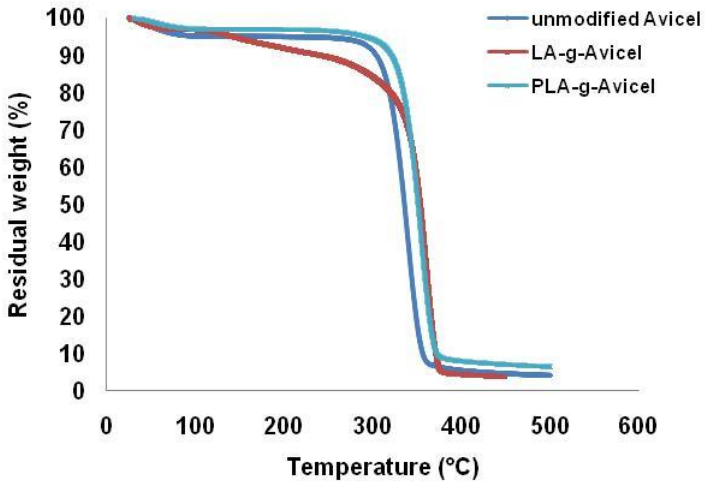

Figure 17. Effect of surface modification on stability of Avicel particles.

5.3 Morphology of PLA-cellulose composites

Composite containing up to 15 wt% of lactic acid grafted Avicel particles were prepared. Higher filler loadings were not prepared due to limited resources for grafting lactic acid. Figures 18-21 show SEM micrograph of cross sections of composite samples containing 5 and 15 wt% of unmodified and surface modified Avicel particles. There is some indication that the surface modified particles are better distributed than the unmodified

particles. However, for these relatively large size particles, grafting of lactic acid had a more pronounced effect on the interfacial adhesion than particle dispersion.

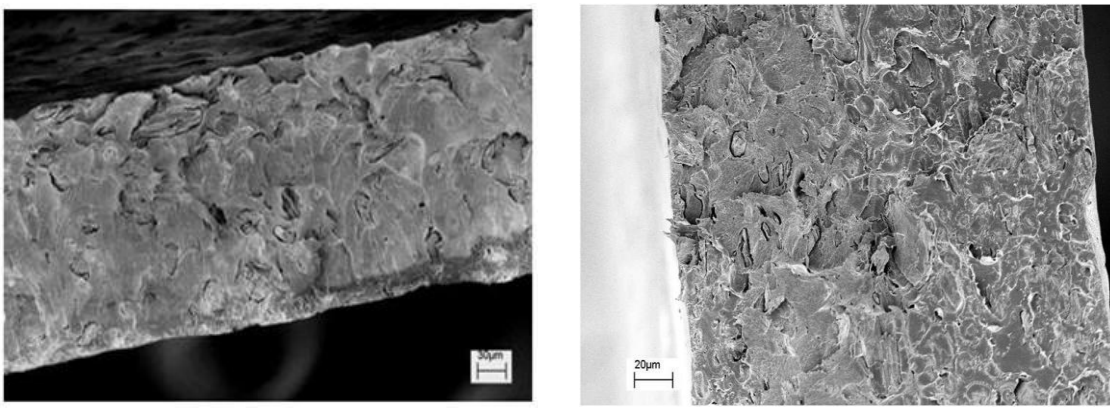

(a) (b)

Figure 18. SEM images of sample cross sections of composite samples (a) 5 wt% unmodified (b) 5 wt% lactic acid grafted Avicel particles.

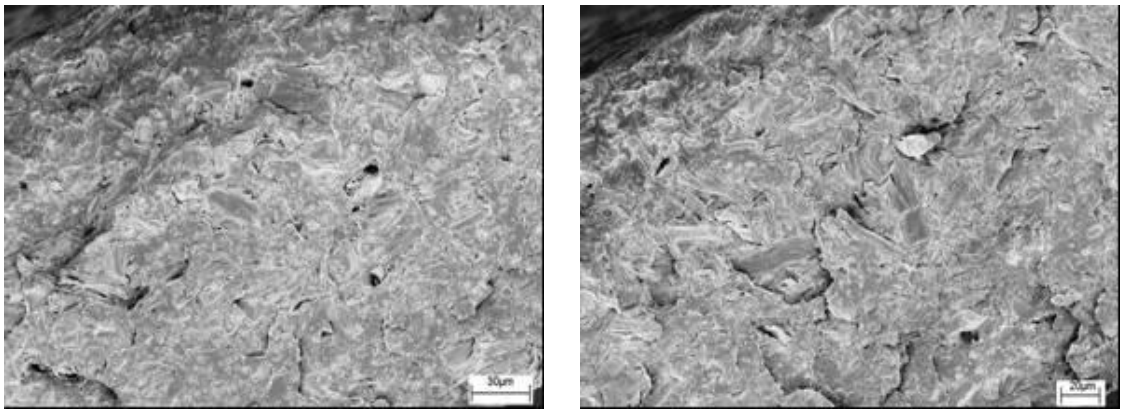

(a) (b)

Figure 19. SEM images of sample cross sections of composite samples (a) 15 wt% unmodified (b) 15 wt% lactic acid grafted Avicel particles.

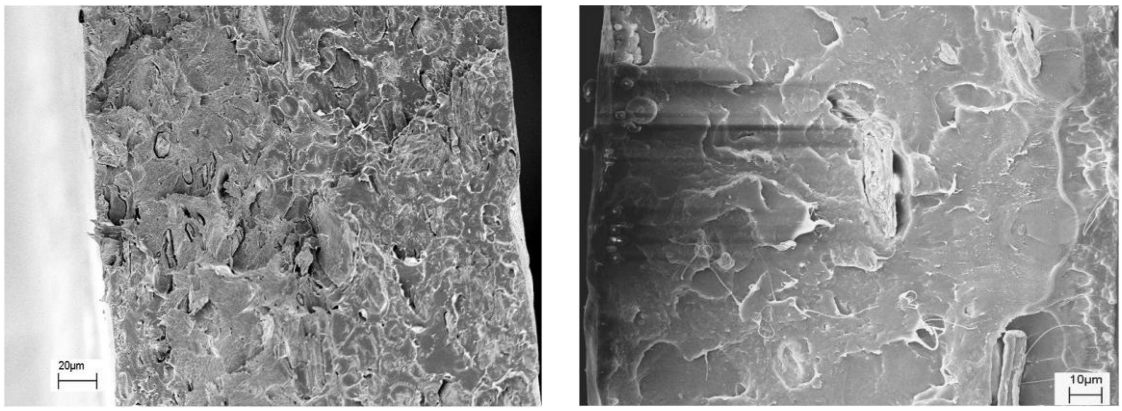

(a) (b)

Figure 20. SEM images of sample cross sections of composite samples (a) 5 wt% lactic acid grafted Avicel particles (b) 5 wt% polylactic acid grafted Avicel particles.

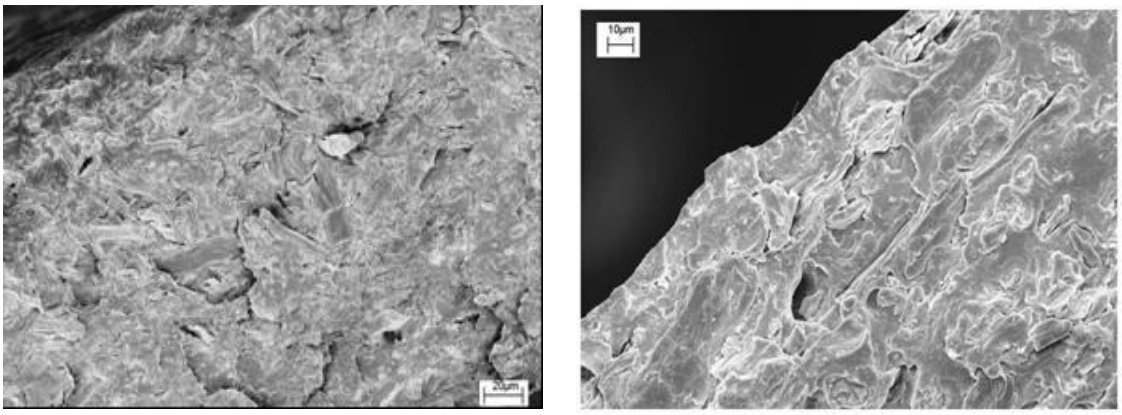

(a) (b)

Figure 21. SEM images of sample cross sections of composite samples (a) 15 wt% lactic acid grafted Avicel particles (b) 15 wt% polylactic acid grafted Avicel particles.

5.4 Tensile properties of lactic acid grafted composites

Figures 22-24 show the tensile modulus, strength and strain at break comparison for unmodified and lactic acid grafted Avicel composites made by solution processing. For each property, "relative" indicates values normalized by those of the neat PLA.

A significant difference is observed between the relative modulus of unmodified and lactic acid grafted samples made by solution processing. As observed earlier the composite samples containing unmodified particles do not show any improvement in modulus up to 15 wt% filler loading. Since the sample crystallinity of all solution processed samples is nearly the same, the improvement in modulus only for samples reinforced with lactic acid grafted particles suggests that the increase is related to the interaction between the filler particles and the PLA matrix. Hiljanen-Vainio et al. [110] also observed the stiffness of composite to depend on the interfacial bonding.

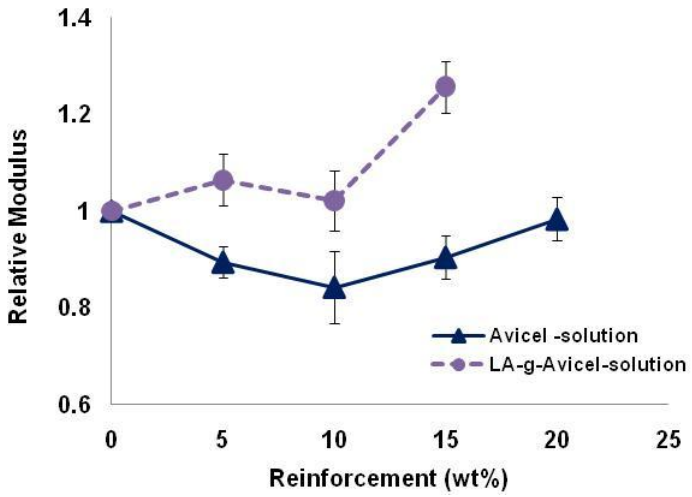

Figure 22. Relative modulus of solution processed PLA samples reinforced with unmodified and lactic acid grafted Avicel particles.

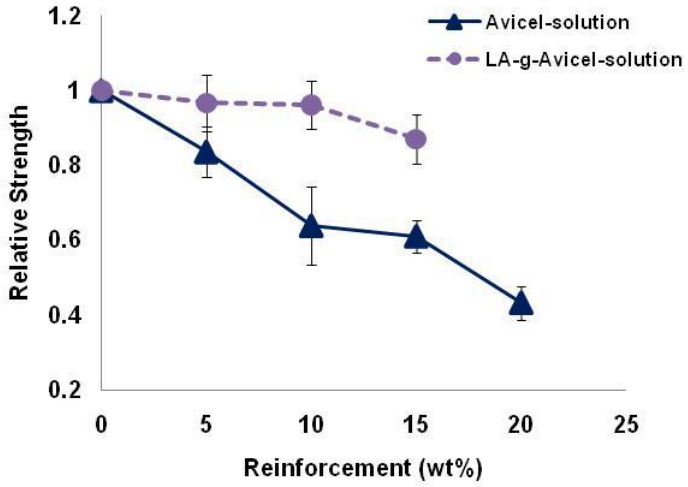

Figure 23. Relative strength of solution processed PLA samples reinforced with unmodified and lactic acid grafted Avicel particles.

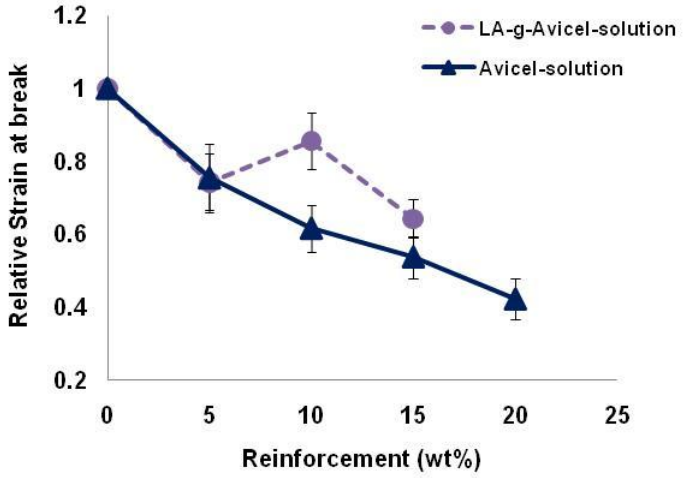

Figure 24. Relative values of strain at break of solution processed PLA samples reinforced with unmodified and lactic acid grafted Avicel particles.

The tensile strength, Figure 23, is observed to remain more or less constant with increasing particle loading. We believe this to be the result better dispersion as well as improved filler-matrix interaction leading to more efficient stress transfer between matrix

and the Avicel particles. An efficient load transfer from the PLA matrix to the Avicel particles would result in a more uniform stress distribution by minimizing or reducing stress concentration centers [111]. The strain at break value also showed a slight improvement for higher loadings of lactic-acid grafted Avicel particles.

The results of tensile testing indicate that grafting lactic acid on Avicel particles improves the interfacial adhesion between Avicel particles and the PLA matrix with the resultant increase in modulus, strength and strain at break of the composite samples.

5.4.1 Model fitting to tensile modulus data for unmodified and modified cellulose reinforcement

For solution processed samples, the tensile modulus data are fitted to existing models as shown in Figure 25 below. The tensile modulus values of composite samples reinforced with LA-g-Avicel particles show good fit to the model values. This is on account of improvement in the PLA-cellulose interactions because of surface modification of cellulose particles by grafting lactic acid. The modulus of the reinforcement obtained by fitting models to experimental data is given in table 6 below. For all models, the predicted modulus of modified Avicel particles is higher than unmodified Avicel particles. The use of surface modified Avicel particles results in constraining of PLA matrix chains because of interfacial interactions. Oksman et al. [38] observed an increase in modulus from 2.9 GPa to 3.9 GPa for PLA reinforced with 5 wt% microcrystalline cellulose and 10 wt% maleated PLA. This reinforcement obtained is similar to modulus increase observed in our case for PLA reinforced with 15 wt% of LA-g-Avicel particles where the modulus increased from ~ 2 GPa to 2.9 GPa.

Table 6. Fitted modulus values for lactic acid grafted Avicel particles of solution processed composite samples

Modulus of reinforcement - lactic acid grafted Avicel particles (MPa)			
	ROM model	Halpin-Tsai model	Paul model
Tensile Testing	7473	8918	11416
DMA (E' at 40˚C)	9646	12427	14289

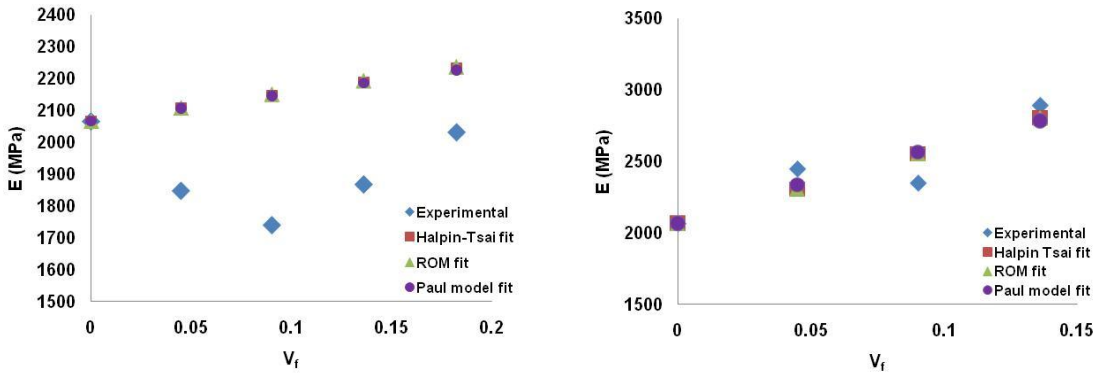

(a) (b)

Figure 25. Comparison of model fitted tensile modulus values of PLA composites reinforced with (a) unmodified and (b) lactic acid grafted Avicel particles.

5.5 Dynamic mechanical properties of lactic acid grafted composites

The effect of grafting lactic acid on the dynamic mechanical properties of composite sample is now considered. First we consider the effect on storage modulus.

A comparison of Figures 26 (a) and 26 (b) reveals that samples reinforced with both un-grafted and grafted Avicel particles show similar storage modulus behavior. This implies that for similar cellulose addition the modified cellulose particles provide greater

reinforcement as will be discussed in chapter 6. With 15 wt% addition of lactic acid grafted Avicel particles, the storage modulus is observed to be higher than that of neat polymer over the entire temperature range considered. The relative increase in storage modulus values below Tg for LA-g-Avicel reinforcement, is likely due to improved compatibility between the lactic acid grafted Avicel particles and the PLA matrix.

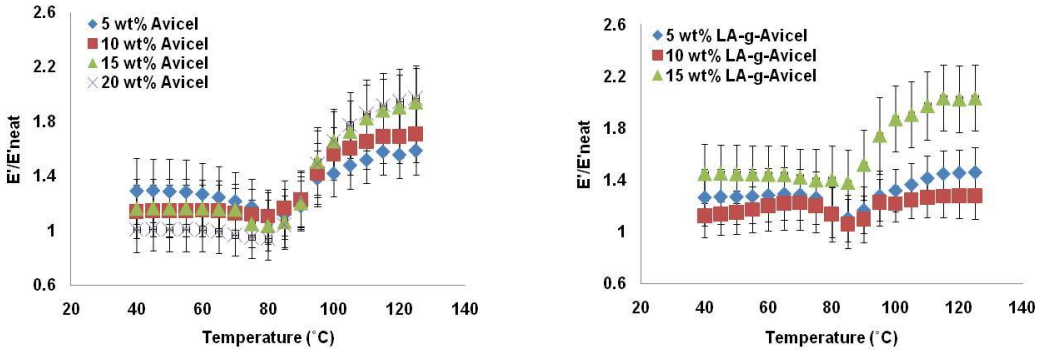

(a) (b)

Figure 26. Normalized storage modulus of solution processed composite samples of PLA reinforced with (a) unmodified and (b) lactic acid grafted Avicel particles.

The effect of using lactic acid grafted Avicel particles on composite loss modulus is shown in Figure 27.

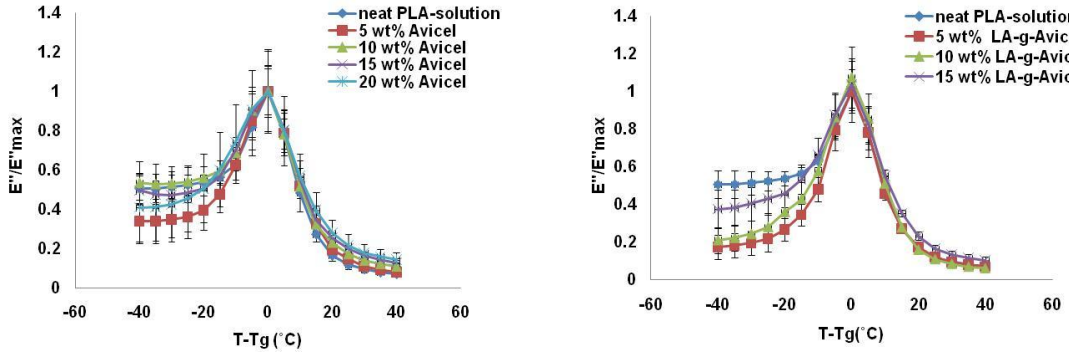

(a) (b)

Figure 27. Normalized loss modulus of solution processed composite samples of PLA reinforced with (a) unmodified and (b) lactic acid grafted Avicel particles.

The loss modulus behavior of lactic acid grafted Avicel samples is similar to samples of unmodified Avicel. Below matrix Tg, loss modulus values for lactic acid grafted samples are lower than samples containing unmodified particles. This implies that PLA samples reinforced with lactic acid grafted Avicel particles are more elastic [112]. For composites reinforced with lactic acid grafted Avicel particles, the grafted PLA chains can have a much stronger interaction with the matrix polymer. Consequently, the mobility of matrix chains in samples with unmodified particles would be higher. Observing the loss modulus behavior both below and above Tg, it is apparent that small scale segmental motion are affected more than long range chain motion. The small length of the grafted chains influences the local interactions but not long range interactions.

5.5.1 Model fitting to storage modulus data for composite samples reinforcement with surface modified cellulose particles - grafted with lactic acid

For LA-g-Avicel reinforced composite samples, the storage modulus data at 40˚C were fitted to existing models described earlier. At temperatures below Tg, 40˚C, the experimental E' values closely match the model predicted values. A factor of two or greater increase in the predicted modulus value is observed using lactic acid grafted Avicel particles for reinforcement as reported in table 6. Storage modulus data above Tg is not reported as the models do not account for the influence of temperature and predict unreasonably high modulus values of reinforcements. Above the composite Tg, due to higher matrix chain mobility the interfacial interactions are not as effective in restraining the matrix chains.

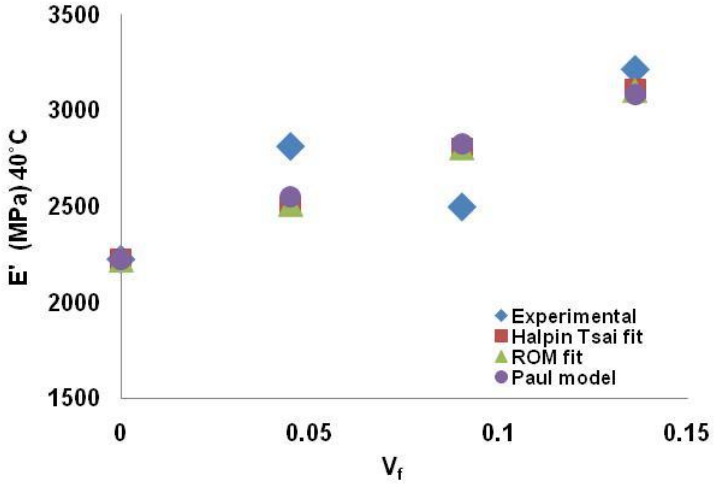

Figure 28. Comparison of model fitted storage modulus values of PLA samples reinforced with lactic acid grafted Avicel at 40˚C

5.6 Effect of surface modification of Avicel particles by grafting polylactic acid, PLA chains

Significant difference in the mechanical properties was observed between the composites reinforced with unmodified and lactic acid grafted microcrystalline cellulose particles. The improvements in properties were observed with modified cellulose particles even when size of cellulose particles was large compared to the length of grafted chains and in absence of entanglements between grafted lactic acid chains and matrix PLA chains. Entanglement formation which could result in higher reinforcement was achieved by grafting relatively larger polylactic acid, PLA chains on cellulose particles. Surface modification of cellulose particles with PLA chains was done using the same procedure as used for grafting lactic acid and is reported in chapter 3. Compared to the expensive lactic acid monomer, use of the polymer PLA for surface grafting was more economical option. The properties of composite samples reinforced with modified cellulose particles, obtained by surface grafting PLA chains are now reported.

5.7 Tensile properties of polylactic acid grafted composites

The tensile properties of PLA samples reinforced with PLA grafted cellulose particles are shown in Figures 29-31. Surface modification by grafting PLA chains resulted in composite samples with similar values for modulus as those obtained by surface modification with lactic acid - Figure 29. The relative strength of composites reinforced with PLA grafted cellulose particles was higher than corresponding samples reinforced with lactic acid grafted samples. PLA-g-Avicel reinforced samples show higher values for strain break up to 10 wt% filler loading. The improvement in strength and strain at break is believed to be the result of entanglements between matrix PLA chains and

grafted PLA chains. This is based on our GPC analysis of un-grafted PLA remaining after grafting reaction which showed no significant reduction in molecular weight compared to PLA pellets which had molecular weight much greater than entanglement molecular weight of PLA.

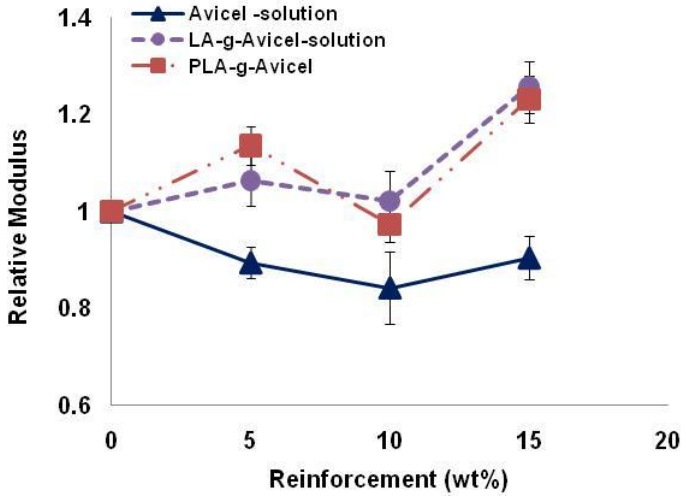

Figure 29. Relative modulus of solution processed PLA samples reinforced with lactic acid grafted and polylactic acid grafted cellulose particles.

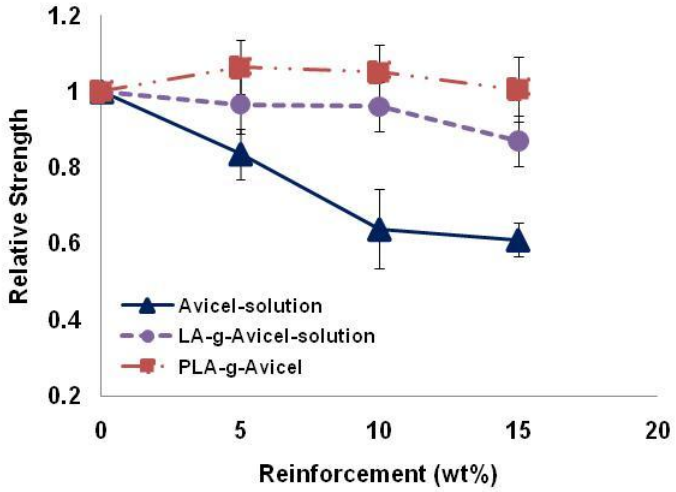

Figure 30. Relative strength of solution processed PLA samples reinforced with lactic acid grafted and polylactic acid grafted cellulose particles.

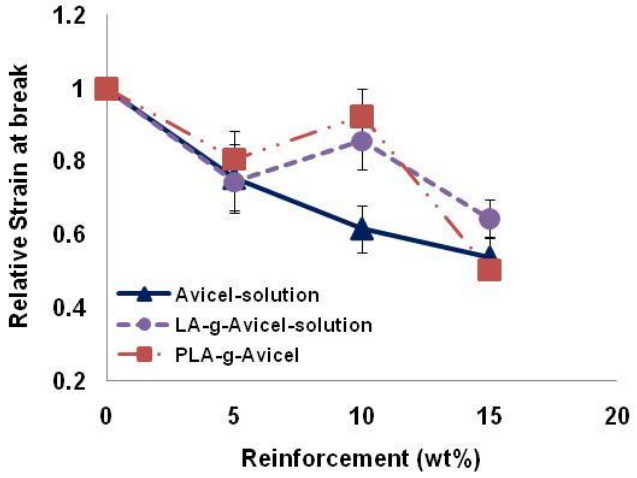

Figure 31. Relative strain at break of solution processed PLA samples reinforced with lactic acid grafted and polylactic acid grafted cellulose particles.

5.7.1 Model fitting to tensile modulus data for composite samples reinforced with surface modified cellulose particles grafted with polylactic acid

The tensile modulus data was fitted to the same three models as reported before. A comparison of data from tables 6 and 7 revealed that reinforcement obtained using PLA-g-Avicel particles was similar to that obtained with LA-g-Avicel particles. The model fitting data for PLA-g-Avicel particle reinforced samples is shown in Figure 32. The figure for LA-g-Avicel particles reinforced samples is shown again for comparison.

Table 7. Fitted modulus values for polylactic acid grafted Avicel particles of solution processed composite samples

Modulus of reinforcement - polylactic acid grafted Avicel particles (MPa)			
	ROM model	Halpin-Tsai model	Paul model
Tensile Testing	7760	9407	10491
DMA (E' at 40˚C)	8741	10790	12085

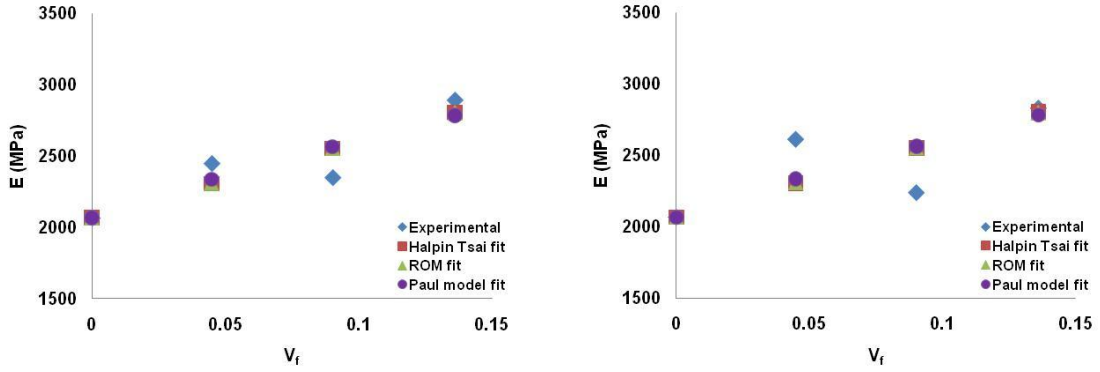

Figure 32. Comparison of model fitted tensile modulus values of PLA composites reinforced with (a) lactic acid grafted Avicel particles (b) polylactic acid grafted Avicel particles.

Figure 32 revealed a good model fit with experimental data even at the highest filler loading level. An assumption made with all models is good interfacial interaction between phases, surface modification improved interfacial interactions resulting in a better fit between model and experimental values.

5.8 Dynamic mechanical properties of polylactic acid grafted composites

The dynamic mechanical properties of PLA-g-Avicel reinforced samples are shown in Figures 33 and 34. Comparison of Figure 33 (a) and 33 (b) shows surface modification of cellulose particles with lactic acid or polylactic acid results in similar values of relative storage modulus both of which are higher than values observed with samples reinforced with unmodified cellulose particles. Thus surface modification by grafting longer PLA chains did not result in additional restraining of the matrix chains compared with lactic acid grafting.

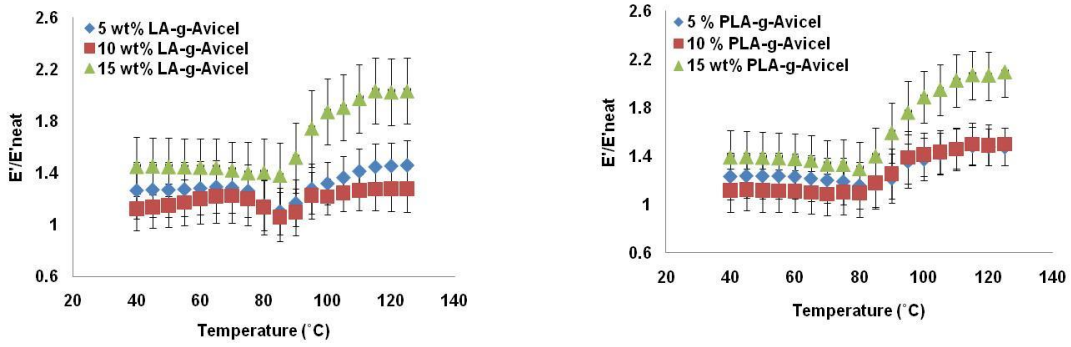

(a) (b)

Figure 33. Normalized storage modulus of solution processed samples of PLA reinforced with (a) lactic acid grafted Avicel particles and (b) polylactic acid grafted Avicel particles.

A comparison of normalized loss modulus for samples reinforced with lactic acid grafted Avicel particles and polylactic acid grafted Avicel particles is shown in Figure 34. Reinforcing PLA with surface modified cellulose particles by grafting monomeric lactic acid chains or polylactic acid chains influenced the short chain motion below Tg but had no significant effect on large scale chain motion above the composite Tg. Thus both these reinforcements resulted in similar level of interfacial interactions between PLA matrix and cellulose particles and consequently lead to these samples having similar dynamic mechanical properties.

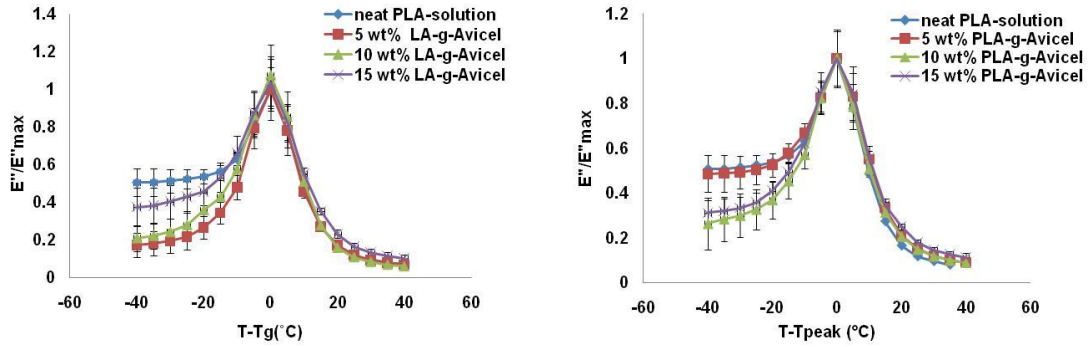

(a) (b)

Figure 34. Normalized loss modulus data of solution processed samples of PLA reinforced with (a) lactic acid grafted Avicel particles and (b) polylactic acid grafted Avicel particles.

5.8.1 Model fitting to storage modulus data for composite samples reinforcement with surface modified cellulose particles - grafted with polylactic acid

The storage modulus data at 40˚C were fitted to existing models described earlier. No relative increase in the storage modulus values over that obtained using particles modified with lactic acid was observed. All these results show no distinction, in terms of any specific property improvement, of modifying cellulose particle surface by grafting polylactic acid compared to lactic acid. However grafting polylactic acid is economical due to the comparatively lower cost of polymer, PLA.

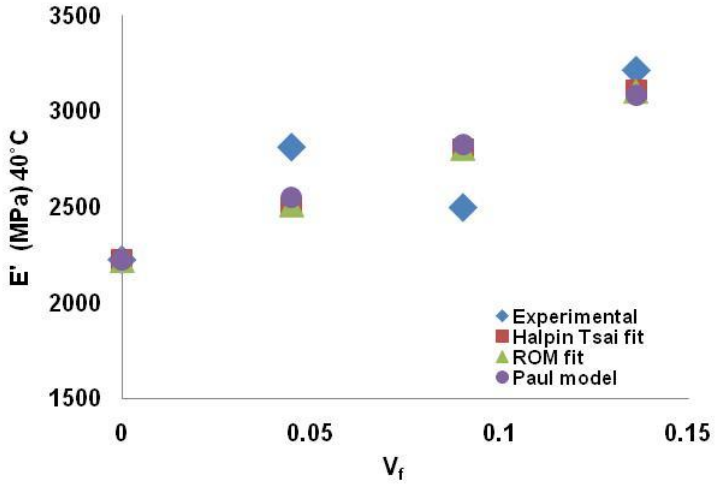

Figure 35. Comparison of model fitted storage modulus values of PLA samples reinforced polylactic acid grafted Avicel particles at 40˚C.

5.9 Effect of grafting on mechanical loss

The magnitude of loss modulus peak (E''_{max}) gives information about the mechanical loss in the interface regions. In Figure 36, the E''_{max} values are plotted as a function of filler content.

The E''_{max} value for lactic acid grafted Avicel reinforced samples increased with increasing filler loading of grafted Avicel particles. This suggests that the loss in the interface region increased with increasing filler content for the lactic acid grafted composite samples [113]. For particles modified by grafting high molecular weight PLA chains the E''_{max} values lie between those for unmodified and lactic acid grafted Avicel particles. This indicated more effective surface modification was achieved using the "grafting from" approach. This observed increase in E''_{max} is on account of the composite samples ability to dissipate energy into heat with increasing filler content [114]. The

higher E''_{max} value can be explained as the result of improved filler-matrix interaction resulting in better filler dispersion of the surface modified particles in the PLA matrix. For samples reinforced with unmodified Avicel, the highest E''_{max} value were obtained with the lowest that is 5 wt% loading. This implies that particle dispersion becomes worse above 5 wt% loading of unmodified Avicel particles. Since the temperature of loss modulus peak corresponds to Tg, an increase in E''_{max} indicates increased resistance to flow.

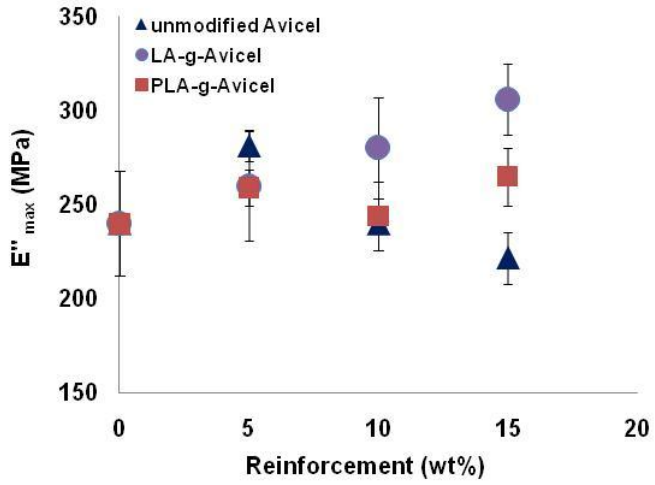

Figure 36. Loss modulus peak value as function of Avicel particle content.

5.10 Summary

The composite properties were found to depend on the relative amount of microcrystalline cellulose, the level of dispersion of the microcrystalline cellulose particles and interfacial interactions. It was found that the compatibility between matrix and filler is an important parameter that affected the dispersion of microcrystalline

cellulose in PLA matrix. Better dispersion led to increase in both static and dynamic mechanical properties of the composite.

Surface modification of Avicel particles by grafting polylactic acid was achieved with simple polycondensation reaction without employing any catalyst. DSC analysis showed surface modification lowered the crystallinity of cellulose particles. Surface modification improved the interfacial interactions resulting in improved tensile strength and modulus. For surface modification the "grafting from" approach for polymerizing lactic acid on cellulose surface was more effective than "grafting to" approach for grafting existing higher molecular weight PLA chains. This is reflected in comparatively higher weight fraction of grafted lactic acid. Use of surface modified particles resulted in higher magnitude of loss modulus peak (E" max) value and the value increased with increasing loading of these particles. Increased filler matrix interaction with surface modification resulted in decrease in loss modulus values below composite Tg. Above matrix Tg, increased friction between matrix chains and the filler particles increased the loss modulus for all composite samples. Surface modification of cellulose particles influenced the short range segmental interactions but not the long range chain motion.

CHAPTER 6

PLA-HYDROLYZED MICROCRYSTALLINE CELLULOSE COMPOSITES

6.1 Polymer nanocomposites

During the past few years research for developing nanocomposite systems has received attention. The uniform dispersion and controlled interaction of nano-sized filler with matrix can provide improvements like decreased swellability, electrical and thermal conductivity, optical clarity, enhanced barrier to small molecules, better mechanical and thermal properties etc. [115]. Improvements in properties have been reported with as low as 1 volume percent addition of nano-sized constituents for e.g., layered silicates [116-120]. Considerably large amount of traditional filler (micron in size or larger) is required for obtaining comparable property enhancements. The improvement in properties obtained at low filler loadings in nanocomposite systems are on account of the increase in surface area per volume of material. Polymer nanocomposites systems also have the potential for enabling larger recycling of plastics materials used in packaging applications by eliminating multilayer designs [121].

Cellulose whiskers obtained by acid hydrolysis of microcrystalline cellulose particles is a potential nano reinforcement material for PLA and is reported to have good mechanical properties, low cost and is available from a renewable resource that is abundantly available. Combination of PLA and cellulose results in formation of completely degradable composite in which both the constituents are derived from renewable resources.

Several researchers [122-124] have reported enhancement in composite properties when using cellulose whiskers as the reinforcing material. It is possible to develop completely degradable nanocomposites with cellulose as the reinforcing material, provided it is possible to isolate the crystalline cellulose whiskers.

In the previous chapters, we studied the effects of processing technique and surface modification of microcrystalline cellulose particles on thermal and mechanical properties of PLA-Cellulose based composites. In this chapter, the relative influence of filler particle size and interfacial adhesion in composite materials is studied using hydrolyzed Avicel particles and surface modified hydrolyzed Avicel particles. Surface modification was done by grafting the hydrolyzed microcrystalline cellulose particles with lactic acid (LA-g-hydrolyzed Avicel) and polylactic acid (PLA-g-hydrolyzed Avicel) via esterification reaction between hydroxyl group of hydrolyzed Avicel particles and carboxyl of lactic acid without using any external catalyst.

6.2 Results and discussion

6.2.1 Hydrolyzed cellulose particle morphology

The morphology of hydrolyzed Avicel particles was studied using SEM and is reported in Figure 37. The hydrolysis conditions employed are observed to result in incomplete hydrolysis of the microcrystalline cellulose particles and lead to formation of a fibrous morphology. The SEM micrographs also revealed that acid hydrolysis resulted in transverse cleavage along the particles that resulted in formation of different sized whiskers and the diameter of some whiskers were observed to be less than 1 micrometer. This is on account of the non-selectivity of the hydrolysis process, a common

phenomenon observed with acid hydrolysis of cellulose [22]. Also, complete whisker separation was not achieved.

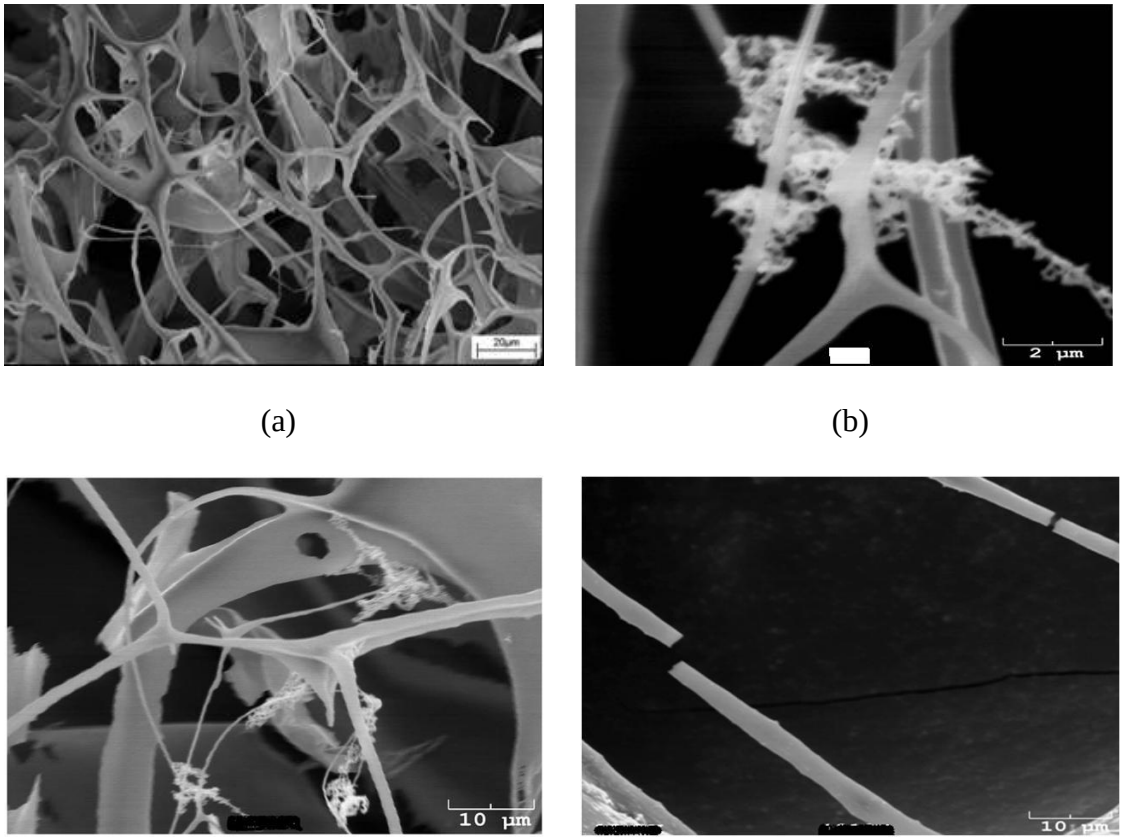

(a) (b)

(c) (d)

Figure 37. Morphology of hydrolyzed Avicel particles.

6.2.2 Morphology of composites reinforced with hydrolyzed and surface modified cellulose particles

Figure 38 shows SEM micrographs of cross sections of composite samples containing 15 wt% of hydrolyzed and lactic acid grafted hydrolyzed Avicel particles. The presence of relatively large particles indicates that the hydrolysis of cellulose particles was not complete. There is also indication that the surface modified particles had better interfacial adhesion than the unmodified particles.

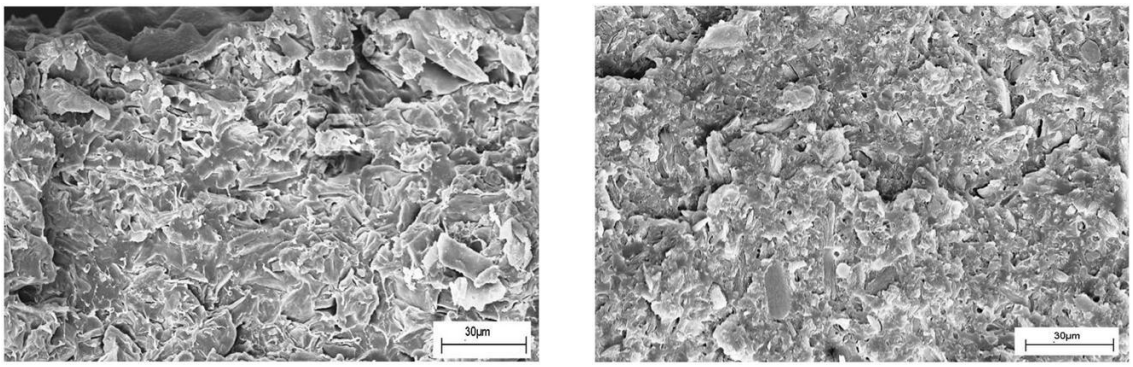

(a) (b)

Figure 38. SEM images of sample cross sections of composite samples (a) 15 wt% hydrolyzed and (b) 15 wt% lactic acid grafted hydrolyzed Avicel particles.

6.2.3 Wide angle X-ray diffraction

WAXD studies were carried out to analyze the effect of acid hydrolysis and the grafting conditions used on the crystal structure of the Avicel particles and the corresponding plot is given in Figure 39. The data are normalized by value of intensity at 2 theta = 50. For all samples, sharp peaks are observed at 2θ = 22.5 and 34.5. In addition a shoulder is observed around the region 2θ= 14 to 17. These peaks correspond to the cellulose I structure [39]. No relative shift in peak position observed after acid hydrolysis of the Avicel particles confirmed that there was no change in crystal structure of Avicel particles. The WAXD results indicate that acid hydrolysis was non selective and affected both the amorphous and crystalline regions.

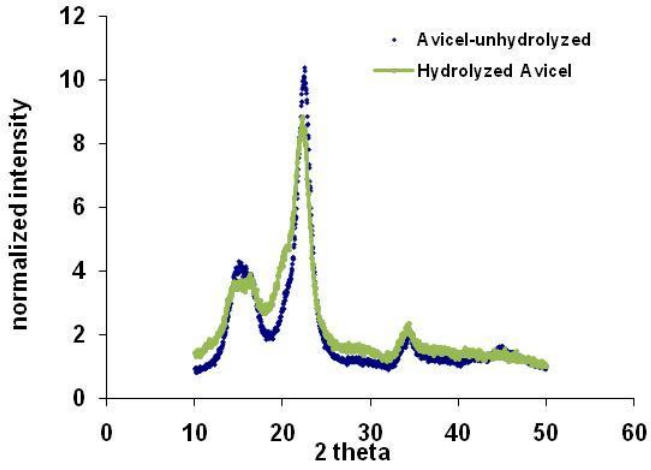

Figure 39. WAXD pattern of unmodified Avicel particles and hydrolyzed Avicel powder.

6.2.4 Thermal stability of hydrolyzed and surface modified hydrolyzed cellulose particles

The effect of grafting and acid hydrolysis on the thermal stability of the cellulose was studied using TGA and is shown in Figure 40. For comparison of thermal stability, the temperature of maximum weight loss rate was taken as reference. Hydrolyzed Avicel obtained by sulfuric acid hydrolysis of Avicel particles reduced the thermal stability of the cellulose particles. Lactic acid grafting did not change the degradation temperature of the hydrolyzed Avicel particles. The lower thermal stability of hydrolyzed Avicel is likely due to presence of residual acid. However, even for hydrolyzed Avicel particles no significant weight loss is observed till well over 200°C. Since the melting point of PLA resin is around 170°C, addition of hydrolyzed cellulose particles in PLA will not adversely affect the thermal stability of the PLA-cellulose composites when processed via melt mixing technique.

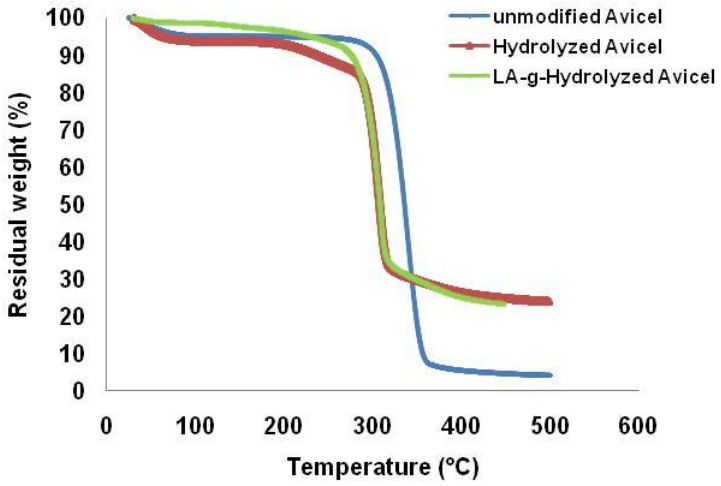

Figure 40. Effect of acid hydrolysis and surface modification on stability of Avicel particles.

6.2.5 Grafting efficiency

The efficiency of grafting Lactic Acid to hydrolyzed Avicel particles was calculated with DSC following the procedure discussed in section 5.2.2. The weight fraction of Avicel in the LA-g-hydrolyzed Avicel sample was obtained by dividing the heat of melting of lactic acid grafted hydrolyzed Avicel particles by the corresponding heat of melting of hydrolyzed Avicel particles. Table 8 gives the values of melting enthalpies and weight fractions of cellulose and lactic acid in surface modified samples. Higher grafting levels achieved with hydrolyzed Avicel sample is on account of increase in the number of accessible surface hydroxyl groups.

Table 8. Heat of melting (ΔH_m) and weight fractions of cellulose grafted polymer in hydrolyzed Avicel and lactic acid grafted hydrolyzed Avicel particles.

Sample	Degradation temperature from TGA (˚C)	ΔH_m (J/g)	% lactic acid (wt%)
Hydrolyzed Avicel	307	376	0
LA-g-hydrolyzed Avicel	305	280	25±1.7

The dsc thermograms of un-hydrolyzed and hydrolyzed microcrystalline cellulose samples shown in Figure 41 shows that hydrolysis affects both the amorphous and crystalline phases and reduces sample crystallinity.

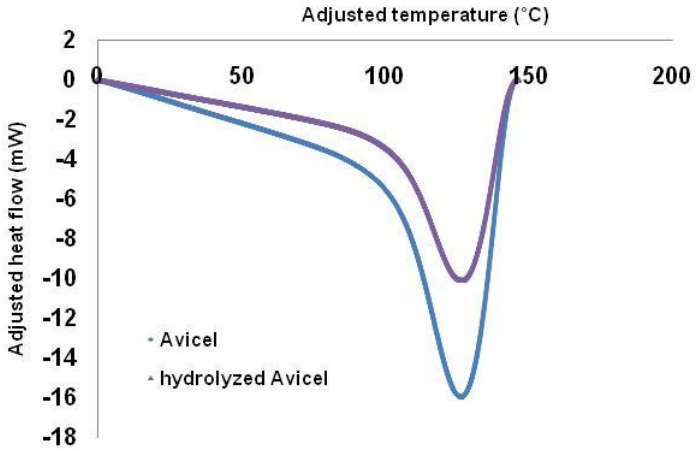

Figure 41. DSC thermograms of un-hydrolyzed and hydrolyzed Avicel particles.

6.2.6 Crystallization kinetics

In composite materials, the crystallinity of matrix affects a variety of different properties including mechanical, thermal and degradability of the composite. Slow crystallization rate is a drawback associated with PLA. A number of researchers [1, 125] have studied the role of cellulose reinforcements as nucleating agents in PLA in an attempt to increase the PLA crystallization rate. We have carried out isothermal crystallization studies on samples of neat PLA and PLA reinforced with hydrolyzed and surface modified Avicel particles to observe the nucleating efficiency of these reinforcements in PLA. The isothermal crystallization studies were done at 120°C. Samples were cooled rapidly (-100˚C min^{-1}) from melt to the crystallization temperature. The crystallization kinetics was analyzed using an Avrami type of fitting as given in equation 6.

The crystallization half times of PLA-Cellulose solution processed composite samples are plotted as a function of weight percent reinforcement (cellulose) in Figure 42.

For all samples, increasing the cellulose content leads to lower half times of crystallization, $t_{1/2}$ time. Decrease in size of cellulose particles, achieved through acid hydrolysis of cellulose particles, resulted in lowest $t_{1/2}$ times and corresponded to more than two fold increase in the crystallization rate at loading levels considered. This could be expected as reduction in particle size increases the surface area of particles and the increased surface area results in increased activity of the particle surface [35]. The number of crystals nucleated was shown to be proportional to fillers surface area for PP-SWNT nanocomposite [126]. Grafting of lactic acid on surface of hydrolyzed particles (LA-g-hydrolyzed Avicel) reduced their nucleating efficiency because cellulose surface was chemically modified. Mathew et al. [19] have observed the roughness of

microcrystalline cellulose particles to help initiation and growth of crystals. Lactic acid grafting could also lead to change in the surface roughness of cellulose particles affecting rate of crystallization. Particles surface modified by grafting preformed high molecular weight PLA chains showed similar nucleation efficiency as unmodified hydrolyzed particles. This indicates that the monomeric or oligomeric lactic acid grafts acted as defects similar to chain ends adversely affecting the crystallization rate of the PLA matrix chains. These observations are similar to findings of Su et al.[127] who observed that reducing particle size and improving the filler-matrix interactions affected the nucleating ability of carbon black particles in PLA.

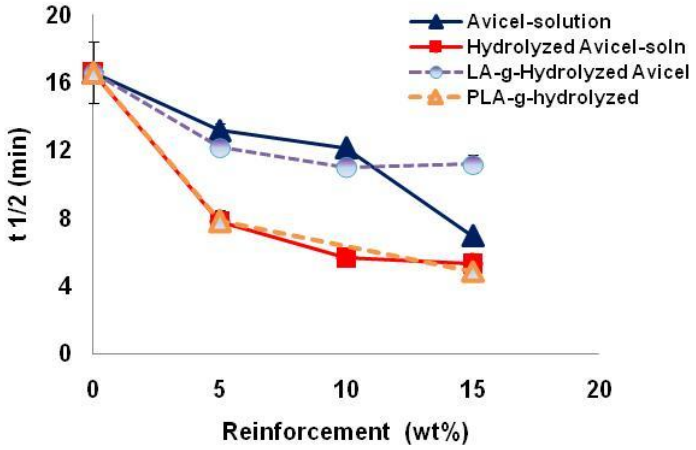

Figure 42. Influence of size and surface modification on the nucleating ability of the cellulose particles.

GPC studies done for calculating the molecular weights of the neat PLA and those of the composite samples showed no significant difference in the molecular weights of neat PLA and composite samples. This shows that the increase in crystallization rate observed is only on account of the cellulose particles acting as nucleating agents and not a function of molecular weight of PLA.

The total percent crystallinity, calculated from the heat of fusion by melting the samples after isothermal crystallization, and from DSC studies carried out separately, showed crystallinity of all the solution processed samples was nearly same. The addition of cellulose particles only increased the rate but not the extent of crystallization which implies the observed improvements in physical properties of composites are not dependent on equilibrium crystallinity but depend on other factors like interfacial interactions in the sample [128]. Similar results were reported by Jiang et al. [129] for poly(3-hydroxybutyrate-co-3-hydroxyvalerate) (PHBV) copolymer reinforced with cellulose whiskers obtained by acid hydrolysis of microcrystalline cellulose.

DSC studies done on composite samples reinforced with hydrolyzed Avicel and LA-g-hydrolyzed Avicel particles also showed that the melting temperature remained more or less constant (170 ± 1°C). This is also an indication that the crystal growth was not significantly affected when reinforcing PLA with hydrolyzed Avicel or surface modified hydrolyzed Avicel particles [130].

6.2.7 Tensile properties

The static mechanical properties of samples reinforced with hydrolyzed and surface modified hydrolyzed Avicel particles are now considered. Figure 43-45 shows the tensile modulus, strength and strain at break comparison for PLA samples reinforced with unhydrolyzed Avicel particles, hydrolyzed Avicel particles and surface modified hydrolyzed particles. The term “relative” indicates values that are normalized by those of neat PLA. For the larger unmodified Avicel particles, the relative modulus showed no significant change with increasing filler concentration while the values of relative

strength and strain at break decreased with increasing particle loading. Addition of hydrolyzed microcrystalline cellulose particles increased the composite stiffness but decreased the composite strength. The change in morphology of the cellulose particles obtained on hydrolysis could have resulted in increasing surface area of the particles as also their tendency to agglomerate. Formation of aggregates is expected to influence the strength more than the stiffness of the composite sample as particle aggregation results in increased stress concentration regions which act as weak points. Addition of the smaller sized hydrolyzed Avicel particles lead to greater restraining of matrix chains and is likely the result of the fibrous particle morphology developed on acid hydrolysis. The reduction in matrix chain mobility increased the macroscopic rigidity of matrix layer in contact with particles as compared to bulk matrix which is not influenced by the filler particles and resulted in increased modulus of the composite [131]. The formation of fibrous particle morphology did not result in increased filler-matrix compatibility as was evident from decrease in value of relative strength.

The composite samples synthesized with surface modified hydrolyzed cellulose particles showed increase in both stiffness and strength. Surface modification of hydrolyzed cellulose particles by surface grafting of oligomeric or monomeric lactic acid improved the interfacial interaction between the cellulose particles and PLA matrix. Better compatibility between matrix and filler particles increased the effective volume fraction of the filler and reduced regions of stress concentration which are introduced in the sample by particle addition.

Figure 45 shows the influence of filler size (hydrolyzed Avicel) and filler-matrix compatibility (LA-g-hydrolyzed Avicel) on the ability of the matrix to strain before

failure. Reduction of filler size decreased the ability of the matrix to strain compared to composites synthesized with larger un-hydrolyzed microcrystalline cellulose particles. Surface modification of hydrolyzed Avicel by grafting lactic acid is observed to improve the strain at break values of the composite samples. Improvements in interfacial interaction results in fewer stress concentration regions being formed and increases resistance to crack propagation and lead to increase in strain at break values compared to the values of samples reinforced with hydrolyzed Avicel particles. By comparing Figures 43-45 it is observed that addition of LA-g-hydrolyzed Avicel particles increased the modulus, strength and strain at break of the composite samples. Potentially, the use of surface modified hydrolyzed Avicel particles could improve the stiffness, strength as well as the toughness of composite samples.

It should be noted, at any loading level for lactic acid grafted cellulose particles the actual amount of cellulose particles added is less compared to the amount of unmodified cellulose particles added. This is because the lactic acid grafted particles contain around 25 % by weight of lactic acid which is grafted on the surface. The use of lactic acid grafted particles resulted in property improvement at relatively lower particle loadings.

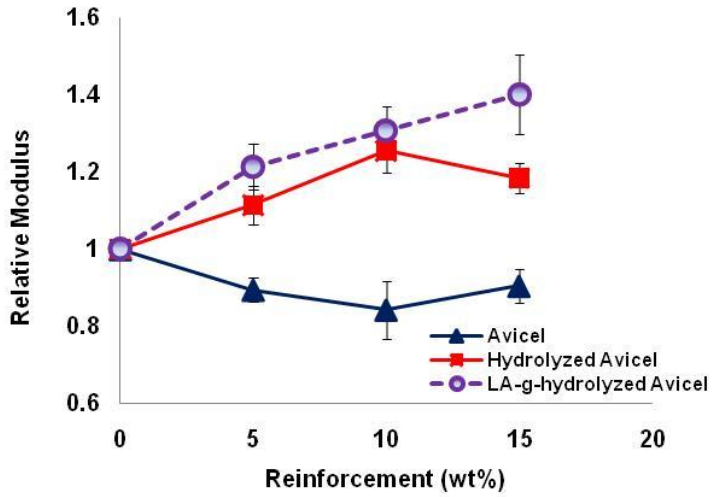

Figure 43. Comparison of relative tensile modulus of PLA composites reinforced with unmodified Avicel particles, hydrolyzed Avicel particles and lactic acid grafted hydrolyzed Avicel (LA-g-hydrolyzed) particles.

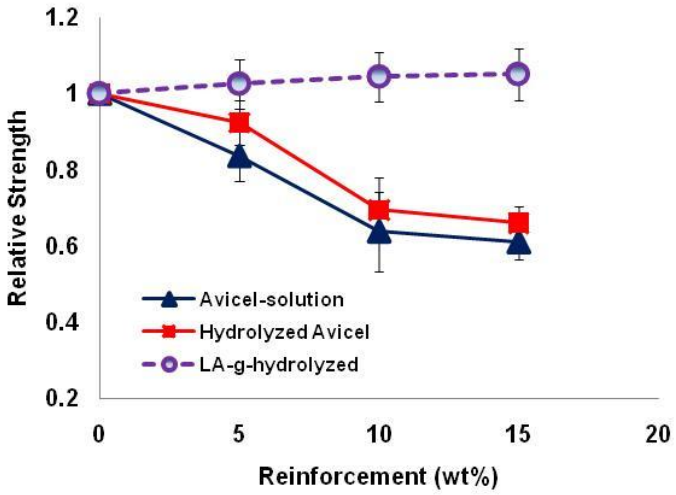

Figure 44. Comparison of relative tensile strength of PLA composites reinforced with unmodified Avicel particles, hydrolyzed Avicel particles and lactic acid grafted hydrolyzed Avicel (LA-g-hydrolyzed) particles.

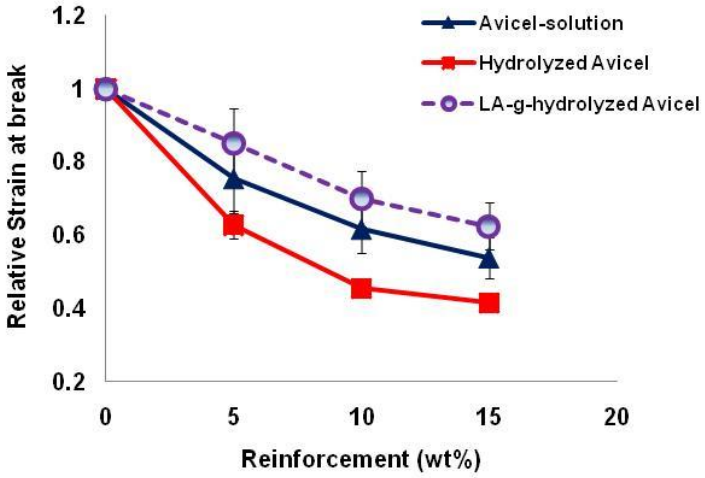

Figure 45. Comparison of relative strain at break of PLA composites reinforced with unmodified Avicel particles, hydrolyzed Avicel particles and lactic acid grafted hydrolyzed Avicel (LA-g-hydrolyzed) particles.

6.2.8 Model fitting to tensile modulus data with hydrolyzed and surface modified hydrolyzed cellulose reinforcement

Addition of modified hydrolyzed cellulose particles to PLA matrix results in increased interaction between matrix and filler particles. The observed increase in the modulus of this modified reinforcement is on account of the increased interfacial interactions. For hydrolyzed cellulose particle reinforcement the higher experimental values observed are on account of increase in the surface area of the cellulose particles due to acid hydrolysis, which increases the interaction potential of cellulose particles with the polylactic acid matrix. Tables 9 and 10 give fitted modulus values of the reinforcement obtained by fitting models to experimental data. Surface modification of hydrolyzed cellulose particles with lactic acid enhanced interfacial interactions and is reflected in higher fitted modulus values for samples reinforced with surface modified particles. The experimental and model fitted data is shown in Figure 46. The effective modulus of hydrolyzed

microcrystalline cellulose is lower than predicted value of ~100GPa. The lowering of crystallinity during hydrolysis and absence of whisker-whisker network may be responsible for the observed decrease in modulus. The 25 % increase in modulus achieved using 10 wt% of hydrolyzed microcrystalline cellulose is comparable to the 90 % modulus increase reported by Huda et al. [132] for PLA reinforced with 30 wt% recycled newspaper cellulose fibers.

Table 9. Fitted modulus values for hydrolyzed Avicel particles of solution processed composite samples

Modulus of reinforcement - hydrolyzed Avicel particles (MPa)			
	ROM model	Halpin-Tsai model	Paul model
Tensile Testing	6560	7286	7871
DMA (E' at 40˚C)	10628	14191	18270

Table 10. Fitted modulus values for lactic acid grafted hydrolyzed Avicel particles of solution processed composite samples

Modulus of reinforcement - lactic acid grafted hydrolyzed Avicel particles (MPa)			
	ROM model	Halpin-Tsai model	Paul model
Tensile Testing	12230	17737	20295
DMA (E' at 40˚C)	19974	54108	123749

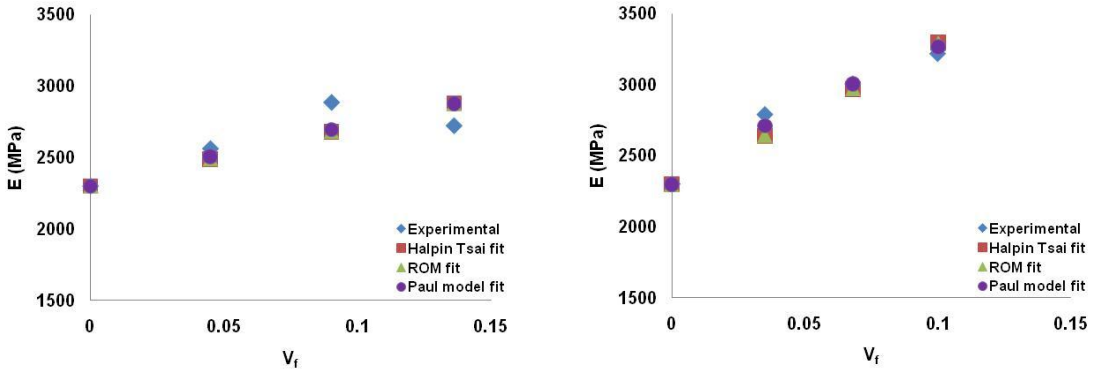

(a) (b)

Figure 46. Comparison of model fitted tensile modulus values of PLA composites reinforced (a) unmodified hydrolyzed Avicel particles (b) lactic acid grafted hydrolyzed Avicel particles.

6.2.9 Dynamic mechanical properties

The dynamic mechanical properties of the samples reinforced with hydrolyzed and surface modified hydrolyzed microcrystalline cellulose particles are now considered. In Figure 46 the relative storage modulus of composite samples reinforced with hydrolyzed Avicel and lactic acid grafted hydrolyzed Avicel are plotted as function of temperature. Comparison of Figures 47 (a) and 47 (b) revealed that below Tg, the relative storage modulus of lactic acid grafted samples is higher than un-grafted samples. On the contrary above Tg, the un-grafted samples exhibit higher storage modulus than lactic acid grafted samples. This reversal in reinforcement behavior is likely due to the lower amount of equivalent cellulose particles added in case of lactic acid grafted cellulose particles as was pointed out earlier. Below Tg, use of LA-g-hydrolyzed Avicel particles results in better filler-matrix interaction and increases the storage modulus. Above Tg, the

increased mobility of the matrix chains overcomes any restrictions imposed by filler-matrix interactions on matrix chain mobility. In both cases reinforcement achieved above the composite Tg is greater than achieved below composite Tg since the ratio of modulus of hydrolyzed Avicel particles to modulus of PLA is higher above Tg when matrix polymer is in the rubbery state [133]. Comparing the values of relative storage modulus for the 10 wt% samples, at 120°C the reinforcement obtained with hydrolyzed Avicel is 2.7 times while that obtained with LA-g-hydrolyzed Avicel is 2.2 times that of neat PLA. Both these values are greater than values obtained with 10 wt% of unmodified or unhydrolyzed Avicel particles.

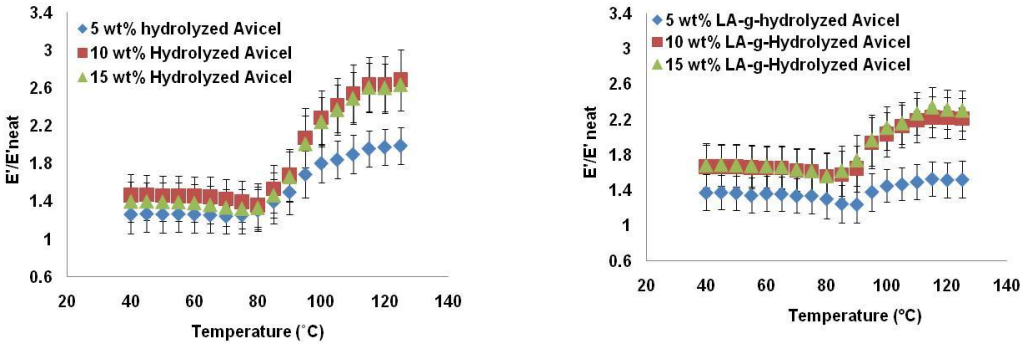

(a) (b)

Figure 47. Normalized storage modulus of solution processed samples of PLA reinforced with (a) hydrolyzed Avicel particles and (b) lactic acid grafted hydrolyzed Avicel particles as function of temperature.

In Figure 48 the relative loss modulus of neat PLA and composite samples is plotted as a function of temperature. The x-axis is normalized by taking the loss modulus peak temperature as reference and the y-axis is normalized by taking the loss modulus peak value as reference. Below Tg, samples reinforced with LA-g-hydrolyzed Avicel particles have lower relative loss modulus compared to the unmodified hydrolyzed Avicel

reinforced composite samples. This is on account of increased matrix-filler interaction in the composites containing LA-g-hydrolyzed Avicel particles. The surface modified particles restrain the PLA chains more than unmodified particles. This is also reflected in higher storage modulus values for LA-g-hydrolyzed Avicel reinforced samples in the region below composite Tg as observed in Figure 47. Above Tg, the relative loss modulus of samples containing unmodified hydrolyzed particles are only slightly higher than samples containing lactic acid grafted Avicel particles and is also likely due to comparatively lower cellulose content of lactic acid grafted cellulose particles.

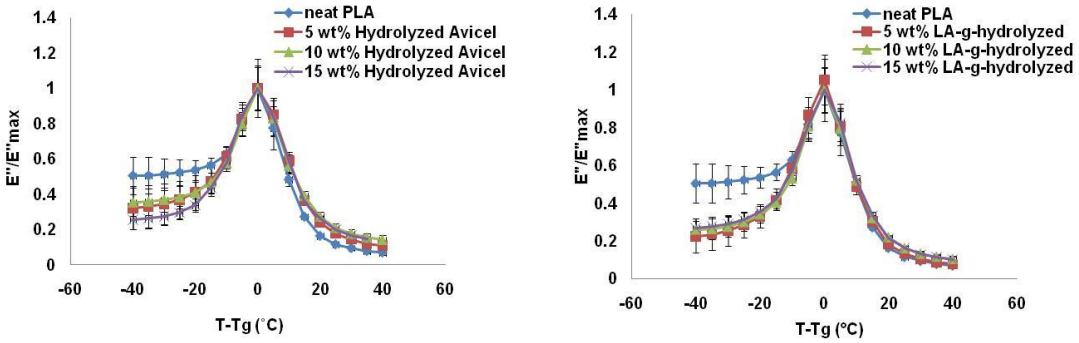

(a) (b)

Figure 48. Normalized loss modulus values of solution processed samples of PLA reinforced with (a) hydrolyzed Avicel particles and (b) lactic acid grafted hydrolyzed Avicel particles as function of temperature.

6.2.10 Model fitting to storage modulus data for composites with hydrolyzed and surface modified hydrolyzed cellulose reinforcement

Comparison of experimental E' values and fitted model values for composite samples reinforced with hydrolyzed and lactic acid grafted cellulose particles at 40˚C are given in Figure 49. The modulus of the reinforcement obtained by fitting models to experimental

data is given earlier in tables 9 and 10. The good fit for modulus with all the models is on account of restriction on matrix chains imposed by the hydrolyzed Avicel particles. Use of surface modified cellulose particles, by grafting lactic acid, increased the interfacial interaction and resulted in less error between the model and experimental model values. Comparison with data in table 4 showed hydrolyzed particles restrain the matrix chains more than the un-hydrolyzed particles.

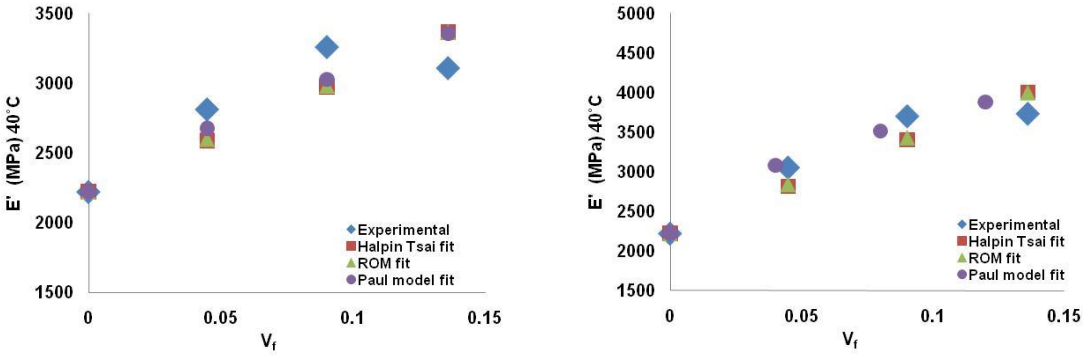

(a) (b)

Figure 49. Comparison of model fitted storage modulus values of PLA samples reinforced with (a) hydrolyzed Avicel particles and (b) lactic acid grafted hydrolyzed Avicel particles at 40°C.

6.3 Effect of surface modification of hydrolyzed cellulose particles by grafting polylactic acid, PLA chains

6.3.1 Tensile properties

Figure 50 shows the relative modulus value of PLA composites reinforced with PLA-g-hydrolyzed cellulose particles. The relative modulus for these composite samples lies in between those obtained with unmodified hydrolyzed cellulose and LA-g-hydrolyzed

cellulose particle reinforced composite samples. Similar observations can be made for the values of relative strength, Figure 51 and the relative strain at break, Figure 52. This indicates that surface modification of cellulose particles by "grafting to" method resulted in comparatively weaker interaction with PLA matrix compared to filler-matrix interactions obtained using cellulose particles modified with "grafting from" method. This behavior may arise due to difference in accessible functional groups for modifying cellulose particles. More number of functional groups may be accessible for surface polymerization of lactic acid compared to reaction with existing high molecular weight polylactic acid chains due to larger size of the polymer chain. Surface modification by grafting polylactic acid chains does result in increasing the strength and strain at break values compared to using unmodified hydrolyzed cellulose particles and is therefore a viable alternative to grafting lactic acid.

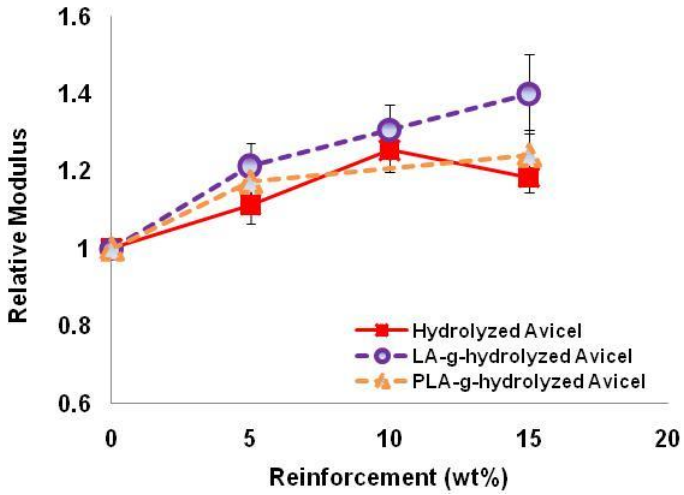

Figure 50. Comparison of relative tensile modulus of PLA composites reinforced with hydrolyzed Avicel particles, lactic acid grafted hydrolyzed Avicel (LA-g-hydrolyzed) particles and polylactic acid grafted hydrolyzed Avicel (PLA-g-hydrolyzed).

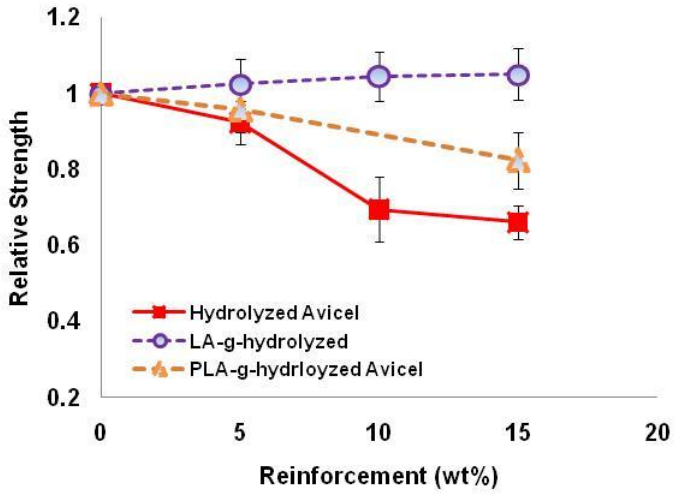

Figure 51. Comparison of relative tensile strength of PLA composites reinforced with hydrolyzed Avicel particles, lactic acid grafted hydrolyzed Avicel (LA-g-hydrolyzed) particles and polylactic acid grafted hydrolyzed Avicel (PLA-g-hydrolyzed).

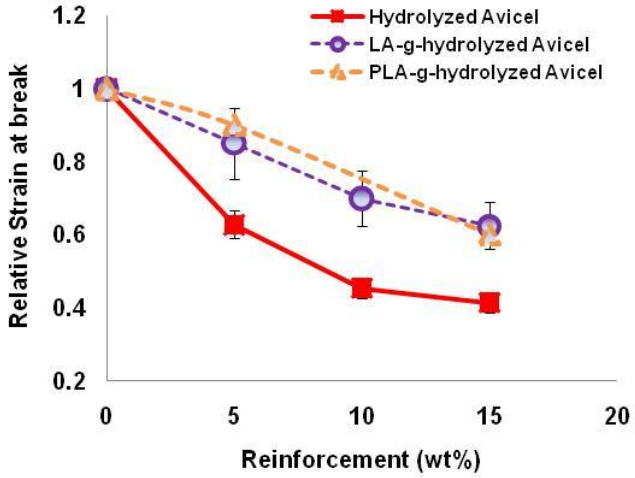

Figure 52. Comparison of relative strain at break of PLA composites reinforced with hydrolyzed Avicel particles, lactic acid grafted hydrolyzed Avicel (LA-g-hydrolyzed) particles and polylactic acid grafted hydrolyzed Avicel (PLA-g-hydrolyzed).

6.3.2 Model fitting to tensile modulus data

The fitted modulus values for samples reinforced with PLA-g-hydrolyzed Avicel particles are given in table 11 and fitted data for different models is plotted along with measured experimental values in Figure 53. The fitted modulus values are observed to be lower than the values for samples reinforced with lactic acid grafted hydrolyzed Avicel particles, table 10. These results suggest that surface modification by grafting lactic acid results in higher interfacial interactions and more efficient transfer of stress.

Table 11. Fitted modulus values for polylactic acid grafted hydrolyzed Avicel particles for solution processed composite samples

Modulus of reinforcement - polylactic acid grafted hydrolyzed Avicel particles (MPa)			
	ROM model	Halpin-Tsai model	Paul model
Tensile Testing	7698	6865	8491
DMA (E' at 40˚C)	18843	42487	80000

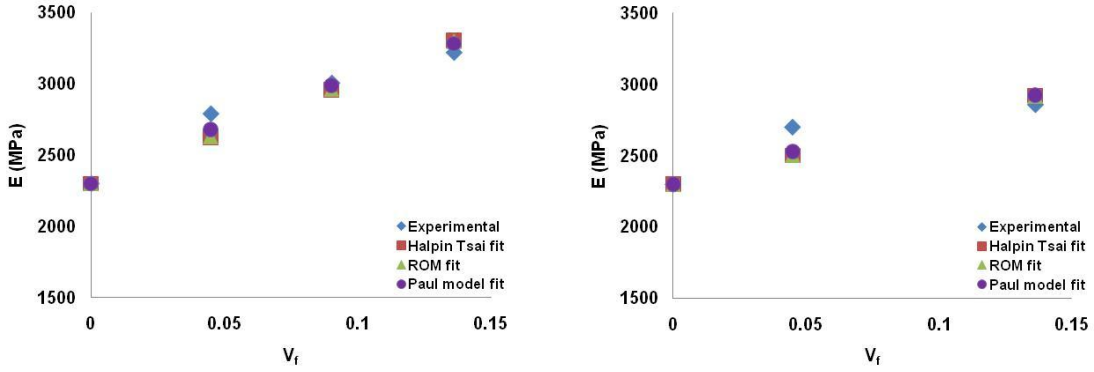

(a) (b)

Figure 53. Comparison of model fitted tensile modulus values of PLA composites reinforced with (a) lactic acid grafted hydrolyzed Avicel particles (b) polylactic acid grafted hydrolyzed Avicel particles.

6.3.3 Dynamic mechanical properties

The length of the grafted PLA chains may be sufficient for entanglements to have formed between the matrix chains and the PLA chains grafted on the filler surface. This can be expected to improve interfacial interactions resulting in strong interface being formed. The E' values of PLA-g-hydrolyzed cellulose particles reinforced samples are higher compared to E' values of LA-g-hydrolyzed cellulose particle reinforced samples. Above Tg, 200 % increase in storage modulus was obtained for PLA samples reinforced with PLA-g-hydrolyzed cellulose particles as observed in Figure 54 (b). These DMA results indicate increased filler matrix interactions for cellulose particles modified by grafting polylactic acid chains. The increase in E' values above Tg may also be due to relatively higher cellulose content of PLA-g-hydrolyzed cellulose particles compared to the cellulose content of Lactic acid –grafted-hydrolyzed cellulose particles.

With PLA grafted particles greater confinement of matrix chains is possible whereas with lactic acid grafted particles greater interfacial interactions between matrix and particles can be expected. Higher filler-matrix interactions lead to better interfacial stress transfer and manifested in higher tensile modulus and strength for composite system reinforced with lactic acid grafted cellulose particles.

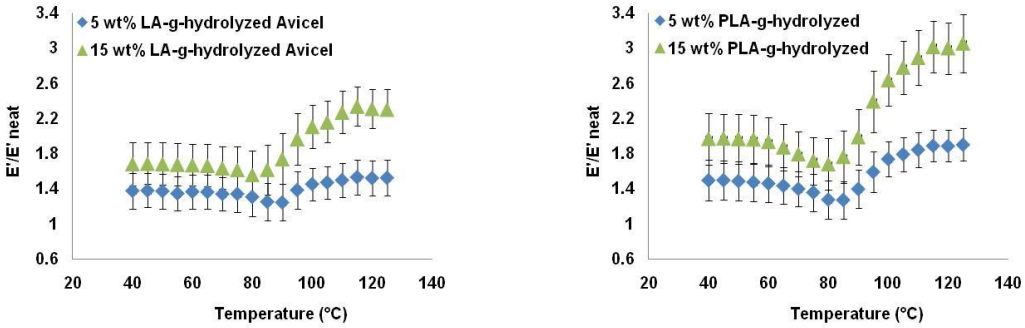

(a) (b)

Figure 54. Normalized storage modulus of solution processed samples of PLA reinforced with (a)lactic acid grafted hydrolyzed Avicel particles and (b) polylactic acid grafted hydrolyzed Avicel particles as function of temperature.

Reinforcing PLA with PLA-g-hydrolyzed cellulose particles resulted in a similar decrease in the relative loss modulus values as was observed for samples reinforced with LA-g-hydrolyzed cellulose particles. This is related to the amount of PLA chains and lactic acid monomer grafted on to the cellulose particles. Matrix chain mobility is reduced by physiochemical interactions with the filler and due to decrease in the allowed conformations (loss of entropy) of the matrix chains in the presence of the filler. The identical chemical nature of matrix PLA chains and graft PLA chains on cellulose particles resulted in lesser than expected restriction on matrix chain conformation. Also, lactic acid grafting on to the cellulose particles resulted in same amount of interfacial

friction as obtained with cellulose particles modified with PLA chains. Since similar improvement in mechanical properties are obtained by reinforcing PLA with cellulose particle modified by grafting lactic acid or polylactic acid, surface modification using PLA polymer chains is recommended as this is a more economical alternative.

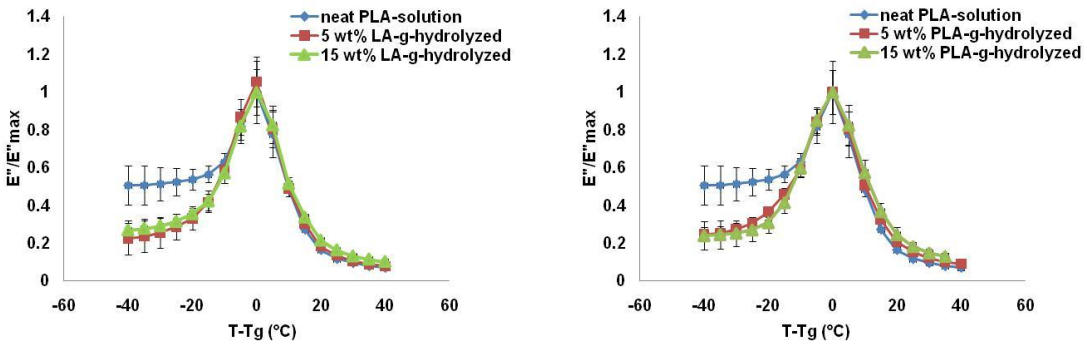

(a) (b)

Figure 55. Normalized loss modulus of solution processed samples of PLA reinforced with (a)lactic acid grafted hydrolyzed Avicel particles and (b) polylactic acid grafted hydrolyzed Avicel particles as function of temperature.

6.3.4 Model fitting to storage modulus data

The fitted storage modulus values for samples reinforced with PLA-g-hydrolyzed Avicel particles are given in table 11 and plotted in Figure 56. The fitted values for modulus of PLA-g-hydrolyzed Avicel particle reinforcement are observed to be lower than those obtained for modulus of hydrolyzed cellulose particles surface modified with lactic acid. Thus surface modification with polylactic acid is not observed to increase the reinforcement modulus values as compared to modulus of particles surface modified by

grafting lactic acid. Similar trend was observed for un-hydrolyzed cellulose particle surface modified with lactic acid and polylactic acid.

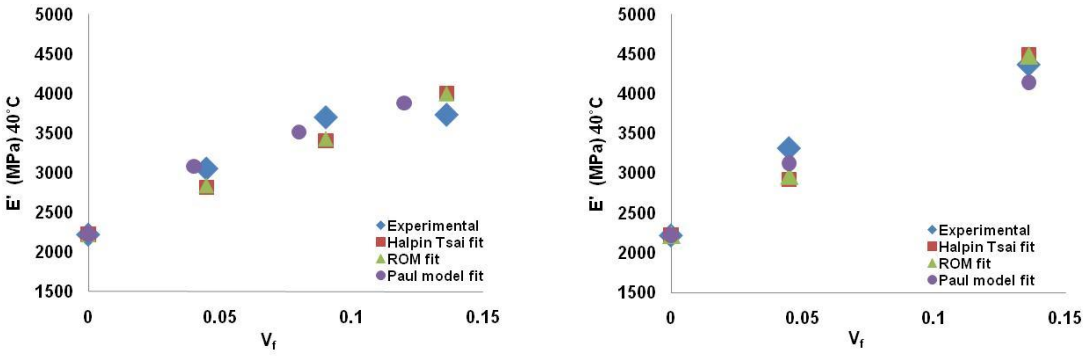

(a) (b)

Figure 56. Comparison of model fitted storage modulus values of PLA samples reinforced with (a) lactic acid grafted hydrolyzed Avicel particles and (b) polylactic acid grafted hydrolyzed Avicel particles.

6.4 Mechanical loss

In Figure 57 the loss modulus peak values (E''_{max}) are plotted as function of the weight percent reinforcement of different cellulose particles. For a given filler loading, the lowest E''_{max} values are observed for samples containing unmodified hydrolyzed Avicel particles and the highest E''_{max} values are observed for samples reinforced with polylactic acid grafted hydrolyzed particles. The higher mechanical loss in samples reinforced with modified cellulose particles is again consequence of higher interfacial interaction that results from better dispersion of modified cellulose particles in the PLA matrix.

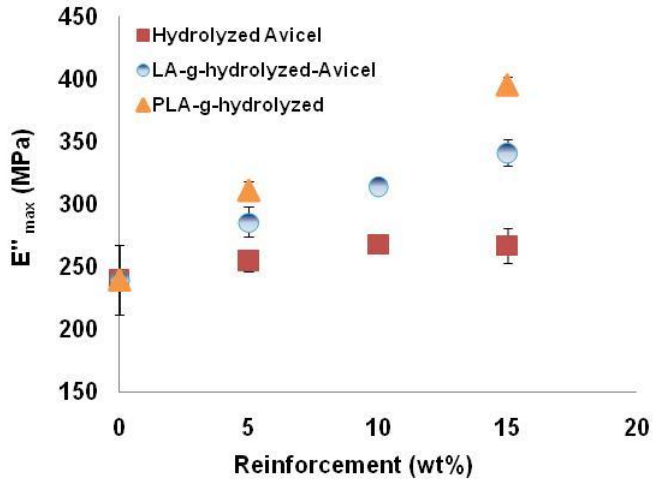

Figure 57. Influence of particle size and surface modification on mechanical loss in the interface regions as observed from magnitude of loss modulus peak values.

Comparison of Figures 36 and 57 showed, for the composite samples, the loss in the interface regions is observed to be dependent on filler size and surface chemical composition of Avicel particles. A reduction of filler size achieved using hydrolyzed Avicel particles, resulted in particles having larger surface area and hence greater interaction potential and resulted in higher E''_{max} values for the samples reinforced with hydrolyzed particles compared to samples containing larger un-hydrolyzed Avicel particles. The tendency of smaller hydrolyzed particles to agglomerate prevented them from achieving the higher interfacial interactions observed with surface modified Avicel particles. Particle aggregation has been shown to be influenced by particle size and surface tension of the particles [28]. Surface modification of particles by grafting lactic acid or polylactic acid reduced their surface tension, a driving force for particle aggregation and the tendency to agglomerate. This aided in better dispersing of the

particles and improved interfacial stress transfer resulting in the maximum mechanical loss in the interfacial region.

6.5 Summary

Acid hydrolysis of microcrystalline cellulose particles resulted in an order of magnitude reduction in size of the particles and lead to formation of fibrous particle morphology. WAXD and DSC studies indicated that hydrolysis occurred in both the amorphous and crystalline phases. The surface of hydrolyzed microcrystalline cellulose particles was chemically modified by surface polymerization of lactic acid using "grafting from" approach and by grafting existing high molecular weight polylactic acid chains using "grafting to" approach. SEM studies indicated that the hydrolysis conditions employed did not result in complete hydrolysis. Static and dynamic mechanical analysis showed surface modification of hydrolyzed microcrystalline cellulose particles improved the interfacial interactions leading to higher values of storage modulus, greater mechanical loss in the interface regions and increase in stiffness, strength and strain at break of the composite samples. The property improvements observed using surface modified particles were also obtained at relatively lower cellulose loadings. The cellulose particles were also observed to act as nucleating agents increasing the crystallization rate of PLA and their nucleation efficiency increased with decrease in particle size. Particle's surface chemical composition was found to influence its effectiveness as a nucleating agent. Surface modification of hydrolyzed cellulose particles by lactic acid or polylactic acid resulted in similar increase in the static and dynamic mechanical properties of the PLA-cellulose composites. This is on account of the difference in the grafting efficiency of

"grafting from" and "grafting to" type reactions which resulted in different amounts of polymer being grafted on cellulose surface.

CHAPTER 7

DEGRTADATION STUDIES OF PLA-CELLULOSE COMPOSITES

7.1 Introduction

PLA is an aliphatic polyester that is reported to degrade mainly by hydrolysis and not by microbial or enzymatic attack [134, 135]. Degradation involves either random chain scission or chain end scission of terminal ester linkages to form monomeric hydroxy acids. In general there are four steps in the hydrolytic degradation of PLA [77]

1) Absorption of water by the polymer

2) Ester cleavage with formation of oligomer fragments

3) Solubilization of the oligomer fragments formed

4) Diffusion of soluble oligomers into the reaction medium

The degradation rate has been observed to depend on initial sample crystallinity, molecular weight, molecular weight distribution, stereo isomeric content (L to D ratio) and rate of water diffusion [136]. As stated earlier, in certain applications, the comparatively slow rate of PLA degradation is a drawback. This has lead to a longer than necessary in vivo life for some PLA based biomedical implants requiring additional surgeries for their removal [70, 137]. The slow degradation rate can also create problems in non-bio related fields, e.g., disposal of consumer products.

Lee et al [138] concluded that for a biodegradable composite polymer film, hydrolysis of matrix polymer depends on transport of water from surface into the bulk of film, i.e. it depends on water permeability. Degradation by chain end scission or random chain scission depends on the relative rate of cleavage of backbone bonds compared to

diffusion of water into sample bulk [139]. For degradation of PLA-layered silicate nanocomposite under compost Ray et al. [77] observed that the rate of degradation of PLA increased significantly after nanocomposite preparation. Tsuji et al. [140] have observed accelerated degradation of PLA matrix in presence of hydrophilic but water insoluble polymers like polyvinyl alcohol, PVA. Similar observations were made by Nijenhuis et al. [141] for blends of PLA and polyethylene oxide, PEO. Thus, factors that increase the hydrolysis tendency of the neat PLA are likely to increase its rate of degradation.

In case of PLA-cellulose composites, since the reinforcement has hydroxyl groups on the surface it may affect the diffusion of water and influence rate and mechanism of degradation. For this reason we studied the effect of this cellulose reinforcement on the degradation rate of composite samples. The degradation of neat PLA and PLA-cellulose composites was carried out in alkaline media using 0.1 N NaOH solution at 37°C. The hydroxyl ions being known to be the active catalytic species that accelerates the hydrolysis of aliphatic polyesters like PLA more than H^+ ions [73]. The degraded samples were characterized by monitoring sample weight loss, GPC for studying the effect on molecular weight and the erosion mechanism and DSC to observe the effect of degradation on samples amorphous and crystalline fractions.

7.2 Weight loss measurement

As the concentration of OH^- ions in the hydrolysis media has been reported to influence the degradation rate of PLA [142], we first determined the conditions, in terms of NaOH normality which would result in degradation of the samples within a reasonable time period. The sample weight loss of neat PLA film samples was monitored at three

different base concentrations of 0.01N, 0.1 N and 0.5 N NaOH and the results are reported in Figure 58. As observed in Figure 58, a very high mass loss rate was observed for samples in 0.5 N NaOH solution with the entire sample being solubilized in two days. On the contrary in 0.01N NaOH solution, less than two percent mass loss was observed after a period of 30 days. The mass loss occurring in 0.5 N and 0.01N NaOH solution were too fast and too slow respectively than the time frame desired for analyzing the degradation process and mechanism. Based on these observations, all degradation studies were carried out in 0.1 N NaOH at 37°C. It should be noted that the degradation mechanism and the mass loss rates observed under these conditions may be different than when using lower alkali concentrations, acidic medium or solutions with pH close to 7.4. However the trends observed give us relevant information about factors influencing PLA hydrolysis.

For any NaOH concentrations considered, Figure 58, no induction time for start of weight loss was observed and the weight loss showed an almost linear type of relationship with time in the degradation media. These observations point to degradation occurring via surface erosion mechanism. Also, the solution in vials turned cloudy indicating the degradation products formed were suspended in the alkali media. The weight loss calculated using equation 7 was obtained by comparing the initial sample weight and sample weight after given hydrolysis time.

We also verified that the microcrystalline cellulose particles were not undergoing degradation under these conditions by subjecting the microcrystalline cellulose sample to same hydrolysis conditions as PLA and monitoring the sample weight loss. Since no significant weight loss occurred in the microcrystalline cellulose sample, the weight loss

occurring in the PLA-cellulose composite samples is believed entirely to be the result of PLA degradation.

$$\%\, weight\ loss = \left(\frac{x_o - x_t}{x_o}\right) x\ 100 \qquad (7)$$

where x_o = sample weight at t = 0 days and x_t = sample weight at t = t days

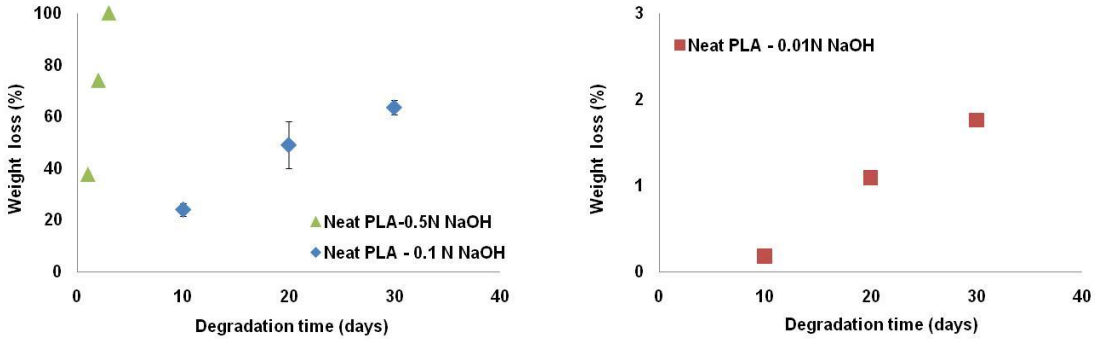

(a) (b)

Figure 58. Percentage weight loss of neat PLA film samples at 37˚C in (a) 0.5 N and 0.1 N NaOH and (b) 0.01N NaOH solution.

In Figure 59 the weight loss observed for neat PLA and PLA-cellulose composite samples in 0.1 N NaOH solutions is reported. For all samples the weight loss increased with increasing hydrolysis time with no induction period observed before start of weight loss.

Addition of cellulose particles unmodified or modified increased the weight loss rate and the increase was prominent at early stages, after 10 days than at the end after 30 days.

This is believed to be on account of low molecular weight chains present at the interface diffusing into the degradation medium. For the neat PLA samples and PLA-cellulose composite samples the mass loss rate decreased after 20 days in the hydrolysis media. This decrease is related to the increase in sample crystallinity after hydrolysis [143] and is discussed in section 7.3. The acidic degradation products i.e. lactic acid, formed during PLA hydrolysis may also lower the hydrolysis rate as a result of increase in hydronium H_3O^+ ion concentration and the effect is termed as "auto-inhibition effect" [144]. The molecular weight of the degrading samples was observed to increase with time in the degradation media as discussed later. This increase in chain length may require a greater number of bonds to be cleaved for erosion to occur resulting in the observed decrease in the rate of weight loss [145].

Comparison of neat PLA samples obtained using melt and solution processing revealed that solution processed samples underwent greater weight loss after 30 days in the hydrolysis media. This may be due to the amorphous regions being easier to hydrolyze than crystalline regions and the sample crystallinity affecting the diffusion of water during hydrolytic degradation [71, 146]. In a particular study, Fischer et al. [87] studied degradation of solution grown DL-lactide copolymer single crystals in 1: 2 water-methanol mixture containing 0.02 to 0.04 moles of NaOH. They observed that cleavage of ester bonds starts in the amorphous surface regions of the single crystals and the reaction rate decreases when degradation proceeds in the crystalline region. Our result corroborates this observation because the solution processed samples of PLA having higher molecular weight and lower crystallinity than the melt processed samples showed higher weight loss.

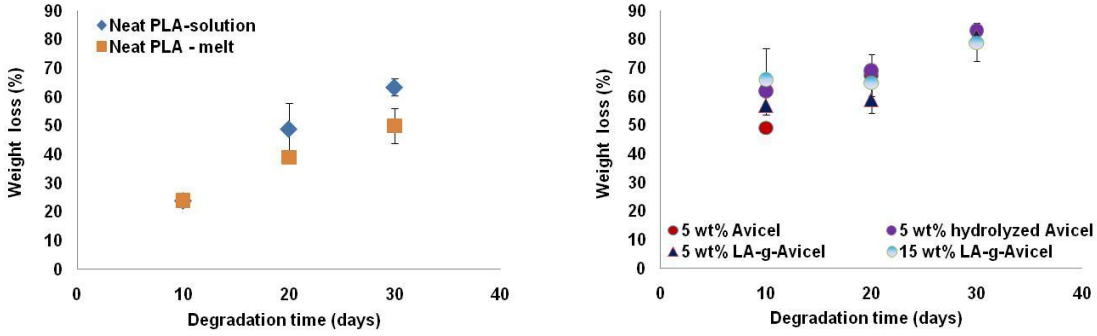

(a) **(b)**

Figure 59. Percentage weight loss of (a) neat PLA and (b) PLA-cellulose composite film samples as function of incubation time in 0.1 N NaOH solution at 37˚C.

7.3 Effect of degradation on sample crystallinity and Tg

To observe the effect of degradation on sample crystallinity and to verify whether the amorphous regions were easier to hydrolyze, the degraded samples were analyzed with DSC. The results obtained are plotted in Figure 60. For all samples, the % crystallinity was observed to increase with increasing time in the hydrolysis medium. This indicated that during alkaline hydrolysis, the amorphous phase was influenced more and the hydrolytic chain cleavage proceeded mainly in the amorphous regions [147]. This could have led to the observed increase in samples crystalline fraction [148, 149]. The increase in crystallinity was observed without accompanying increase in melting temperature, Tm which indicates that the ratio of amorphous phase to crystalline phase was changed without altering the crystal size in the crystalline phase [69]. The calculated percentage crystallinity was obtained after normalizing with fraction of PLA remaining in the sample.

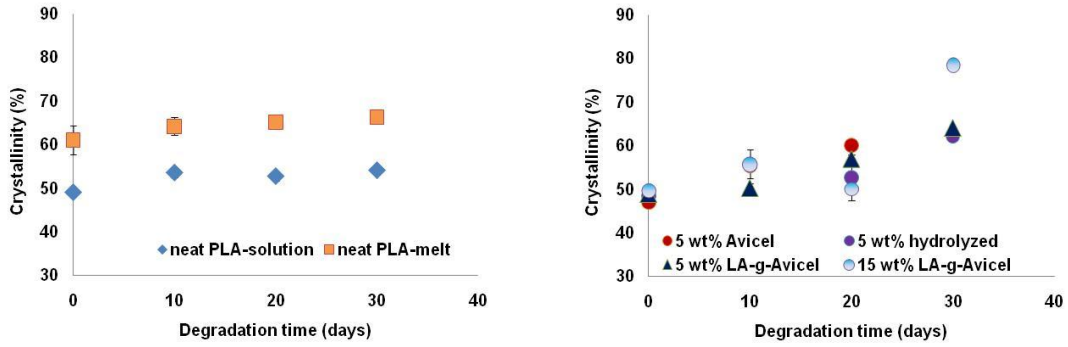

(a) **(b)**

Figure 60. PLA crystallinity of (a) neat PLA and (b) PLA-cellulose composite film samples as a function of incubation time in 0.1 N NaOH solution at 37˚C.

The Tg of neat PLA and PLA-cellulose composite samples, measured with DSC and shown in Figure 61, increased with increasing time in the hydrolysis media. This increase in Tg indicated that the degradation products formed, e.g. PLA oligomers, lactic acid etc. did not exert plasticizing effect on the sample. This is further evidence of the degradation products being suspended in the alkaline media used and not being trapped inside the degrading sample, another indication of degradation occurring via surface erosion mechanism. Paul et al. [148] had observed a decrease in Tg for PLA-clay nanocomposite during hydrolysis in phosphate-buffer solution and explained this phenomenon as arising due to the plasticizing effect of the degradation products formed after degradation.

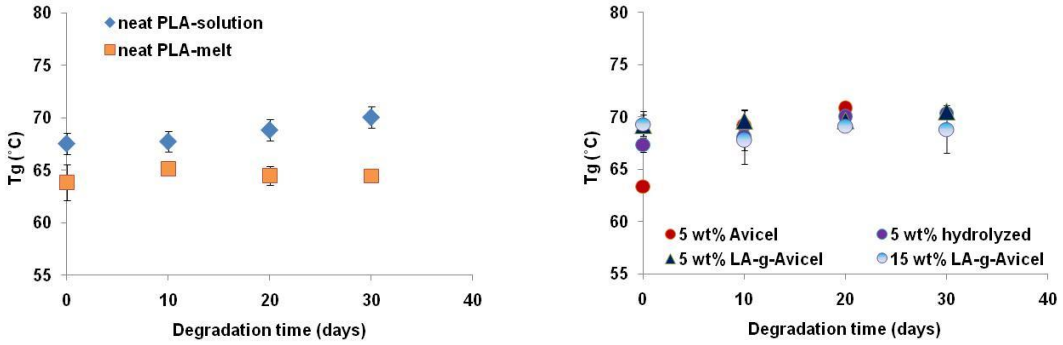

(a) **(b)**

Figure 61. Tg of (a) neat PLA and (b) PLA-cellulose composite film samples as a function of incubation time in 0.1 N NaOH solution at 37˚C.

7.4 Effect of degradation on molecular weight and mechanism of degradation

The influence of degradation on sample molecular weight and the degradation mechanism was analyzed using GPC and the results are given in Figure 62. As seen in Figure 62 (b), the number average molecular weight, Mn of PLA-cellulose composite increased with increasing time in the hydrolysis medium. This is on account of degradation occurring via surface erosion mechanism. It should be noted, increase in molecular weight was not the result of increased chain length but the result of small molecules getting excluded as explained below. As such, the increase observed is only an "apparent" increase in the molecular weight.

For solution processed samples made via film casting method, sufficient time may be available for low molecular weight PLA chains to diffuse to the interface. Such a diffusion of low molecular weight chains would be entirely entropy driven. The low molecular weight chains present near the interface diffused into the degradation medium and resulted in the recorded sample mass loss and apparent increase in samples Mn values. Tsuji and Ishida [150] have reported increase in surface hydrophilicity of PLA

film samples upon treatment with NaOH solution. The base hydrolysis of the PLA films resulted in surface erosion without bulk degradation due to etching action of NaOH. Wang et al. [151] have also shown alkaline surface hydrolysis to result in formation of reactive groups on surface, e.g., hydroxyl (-OH) and carboxylic acid (-COOH). In our case it is also possible that etching action of NaOH could have helped dissolve the low molecular weight PLA chains present at the interface without degradation (leaching). In comparison, relatively lower increase in Mn is observed for melt processed samples of neat PLA, Figure 62 (a). During melt processing not enough time is available for smaller chains to diffuse to the interface and hence concentration of these chains at the interface would be lower than in solution processed samples.

No dramatic lowering of molecular weight was observed for any of the samples studied indicating that random chain scission did not occur. For PLA degradation in alkaline media, Belbella et. al [142] have also observed that degradation does not occur by random chain scission but occurred starting by cleaving of the terminal bond at the chain end. Jong et al. [152] have shown that under both basic and acidic conditions the different ester groups in PLA oligomers have different susceptibility for hydrolysis and that the hydrolysis proceeds by cleavage of ester bond near the hydroxyl end groups. They proposed under acidic conditions the first ester bond gets cleaved while under basic conditions the second ester bond gets cleaved first. Siparsky et. al [143] for hydrolysis of PLA in dioxane/water solution and Shih [153] for PLA hydrolysis in acidic conditions have reported observing dual rate of hydrolysis. They observed the rate of chain-end scission at the terminal ester to be faster than the rate of random ester scission process. Shih has attributed the difference in rates to the difference in the electronic environment

near the reaction sites. Aso et al. [154] have reported temperature dependence on the mechanism of degradation with surface degradation occurring below Tg and bulk degradation above Tg.

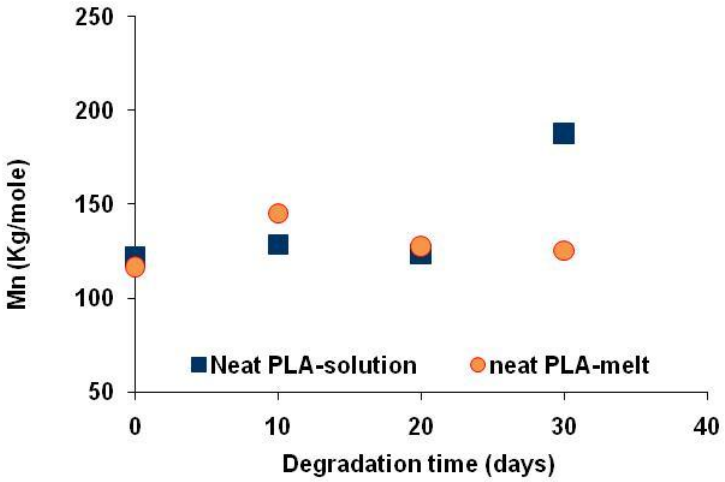

(a)

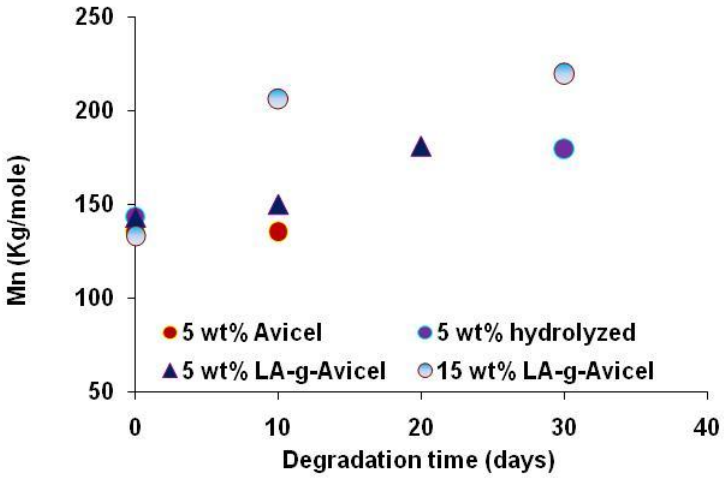

(b)

Figure 62. Effect of degradation on Mn of (a) neat PLA and (b) PLA-cellulose composite film samples as a function incubation time in 0.1 N NaOH solution at 37˚C.

On the basis of the trend observed in molecular weight and the measured mass loss that occurred due to generation and dissolution of degradation products, we believe that the hydrolysis occurred predominantly via non-random chain end scission process [144]. In our case, where the degradation was carried out at 37 °C, the rate of degradation of polymer bonds was faster than the diffusion of water into the polymer resulting in heterogeneous degradation of PLA matrix [139].

It was noted earlier that surface erosion of solution processed samples was easier than melt processed samples due to presence of shorter length PLA chains at the interface in the former. Since the rate of chain end scission depends on the number of chain ends in the sample, after 30 days in the alkaline media, the solution processed sample of neat PLA showed a sudden "apparent" increase in the number average molecular weight [155].

GPC chromatograms of solution and melt processed neat PLA film samples both un-degraded and degraded are shown in Figures 63 and 64. The data are shifted vertically for clarity. The concentration of samples used for doing the GPC were not the same as sufficient sample was not available in case of samples degraded for longer times. Therefore we only consider the peak position of the degraded and the un-degraded samples. For solution processed samples, Figure 63, it is observed that for samples subjected to degradation time of 20 days and more, the peaks shift to higher molecular weight side and from multimodal to unimodal distribution. The observed shifts are likely due to the low molecular weight chains getting dissolved in the degradation medium and the degradation products formed not getting trapped in sample bulk [156]. For samples degraded for 10 days, no significant difference between the chromatograms of un-

degraded and degraded samples was observed. This is on account of degradation occurring by surface erosion mechanism. In the alkaline medium employed here, the carboxylate ions can form a negatively charged screen trapping the hydroxyl ions on the surface and hinder the diffusion of hydroxyl ions into the bulk [142]. For melt processed samples no peak shift is observed for samples subjected to degradation time of 20 days and more. Presence of comparatively lower number of low molecular weight chains at the interface in melt processed samples is believed to be responsible for this observed behavior.

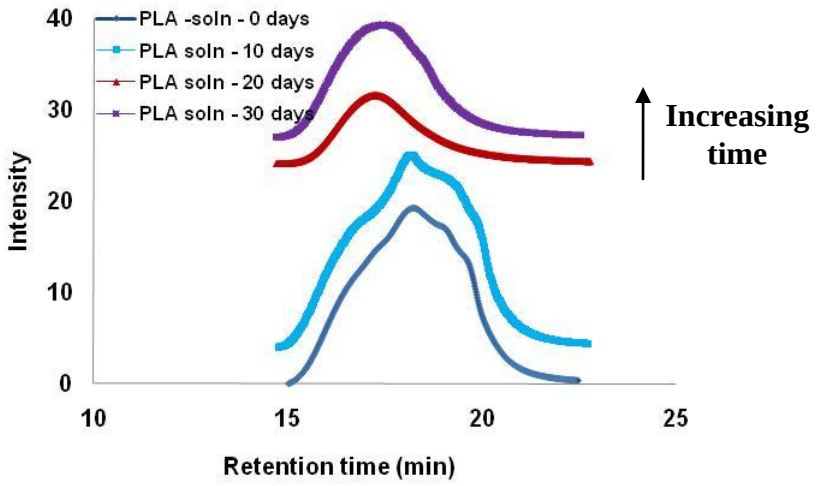

Figure 63. Effect of degradation on molecular weight of neat PLA film samples made by solution processing as a function of incubation time in 0.1 N NaOH solution at 37˚C.

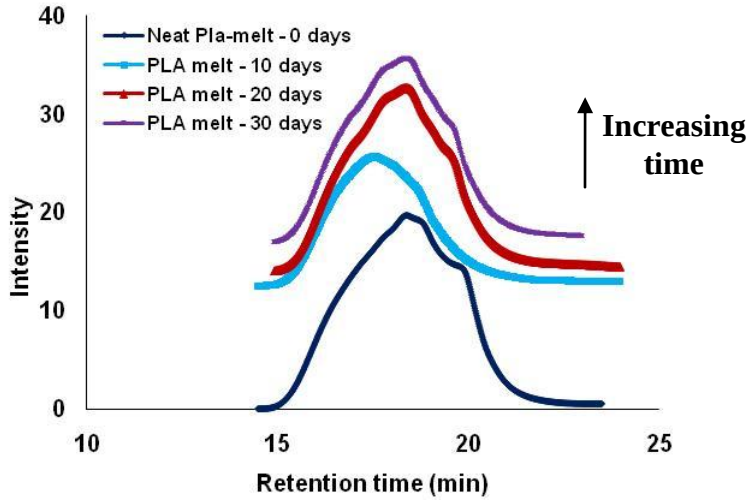

Figure 64. Effect of degradation on molecular weight of neat PLA film samples made by melt processing as a function of incubation time in 0.1 N NaOH solution at 37˚C.

7.5 Summary

The degradation of PLA and PLA-cellulose composite in the alkaline medium of 0.1 N NaOH at 37 °C occurred predominantly via surface erosion mechanism. Addition of cellulose to PLA matrix was observed to increase the hydrolysis rate of PLA as characterized by weight loss measurements and GPC. The addition of hydrophilic cellulose increased the diffusion rate of water into samples resulting in faster hydrolysis of PLA chains. The amorphous regions were influenced more and the fraction of amorphous phase in the degrading sample decreased with increasing time in the hydrolysis medium. Hydrolysis occurred predominantly via chain end scission and the degradation products formed were suspended in the alkaline medium. The rate of degradation could be controlled by controlling the concentration of OH^- ions in the degradation medium and the samples molecular weight. The rate of water diffusion into

polymer bulk and rate of cleaving of backbone bonds controlled the mechanism of degradation. Surface erosion occurred since the rate of degradation of main chain bonds was faster than bulk diffusion of water.

CHAPTER 8

CONCLUSIONS AND RECOMMENDATIONS

A processing-structure-property relationship study of PLA-cellulose composites was done and the effectiveness of cellulose as reinforcement for PLA was demonstrated.

Degradable polymer composites from renewable resources based on PLA and Cellulose were synthesized by melt mixing and solution processing techniques. For our system, the different processing techniques used resulted in samples having different molecular weights affecting the samples crystallinity. The melt processed samples had lower molecular weight, lower half time for crystallization and higher crystallinity were stiffer compared to solution processed samples.

Addition of unmodified microcrystalline cellulose particles to PLA resulted in increased stiffness but lowering of strength and strain at break values. It also resulted in increased elasticity as measured by DMA. The use of surface modified microcrystalline cellulose particles resulted in improved interfacial interaction between PLA and cellulose.

Hydrolysis of microcrystalline cellulose particles was done by reaction with sulfuric acid and lead to increase in the surface area of these cellulose particles.

The surface of microcrystalline cellulose particles, either un-hydrolyzed or hydrolyzed, was modified by grafting lactic acid and polylactic acid chains. The surface modification was done using an esterification reaction that required no catalyst. Surface modification of cellulose particles resulted in improved compatibility between PLA and cellulose and lead to relative increase in values of stiffness, strength and strain at break. With surface modified cellulose particles, significant increases in the static and dynamic mechanical

properties were obtained at relatively lower cellulose content. A 100 % increase in values for Young's Modulus and more than 200% increase in the storage modulus values were recorded. Higher reinforcement was achieved above the composites Tg than below it. For the composite samples, the loss in the interface regions was observed to be dependent on surface area and surface chemical composition of reinforcement (cellulose particles). Model fitting to measured static and dynamic modulus values revealed that use of surface modified cellulose particles resulted in greater restraining of the PLA matrix.

Surface modification of cellulose particles by grafting polylactic acid chains as compared to grafting lactic acid chains did not result in any significant difference in composite properties. The only advantage of grafting PLA chains was the lower cost of PLA compared to the high cost of lactic acid monomer. To the best of our knowledge, we have shown for the first time that effective surface modification of cellulose particles by grafting long length or short length polymer chains could be done using same procedure that involved a single step process and required no catalyst.

Microcrystalline cellulose particles (un-hydrolyzed or hydrolyzed) were also observed to act as nucleating agents and increased the rate of crystallization of PLA. The nucleation efficiency depended on the particles surface area and surface chemical composition. Increase in particles surface area via hydrolysis increased its nucleation ability. Presence of short length lactic acid chains on cellulose surface acted as defects and reduced the cellulose particles efficiency to act as nucleating agent.

Degradation of neat PLA and PLA-cellulose composites was studied in alkaline media. The rate of degradation was found to depend on pH of the degradation medium and initial sample crystallinity.

The degradation in NaOH solution was observed to occur predominantly via surface erosion mechanism and the degradation products were suspended in alkaline media used. Degradation occurred through hydrolysis of chains mainly in the amorphous regions and resulted in increasing the crystalline fraction of the degraded samples without affecting the crystal size. These observations are valid for the samples studied under these specific conditions and having the specified size and shape.

The processing method employed influenced the molecular weight of samples which had a direct effect on the polymers ability to crystallize. Samples having higher crystallinity were stiffer and had lower toughness. With the choice of appropriate processing method it is possible to control the crystallinity of the composite samples. This would be beneficial for improving the barrier properties of the material which is an important property for packaging applications. By controlling the sample crystallinity, the mechanical energy loss in the system could also be manipulated. The rate of polymer degradation can also be varied by changing sample crystallinity.

We found that the dispersion of microcrystalline cellulose particles in the PLA matrix can be improved by surface polymerization on the particles. Improving the filler dispersion increased its effective volume fraction in the composite and resulted in increased reinforcement with the same filler. It also resulted in higher tensile strength due to increased filler matrix interactions and higher values of strain at break. Improvement in tensile modulus can be attained by incorporation of a stiffer material which acts as a nucleating agent and increases the sample crystallinity or by improving the dispersion of the filler without the need for the filler to act as a nucleating agent. With better control of

the filler matrix interactions, tuning of mechanical properties would be possible which will help to increase the materials usefulness.

It is recommended to synthesize cellulose nano-fibers via electrospinning of the hydrolyzed cellulose suspension. These high aspect ratio fibers with high surface area will have greater interfacial interaction and can form percolation network further improving the properties. It is also recommended to study the rheological properties of the PLA-cellulose composite in order to study influence on processing.

A comparative study, wherein surface modification is carried out in presence of a suitable catalyst is proposed. Such an investigating would analyze the scope of using catalyst for surface modification reactions. Also in future work, surface modification of cellulose particles by reactive extrusion under inert atmosphere is recommended.

Different polymer matrices should be studied and surface modification of cellulose particles should be carried out by grafting different polymers.

APPENDIX A

Crystallinity data for melt and solution processed samples of PLA reinforced with unmodified microcrystalline cellulose particles

Table 12. Effect of cellulose addition on crystallinity of melt processed neat PLA and PLA-cellulose composite samples.

Melt processed samples	% Crystallinity (Avg)	Standard Deviation
Neat PLA	60.60	3.3
5 wt% Avicel	71.26	5.8
10 wt% Avicel	67.19	8.3
15 wt% Avicel	68.05	3.4
20 wt% Avicel	76.06	5.7

Table 13. Effect of cellulose addition on crystallinity of solution processed neat PLA and PLA-cellulose composite samples.

Solution processed samples	% Crystallinity (Avg)	Standard Deviation
Neat PLA	47.18	0.9
5 wt% Avicel	44.68	2.4
10 wt% Avicel	54.63	5.3
15 wt% Avicel	47.88	0.8
20 wt% Avicel	46.33	1.39

APPENDIX B

Tensile testing data of PLA samples reinforced with microcrystalline cellulose particles

Table 14. Tensile modulus of melt processed PLA and PLA-cellulose composite samples.

Melt processed samples	Young's Modulus (MPa)	Std Dev	Reinforcement	Error Reinforcement
Neat PLA	2336	132	1	
5 wt% Avicel	2275	159	0.97	0.09
10 wt% Avicel	2773	191	1.18	0.11
15 wt% Avicel	2753	264	1.18	0.13
20 wt% Avicel	2703	185	1.16	0.10

Table 15. Tensile strength of melt processed PLA and PLA-cellulose composite samples.

Melt processed samples	Tensile Strength (MPa)	Std Dev	Reinforcement	Error Reinforcement
Neat PLA	37	4.5	1	0
5 wt% Avicel	36	0.14	0.97	0.12
10 wt% Avicel	31	2.3	0.82	0.12
15 wt% Avicel	26	1.3	0.69	0.09
20 wt% Avicel	24	1	0.65	0.08

Table 16. Tensile modulus of solution processed PLA and PLA-cellulose composite samples.

Solution processed samples	Young's Modulus (MPa)	Std Dev	Reinforcement	Error Reinforcement
Neat PLA	2066	67	1	0
5 wt% Avicel	1848	24	0.89	0.03
10 wt% Avicel	1740	142	0.84	0.074
15 wt% Avicel	1868	70	0.9	0.045
20 wt% Avicel	2032	78	0.98	0.045

Table 17. Tensile strength of solution processed PLA and PLA-cellulose composite samples.

Solution processed samples	Tensile Strength (MPa)	Std Dev	Reinforcement	Error Reinforcement
Neat PLA	59	3.6	1	0
5 wt% Avicel	49	2.5	0.84	0.07
10 wt% Avicel	38	5.6	0.64	0.10
15 wt% Avicel	36	1.4	0.61	0.04
20 wt% Avicel	25	2.1	0.43	0.04

APPENDIX C

Length of lactic acid chains grafted on microcrystalline cellulose particles

Assume cylindrical shape for particles, with length = 20 µm and width = 2 µm

Surface area of one particle = $2\pi r^2 + 2\pi rh$

= 276 µm^2 = 276×10^{-12} m^2

Volume of particle = $\pi r^2 h$ = 251 µm^3 = $251 \times 10^{-18}\ m^3$

$density\ of\ microcrystalline\ cellulose = 1.4\ g/cm^3$

$1\ g\ of\ microcrystalline\ cellulose = \frac{1}{1.4} \sim 0.7 cm^3 = 0.7 \times 10^{-6} m^3$

Total number of particles in 1 g of microcrystalline cellulose = 2.8 x 10^9 particles

Total surface area of particles = $276 \times 10^{-12} \times 2.8 \times 10^9 = 0.78\ m^2$

Surface area of one cellulose unit = 6 A x 6 A = 36 A^2 = 36 x 10^{-20} m^2

The total number of cellulose units on surface = 2.1 x 10^{18} in 1 g of cellulose

1 g of lactic acid grafted microcrystalline cellulose contains 14 wt% lactic acid

or 0.14 g of lactic acid.

Therefore, the total number of cellulose units = 2.1 x 10^{18} x 0.86

= 1.8 x 10^{18} cellulose units in $0.67 m^2$

$molecular\ weight\ of\ lactic\ acid = 90\ \frac{g}{mole}$

0.14 g of lactic acid = $\frac{0.14}{90} = 1.56 \times 10^{-3}\ moles\ of\ lactic\ acid$ in 0.86 g of cellulose

0.86 g of microcrystalline cellulose per 0.67m^2 cellulose

= 2.3 x 10^{-3} moles of lactic acid/ 0.67 m^2 cellulose

= 1.4 x 10^{21} lactic acid molecules / 0.67 m^2 cellulose

1 cellulose unit contains 3 –OH groups

Total number of –OH groups in 1.8 *x* 10^{18} cellulose units = 5.4 *x* 10^{18} –OH groups in 0.67 m^2 cellulose

= 1.4 x 10^{21} lactic acid molecules per 5.4 *x* 10^{18} –OH groups

~ 250 lactic acid molecules per –OH group

APPENDIX D

Tensile testing data of PLA samples reinforced with lactic acid-g-microcrystalline cellulose particles

Table 18. Tensile modulus of solution processed samples reinforced with lactic acid-g-microcrystalline cellulose particles.

Solution processed samples	Young's Modulus (MPa)	Std Dev	Reinforcement	Error Reinforcement
Neat PLA	2066	67	1	0
5 wt% LA-g-Avicel	2448	78	1.06	0.05
10 wt% LA-g-Avicel	2349	100	1.02	0.06
15 wt% LA-g-Avicel	2892	57	1.26	0.05

Table 19. Tensile strength of solution processed samples reinforced with lactic acid-g-microcrystalline cellulose particles.

Solution processed samples	Tensile Strength (MPa)	Std Dev	Reinforcement	Error Reinforcement
Neat PLA	59	3.6	1	0
5 wt% LA-g-Avicel	57	1.8	0.97	0.08
10 wt% LA-g-Avicel	57	1.5	0.96	0.06
15 wt% LA-g-Avicel	51	1.5	0.81	0.07

Table 20. Strain at break values for solution processed samples reinforced with lactic acid-g-microcrystalline cellulose particles.

Solution processed samples	Strain at break (mm/mm)	Std Dev	Reinforcement	Error Reinforcement
Neat PLA	0.04	0.003	1	0
5 wt% LA-g-Avicel	0.03	0.002	0.97	0.08
10 wt% LA-g-Avicel	0.034	0.002	0.96	0.08
15 wt% LA-g-Avicel	0.026	0.0008	0.81	0.05

APPENDIX E

Tensile testing data of PLA samples reinforced with hydrolyzed-microcrystalline cellulose particles

Table 21. Tensile modulus of samples reinforced with hydrolyzed-microcrystalline cellulose particles.

Solution processed samples	Young's Modulus (MPa)	Std Dev	Reinforcement	Error Reinforcement
Neat PLA	2300	67	1	0
5 wt% hydrolyzed Avicel	2562	25	1.11	0.05
10 wt% hydrolyzed Avicel	2886	99	1.25	0.06
15 wt% hydrolyzed Avicel	2723	44	1.18	0.04

Table 22. Tensile strength of samples reinforced with hydrolyzed-microcrystalline cellulose particles.

Solution processed samples	Tensile Strength (MPa)	Std Dev	Reinforcement	Error Reinforcement
Neat PLA	59	3.6	1	0
5 wt% hydrolyzed Avicel	55	0.7	0.92	0.08
10 wt% hydrolyzed Avicel	41	4.3	0.69	0.06
15 wt% hydrolyzed Avicel	39	1	0.66	0.07

Table 23. Strain at break values for samples reinforced with hydrolyzed-microcrystalline cellulose particles.

Solution processed samples	Strain at break (mm/mm)	Std Dev	Reinforcement	Error Reinforcement
Neat PLA	0.04	0.002	1	0
5 wt% hydrolyzed Avicel	0.027	0.0007	0.63	0.04
10 wt% hydrolyzed Avicel	0.019	0.0004	0.45	0.03
15 wt% hydrolyzed Avicel	0.018	0.0005	0.41	0.03

APPENDIX F

Tensile testing data of PLA samples reinforced with lactic acid-g-hydrolyzed microcrystalline cellulose particles

Table 24. Tensile modulus of samples reinforced with lactic acid-g-hydrolyzed microcrystalline cellulose particles.

Solution processed samples	Young's Modulus (MPa)	Std Dev	Reinforcement	Error Reinforcement
Neat PLA	2300	67	1	0
5 wt% LA-g-hydrolyzed Avicel	2791	106	1.21	0.06
10 wt% LA-g-hydrolyzed Avicel	3007	117	1.31	0.06
15 wt% LA-g-hydrolyzed Avicel	3221	215	1.40	0.01

Table 25. Tensile strength of samples reinforced with lactic acid-g-hydrolyzed microcrystalline cellulose particles.

Solution processed samples	Tensile Strength (MPa)	Std Dev	Reinforcement	Error Reinforcement
Neat PLA	59	3.6	1	0
5 wt% LA-g-hydrolyzed Avicel	61	0.7	1.03	0.06
10 wt% LA-g-hydrolyzed Avicel	62	0.6	1.05	0.06
15 wt% LA-g-hydrolyzed Avicel	62	1.4	1.05	0.07

Table 26. Strain at break values for samples reinforced with lactic acid-g-hydrolyzed microcrystalline cellulose particles.

Solution processed samples	Strain at break (mm/mm)	Std Dev	Reinforcement	Error Reinforcement
Neat PLA	0.04	0.002	1	0
5 wt% LA-g-hydrolyzed Avicel	0.034	0.003	0.85	0.1
10 wt% LA-g-hydrolyzed Avicel	0.028	0.002	0.70	0.08
15 wt% LA-g-hydrolyzed Avicel	0.025	0.002	0.63	0.06

APPENDIX G

Tensile testing data of PLA samples reinforced with polylactic acid-g-Avicel and polylactic acid-g-hydrolyzed microcrystalline cellulose particles

Table 27. Tensile modulus values of samples reinforced with PLA-g-microcrystalline cellulose particles.

Solution processed samples	Young's Modulus (MPa)	Std Dev	Reinforcement	Error Reinforcement
Neat PLA	2300	67	1	0
5 wt% PLA-g- Avicel	2613	36	1.14	0.04
10 wt% PLA-g-Avicel	2238	42	0.97	0.04
15 wt% PLA-g-Avicel	2832	62	1.23	0.05

Table 28. Tensile strength of samples reinforced with PLA-g-Avicel microcrystalline cellulose particles.

Solution processed samples	Tensile Strength (MPa)	Std Dev	Reinforcement	Error Reinforcement
Neat PLA	59	3.6	1	0
5 wt% PLA-g- Avicel	63	1.7	1.03	0.06
10 wt% PLA-g-Avicel	62	1.7	1.05	0.06
15 wt% PLA-g-Avicel	59	3.5	1.05	0.07

Table 29. Strain at break values for samples reinforced with PLA-g-Avicel microcrystalline cellulose particles.

Solution processed samples	Strain at break (mm/mm)	Std Dev	Reinforcement	Error Reinforcement
Neat PLA	0.04	0.002	1	0
5 wt% PLA-g- Avicel	0.046	0.001	1.27	0.1
10 wt% PLA-g-Avicel	0.053	0.003	1.32	0.08
15 wt% PLA-g-Avicel	0.028	0.0008	0.71	0.06

Table 30. Tensile modulus values of samples reinforced with PLA-g-hydrolyzed microcrystalline cellulose particles.

Solution processed samples	Young's Modulus (MPa)	Std Dev	Reinforcement	Error Reinforcement
Neat PLA	2300	67	1	0
5 wt% PLA-g-hydrolyzed Avicel	2700	133	1.17	0.07
15 wt% PLA-g-hydrolyzed Avicel	2857	158	1.24	0.07

Table 31. Tensile strength of samples reinforced with PLA-g-hydrolyzed microcrystalline cellulose particles.

Solution processed samples	Tensile Strength (MPa)	Std Dev	Reinforcement	Error Reinforcement
Neat PLA	59	3.6	1	0
5 wt% PLA-g-hydrolyzed Avicel	57	0.7	0.96	0.06
15 wt% PLA-g-hydrolyzed Avicel	49	3.2	0.82	0.07

Table 32. Strain at break values for samples reinforced with PLA-g-hydrolyzed microcrystalline cellulose particles.

Solution processed samples	Tensile Strength (MPa)	Std Dev	Reinforcement	Error Reinforcement
Neat PLA	0.04	0.003	1	0
5 wt% PLA-g-hydrolyzed Avicel	0.036	0.003	0.9	0.1
15 wt% PLA-g-hydrolyzed Avicel	0.024	0.002	0.6	0.07

APPENDIX H

GPC data of solution processed neat PLA and PLA-cellulose composites

Table 33. Molecular weight distribution in PLA –microcrystalline cellulose composite samples

Solution processed samples	Mn (kg/mol)	Mw (kg/mol)	PDI
Neat PLA	176 ± 7	316 ± 8.6	1.79 ± 0.1
5 wt% Avicel	175 ± 24	318 ± 36	1.82 ± 0.04
10 wt% Avicel	195 ± 18	319 ± 2.5	1.65 ±0.13
15 wt% Avicel	183 ± 15	346 ± 11.7	1.9 ± 0.2
20 wt% Avicel	188	348	1.85

Table 34. Molecular weight distribution in PLA –lactic acid-g-microcrystalline cellulose composite samples

Solution processed samples	Mn (kg/mol)	Mw (kg/mol)	PDI
Neat PLA	176 ± 7	316 ± 8.6	1.79 ± 0.1
5 wt% LA-g-Avicel	183 ± 15	314 ± 9	1.72 ± 0.09
10 wt% LA-g-Avicel	175 ± 18	371 ± 2.5	2.12 ±0.13
15 wt% LA-g-Avicel	190 ± 3.7	339 ± 6	1.78 ± 0.02

Table 35. Molecular weight distribution in PLA –hydrolyzed microcrystalline cellulose composite samples

Solution processed samples	Mn (kg/mol)	Mw (kg/mol)	PDI
Neat PLA	176 ± 7	316 ± 8.6	1.79 ± 0.1
5 wt% hydrolyzed-Avicel	174 ± 5	336 ± 25	1.95 ± 0.19
10 wt% hydrolyzed -Avicel	177 ±	336 ±	1.89 ±
15 wt% hydrolyzed -Avicel	189 ± 12	322 ± 18	1.7 ± 0.12

APPENDIX I

Avrami constants and half time of crystallization for neat PLA and PLA-cellulose solution processed composite samples

Table 36. Avrami constants with unmodified microcrystalline cellulose as reinforcement

% Reinforcement	K (min^{-1})	n	$t_{1/2}$ (min)
0	0.051 ± 0.007	1.88 ± 0.25	16.6 ± 1.8
5	0.064 ± 0.002	2.24 ± 0.07	13.17 ± 0.42
10	0.069 ± 0	2.29 ± 0.09	12.16 ± 0.14
15	0.125 ± 0.0007	2.8 ± 0.11	6.96 ± 0
20	0.104 ± 0.001	2.53 ± 0.02	8.29 ± 0.06

Table 37. Avrami constants with lactic acid-g-microcrystalline cellulose as reinforcement

% Reinforcement	K (min^{-1})	n	$t_{1/2}$ (min)
0	0.051 ± 0.007	1.88 ± 0.25	16.6 ± 1.8
5	0.06 ± 0.0007	1.97 ± 0.04	14.7 ± 0.2
10	0.064 ± 0.002	2.16 ± 0.02	13.5 ± 0.2
15	0.072 ± 0.002	2.14 ± 0.03	11.8 ± 0.17

Table 38. Avrami constants with PLA-g-microcrystalline cellulose as reinforcement

% Reinforcement	K (min^{-1})	n	$t_{1/2}$ (min)
0	0.051 ± 0.007	1.88 ± 0.25	16.6 ± 1.8
5	0.08 ± 0.0007	2.38 ± 0.035	10.3 ± 0.11
10	0.124 ± 0.0007	2.67 ± 0.007	7.1 ± 0
15	0.12 ± 0.001	2.52 ± 0.007	7.28 ± 0.06

Table 39. Avrami constants with hydrolyzed microcrystalline cellulose as reinforcement

% Reinforcement	K (min^{-1})	n	$t_{1/2}$ (min)
0	0.051 ± 0.007	1.88 ± 0.25	16.6 ± 1.8
5	0.112 ± 0.009	2.47 ± 0.08	7.81 ± 0.64
10	0.15 ± 0.009	2.64 ± 0.04	5.67 ± 0.41
15	0.16 ± 0.004	2.7 ± 0.03	5.33 ± 0.12

Table 40. Avrami constants with lactic acid-g- hydrolyzedmicrocrystalline cellulose as reinforcement

% Reinforcement	K (min^{-1})	n	$t_{1/2}$ (min)
0	0.051 ± 0.007	1.88 ± 0.25	16.6 ± 1.8
5	0.07 ± 0.003	2.21 ± 0.007	12.8 ± 0
10	0.08 ± 0.003	2.35 ± 0.05	11 ± 0.32
15	0.08 ± 0.004	2.37 ± 0.014	11.19 ± 0.55

Table 41. Avrami constants with PLA-g-hydrolyzed microcrystalline cellulose as reinforcement

% Reinforcement	K (min^{-1})	n	$t_{1/2}$ (min)
0	0.051 ± 0.007	1.88 ± 0.25	16.6 ± 1.8
5	0.11 ± 0	2.55 ± 0.007	7.81 ± 0.06
15	0.18 ± 0.0007	2.75 ± 0.04	4.88 ± 0.03

REFERENCES

[1] L. Suryanegara, A. N. Nakagaito, and H. Yano, "The effect of crystallization of PLA on the thermal and mechanical properties of microfibrillated cellulose-reinforced PLA composites," *Composites Science and Technology*, vol. 69, pp. 1187-1192, 2009.

[2] K. Oksman, M. Skrifvars, and J. F. Selin, "Natural fibres as reinforcement in polylactic acid (PLA) composites," *Composites Science and Technology*, vol. 63, pp. 1317-1324, 2003.

[3] M. S. Huda, L. T. Drzal, M. Misra, and A. K. Mohanty, "Wood-fiber-reinforced poly(lactic acid) composites: Evaluation of the physicomechanical and morphological properties," *Journal of Applied Polymer Science*, vol. 102, pp. 4856-4869, 2006.

[4] R. Auras, B. Harte, and S. Selke, "An Overview of Polylactides as Packaging Materials," *Macromolecular Bioscience*, vol. 4, pp. 835-864, 2004.

[5] M. Vert, G. Schwarch, and J. Coudane, "Present and Future of PLA Polymers," *Journal of macromolecular science. Part A, Pure & applied chemistry*, vol. A32, pp. 787-796, 1995.

[6] J. Lunt, "Large-scale production, properties and commercial applications of polylactic acid polymers," *Polymer Degradation and Stability*, vol. 59, pp. 145-152, 1998.

[7] S. Mecking, "Nature or Petrochemistry? - Biologically Degradable Materials," *Angewandte Chemie International Edition*, vol. 43, pp. 1078-1085, 2004.

[8] R. E. Drumright, P. R. Gruber, and D. E. Henton, "Polylactic Acid Technology," *Advanced Materials*, vol. 12, pp. 1841-1846, 2000.

[9] J. Nieuwenhuis, "Synthesis of Polylactides, Polyglycolides and Their Copolymers," *Clinical Materials*, vol. 10, pp. 59-67, 1992.

[10] Y. Ikada and H. Tsuji, "Biodegradable polyesters for medical and ecological applications," *Macromolecular Rapid Communications*, vol. 21, pp. 117-132, 2000.

[11] D. Cam and M. Marucci, "Influence of residual monomers and metals on poly (-lactide) thermal stability," *Polymer*, vol. 38, pp. 1879-1884, 1997.

[12] A. Celli and M. Scandola, "Thermal properties and physical ageing of poly (-lactic acid)," *Polymer*, vol. 33, pp. 2699-2703, 1992.

[13] G. Perego, G. Domenico, and C. C. Bastioli, "Effect of molecular weight and crystallinity on poly(lactic acid) mechanical properties," *Journal of Applied Polymer Science*, vol. 59, pp. 37-43, 1996.

[14] T. Hatakeyama and H. Hatakeyama, *Thermal Properties of Green Polymers and Biocomposites*: Kluwer Academic Publishers, 2004.

[15] M. Samir, F. Alloin, and A. Dufresne, "Review of Recent Research into Cellulosic Whiskers, Their Properties and Their Application in Nanocomposite Field," *Biomacromolecules*, vol. 6, pp. 612-626, 2005.

[16] T. P. Nevell and S. H. Zeronian, *Cellulose Chemistry and its Applications*: Ellis Horwood Limited, 1985.

[17] N. S. Hon David, "Cellulose: a random walk along its historical path," *Cellulose*, vol. 1, pp. 1-25, 1994.

[18] P. A. Fowler, J. M. Hughes, and R. M. Elias, "Biocomposites: technology, environmental credentials and market forces," *Journal of the Science of Food and Agriculture*, vol. 86, pp. 1781-1789, 2006.

[19] A. P. Mathew, K. Oksman, and M. Sain, "The effect of morphology and chemical characteristics of cellulose reinforcements on the crystallinity of polylactic acid," *Journal of Applied Polymer Science*, vol. 101, pp. 300-310, 2006.

[20] T. Zimmermann, E. Pöhler, and T. Geiger, "Cellulose Fibrils for Polymer Reinforcement," *Advanced Engineering Materials*, vol. 6, pp. 754-761, 2004.

[21] T. Chisuzu, T. Keiji, F. Minoru, and S. Hiroshi, "Cellulose Synthesized by Acetobacter Xylinum in the Presence of Acetyl Glucomannan," *Cellulose*, vol. V5, pp. 249-261, 1998.

[22] M. M. d. S. Lima and R. Borsali, "Rodlike Cellulose Microcrystals: Structure, Properties, and Applications," *Macromolecular Rapid Communications*, vol. 25, pp. 771-787, 2004.

[23] Y. Habibi, H. Chanzy, and M. R. Vignon, "TEMPO-mediated surface oxidation of cellulose whiskers," *Cellulose*, vol. V13, pp. 679-687, 2006.

[24] W. Hamad, "On The Development and Applications of Cellulosic Nanofibrillar and Nanocrystalline Materials," *The Canadian Journal of Chemical Engineering*, vol. 84, pp. 513 - 519, 2006.

[25] S. Beck-Candanedo, M. Roman, and D. G. Gray, "Effect of Reaction Conditions on the Properties and Behavior of Wood Cellulose Nanocrystal Suspensions," *Biomacromolecules*, vol. 6, pp. 1048-1054, 2005.

[26] B. G. Ranby, "Aqueous Colloidal Solutions of Cellulose Micelles," *Acta Chem. Scand.*, vol. 3, pp. 649 - 650, 1949.

[27] J. Moczo, E. Fekete, K. Laszlo, and B. Pukanszky, "Aggregation of Particulate Fillers: Factos, determination, Properties," *Macromol. Symp*, vol. 194, pp. 111 - 124, 2003.

[28] B. Pukanszky and E. Fekete, "Adhesion and Surface Modification," *Advances in Polymer Science*, vol. 139, pp. 109 - 153, 1999.

[29] J. W. Ess and P. R. Hornsby, *Plast Rubber Process Appl*, vol. 8, pp. 147, 1987.

[30] B. Pukanszky, "Interfacial interactions in particulate filled thermoplastics: mechanism, strength, properties," *Makromol. Chem., Macromol. Symp.*, vol. 70/71, pp. 213-223, 1993.

[31] T. Vu-Khanh, "Controlling the mechanical performance of composites," *Makromol. Chem, Macromol. Symp.*, vol. 70/71, pp. 225-234, 1993.

[32] J. Jancar, "Influence of filler particle shape on elastic moduli of PP/$CaCo_3$ and PP/$Mg(OH)_2$ composites " *Journal of Materials Science*, vol. 24, pp. 3947 - 3955, 1989.

[33] A. Pozsgay, T. Fráter, L. Papp, I. Sajó, and B. Pukánszky, "Nucleating effect of montmorillonite nanoparticles in polypropylene," *Journal of Macromolecular Science, Part B Physics*, vol. 41, pp. 1249 - 1265, 2002.

[34] R. Rothon, *Particulate-Filled Polymer Composites*: Longman Scientific & Technical, 1995.

[35] K. Mitsuishi, S. Ueno, S. Kodama, and H. Kawasaki, "Crystallization behavior of polypropylene filled with surface-modified calcium carbonate," *Journal of Applied Polymer Science*, vol. 43, pp. 2043-2049, 1991.

[36] D. Garlotta, "A Literature Review of Poly(Lactic Acid)," *Journal of Polymers and the Environment*, vol. 9, pp. 63-84, 2002.

[37] S. S. Ray, Y. Kazunobu, M. Okamoto, Y. Fujimoto, A. Ogami, and K. Ueda, "New polylactide/layered silicate nanocomposites. 5. Designing of materials with desired properties," *Polymer*, vol. 44, pp. 6633-6646, 2003.

[38] K. Oksman, A. P. Mathew, D. Bondeson, and I. Kvien, "Manufacturing process of cellulose whiskers/polylactic acid nanocomposites," *Composites Science and Technology*, vol. 66, pp. 2776-2784, 2006.

[39] A. P. Mathew, K. Oksman, and M. Sain, "Mechanical properties of biodegradable composites from poly lactic acid (PLA) and microcrystalline cellulose (MCC)," *Journal of Applied Polymer Science*, vol. 97, pp. 2014-2025, 2005.

[40] A. Bhatnagar and M. Sain, "Processing of cellulose nanofiber-reinforced composites," *Journal of Reinforced Plastics and Composites*, vol. 24, pp. 1259-68, 2005.

[41] K. Tashiro and M. Kobayashi, "Theoretical evaluation of three-dimensional elastic constants of native and regenerated celluloses: role of hydrogen bonds," *Polymer*, vol. 32, pp. 1516-1526, 1991.

[42] I. Sakurada, Y. Nukushina, and T. Ito, "Experimental determination of the elastic modulus of crystalline regions in oriented polymers," *Journal of Polymer Science*, vol. 57, pp. 651-660, 1962.

[43] P. M. Ajayan, L. S. Schadler, and P. V. Braun, *Nanocomposite Science and Nanotechnology*: WILEY-VCH Verlag GmbH & Co. KGaA, 2003.

[44] N. Hasegawa, M. Kawasumi, M. Kato, A. Usuki, and A. Okada, "Preparation and mechanical properties of polypropylene-clay hybrids using a maleic anhydride-modified polypropylene oligomer," *Journal of Applied Polymer Science*, vol. 67, pp. 87-92, 1998.

[45] K. I. Winey and R. A. Vaia, "Polymer nanocomposites," *MRS Bulletin*, vol. 32, pp. 314-319, 2007.

[46] R. A. Vaia and H. D. Wagner, "Framework for nanocomposites," *Mater. Today*, vol. 7, pp. 32-37, 2004.

[47] S. H. Cypus, W. M. Saltzman, and E. P. Giannelis, "Organosilicate-polymer drug delivery systems: controlled release and enhanced mechanical properties," *Journal of Controlled Release*, vol. 90, pp. 163-169, 2003.

[48] M. S. Huda, A. K. Mohanty, M. Misra, L. T. Drzal, and E. Schut, "Effect of Processing Conditions on the Physio-Mechanical Properties of Cellulose Fiber Reinforced Poly(lactic acid)," in *ANTEC 2004*, vol. 2. Chicago, Illinois, 2004, pp. 1614 - 1618.

[49] P. K. Mallick, *Fiber-Reinforced Composites: materials, manufacturing and design*, 2nd ed: Marcel Dekker, 1993.

[50] J. Antonio, T. O'Reilly, J.-Y. Cavaille, and A. Gandini, "The surface chemical modification of cellulosic fibres in view of their use in composite materials," *Cellulose*, vol. 4, pp. 305 - 320, 1997.

[51] P. Bataille, L. Ricard, and S. Sapieha, "Effects of cellulose fibers in polypropylene composites," *Polymer Composites*, vol. 10, pp. 103-108, 1989.

[52] R. G. Raj, B. V. Kokta, D. Maldas, and C. Daneault, "Use of wood fibers in thermoplastic composites: VI. Isocyanate as a bonding agent for polyethylene-wood fiber composites," *Polymer Composites*, vol. 9, pp. 404-411, 1988.

[53] D. Maldas, B. V. Kokta, and C. Daneault, "Influence of coupling agents and treatments on the mechanical properties of cellulose fiber-polystyrene composites," *Journal of Applied Polymer Science*, vol. 37, pp. 751-775, 1989.

[54] R. G. Raj, B. V. Kokta, D. Maldas, and C. Daneault, "Use of wood fibers in thermoplastics. VII. The effect of coupling agents in polyethylene-wood fiber composites," *Journal of Applied Polymer Science*, vol. 37, pp. 1089-1103, 1989.

[55] M. N. Belgacem and A. Gandini, "The surface modification of cellulose fibres for use as reinforcing elements in composite materials," *Composite Interfaces*, vol. 12, pp. 41-75, 2005.

[56] J. Araki, M. Wada, and S. Kuga, "Steric Stabilization of a Cellulose Microcrystal Suspension by Poly(ethylene glycol) Grafting," *Langmuir*, vol. 17, pp. 21-27, 2001.

[57] L. Heux, G. Chauve, and C. Bonini, "Nonflocculating and Chiral-Nematic Self-ordering of Cellulose Microcrystals Suspensions in Nonpolar Solvents," *Langmuir*, vol. 16, pp. 8210-8212, 2000.

[58] B. Braun, J. R. Dorgan, and D. M. Knauss, "Reactively Compatibilized Cellulosic Polylactide Microcomposites," *Journal of Polymers and the Environment*, vol. V14, pp. 49-58, 2006.

[59] A. K. Bledzki and J. Gassan, "Composites reinforced with cellulose based fibres," *Progress in Polymer Science*, vol. 24, pp. 221-274, 1999.

[60] M. N. Belgacem, P. Bataille, and S. Sapieha, "Effect of corona modification on the mechanical properties of polypropylene/cellulose composites," *Journal of Applied Polymer Science*, vol. 53, pp. 379-385, 1994.

[61] S. Renneckar, A. Zinck-Sharp, A. R. Esker, R. K. Johnson, and W. G. Glasser, "Novel methods for Interfacial Modification of Cellulose-Reinforced Composites," in *Cellulose Nanocomposites Processing, Characterization and Properties*, *ACS Symposium Series 938*, K. Oksman and M. Sain, Eds.: American Chemical Society, 2005, pp. 78 - 96.

[62] P. Cousin, P. Bataille, H. P. Schreiber, and S. Sapieha, "Cellulose-induced crosslinking of polyethylene," *Journal of Applied Polymer Science*, vol. 37, pp. 3057-3060, 1989.

[63] S. Sapieha, P. Allard, and Y. H. Zang, "Dicumyl peroxide-modified cellulose/LLDPE composites," *Journal of Applied Polymer Science*, vol. 41, pp. 2039-2048, 1990.

[64] J. R. Dorgan and B. Braun, in *American Chemical Society*, vol. 93, *PMSE Preprints*, 2005, pp. 954-955.

[65] C. Gousse, H. Chanzy, G. Excoffier, L. Soubeyrand, and E. Fleury, "Stable suspensions of partially silylated cellulose whiskers dispersed in organic solvents," *Polymer*, vol. 43, pp. 2645-2651, 2002.

[66] B. Paul, "Prediction of Elastic Constants of Multiphase Materials," *Transactions of the metlallurgical society of AIME*, vol. 218, pp. 36 -41, 1960.

[67] R. Gauthier, C. Joly, A. C. Coupas, H. Gauthier, and M. Escoubes, "Interfaces in polyolefin/cellulosic fiber composites: Chemical coupling, morphology, correlation with adhesion and aging in moisture," *Polymer Composites*, vol. 19, pp. 287-300, 1998.

[68] S. Singh and S. S. Ray, "Polylactide Based Nanostructured Biomaterials and Their Applications," *Journal of Nanoscience and Nanotechnology*, vol. 7, pp. 2596-2615, 2007.

[69] H. Tsuji and Y. Ikada, "Blends of Crystalline And Amorphous Poly(lactide). III. Hydrolysis of Solution -cast Blend Films," *Journal of Applied Polymer Science*, vol. 63, pp. 855 - 863, 1997.

[70] J. E. Bergsma, W. C. de Bruijn, F. R. Rozema, R. R. M. Bos, and G. Boering, "Late degradation tissue response to poly(-lactide) bone plates and screws," *Biomaterials*, vol. 16, pp. 25-31, 1995.

[71] M. Therin, P. Christel, S. Li, H. Garreau, and M. Vert, "In vivo degradation of massive poly([alpha]-hydroxy acids): Validation of In vitro findings," *Biomaterials*, vol. 13, pp. 594-600, 1992.

[72] S. Gogolewski, M. Jovanovic, S. M. Perren, J. G. Dillon, and M. K. Hughes, "The effect of melt-processing on the degradation of selected polyhydroxyacids: polylactides, polyhydroxybutyrate, and polyhydroxybutyrate-co-valerates," *Polymer Degradation and Stability*, vol. 40, pp. 313-322, 1993.

[73] D. Cam, S.-h. Hyon, and Y. Ikada, "Degradation of high molecular weight poly(-lactide) in alkaline medium," *Biomaterials*, vol. 16, pp. 833-843, 1995.

[74] A. Gopferich, "Mechanisms of Polymer Degradation and Erosion," *Biomaterials*, vol. 17, pp. 103 - 114, 1996.

[75] M. Vert, "Degradation of Polymeric Biomaterials With Respect To Temporary Therapeutic Applications: Tricks and Treats," in *Degradable Materials - Perspectives, Issues, and Opportunities*, S. A. Barenberg, J. L. Brash, R. Narayan, and A. E. Redpath, Eds.: CRC Press.

[76] S. S. Ray, K. Yamada, M. Okamoto, and K. Ueda, "Control of Biodegradability of Polylactide via Nanocomposite Technology," *Macromolecular Materials and Engineering*, vol. 288, pp. 203 - 208, 2003.

[77] S. S. Ray, K. Yamada, M. Okamoto, and K. Ueda, "New polylactide-layered silicate nanocomposites. 2. Concurrent improvements of material properties, biodegradability and melt rheology," *Polymer*, vol. 44, pp. 857-866, 2003.

[78] H. Tsuji and Y. Ikada, "Properties and Morphology of Poly (L-lactide). II. Hydrolysis in Alkaline Solution," *Journal of Polymer Science: Part A: Polymer Chemistry*, vol. 36, pp. 59 - 66, 1998.

[79] H. Tsuji, A. Mizuno, and Y. Ikada, "Properties and morphology of poly(L-lactide). III. Effects of initial crystallinity on long-term In Vitro hydrolysis of high molecular weight poly(L-lactide) film in phosphate-buffered solution," *Journal of Applied Polymer Science*, vol. 77, pp. 1452-1464, 2000.

[80] H. Tsuji and C. A. D. Carpio, "In Vitro Hydrolysis of Blends from Enantiomeric Poly(lactide)s. 3. Homocrystallized and Amorphous Blend Films," *Biomacromolecules*, vol. 4, pp. 7 - 11, 2003.

[81] R. K. Kulkarni, K. C. Pani, C. Neumam, and F. Leonard, "Polylactic acid For Surgical Implants," *Archives of Surgery*, vol. 93, pp. 839 - 843, 1966.

[82] H. Tsuji and K. Nakahara, "Poly(L-lactide). IX. Hydrolysis in acid media," *Journal of Applied Polymer Science*, vol. 86, pp. 186-194, 2002.

[83] D. Xue Min, R. Jean-Francois, and D. G. Gray, "Effect of microcrystallite preparation conditions on the formation of colloid crystals of cellulose," *Cellulose*, vol. V5, pp. 19-32, 1998.

[84] D. Bondeson, A. Mathew, and K. Oksman, "Optimization of the isolation of nanocrystals from microcrystalline cellulose by acid hydrolysis," *Cellulose*, vol. 13, pp. 171-180, 2006.

[85] S. Yan, J. Yin, Y. Yang, Z. Dai, J. Ma, and X. Chen, "Surface-grafted silica linked with l-lactic acid oligomer: A novel nanofiller to improve the performance of biodegradable poly(l-lactide)," *Polymer*, vol. 48, pp. 1688-1694, 2007.

[86] E. Fukada, "Piezoelectricity of biopolymers," *Biorheology*, vol. 32, pp. 593-609, 1995.

[87] E. W. Fischer, H. J. Sterzel, and G. Wegner, "Investigation of the structure of solution grown crystals of lactide copolymers by means of chemical reactions," *Kolloid-Zeitschrift & Zeitschrift fur Polymere*, vol. 251, pp. 980-990, 1973.

[88] *Polymer Handbook*, vol. VII - 15, 3rd edition ed, 1989.

[89] H. Li and M. A. Huneault, "Effect of nucleation and plasticization on the crystallization of poly(lactic acid)," *Polymer*, vol. 48, pp. 6855-6866, 2007.

[90] M. Murariu, A. D. S. Ferreira, M. Alexandre, and P. Dubois, "Polylactide (PLA) designed with desired end-use properties: 1. PLA compositions with low molecular weight ester-like plasticizers and related performances," *Polymers for Advanced Technologies*, vol. 19, pp. 636-646, 2008.

[91] O. Martin and L. Avérous, "Poly(lactic acid): plasticization and properties of biodegradable multiphase systems," *Polymer*, vol. 42, pp. 6209-6219, 2001.

[92] R. G. Sinclair, "The case for polylactic acid as a commodity packaging material," *J.Macromol.Sci.-Pure Appl. Chem*, vol. A33, pp. 587 - 597, 1996.

[93] M. Laka, S. Chernyavskaya, and M. Maskavs, "Cellulose-containing Fillers for Polymer Composites.," *Mechanics of Composite Materials.*, vol. 39, pp. 183-188, 2003.

[94] L. Petersson and K. Oksman, "Biopolymer based nanocomposites: Comparing layered silicates and microcrystalline cellulose as nanoreinforcement," *Composites Science and Technology*, vol. 66, pp. 2187-2196, 2006.

[95] Q. Wu, M. Henriksson, X. Liu, and L. A. Berglund, "A High Strength Nanocomposite Based on Microcrystalline Cellulose and Polyurethane," *Biomacromolecules*, vol. 8, pp. 3687 -3692, 2007.

[96] D. Bondeson, "Strategies for preparation of cellulose whiskers from microcrystalline cellulose as reinforcement in composites," in *Cellulose Nanocomposites Processing, Characterization and Properties, ACS Symposium Series 938*, K. Oksman and M. Sain, Eds.: American Chemical Society 2006, pp. 10-25.

[97] M. Lenes and Ø. W. Gregersen, "Effect of surface chemistry and topography of sulphite fibres on the transcrystallinity of polypropylene," *Cellulose*, vol. 13, pp. 345-355, 2006.

[98] K. Jamshidi, S. H. Hyon, and Y. Ikada, "Thermal characterization of polylactides," *Polymer*, vol. 29, pp. 2229-2234, 1988.

[99] F. Carrasco, P. Pagès, J. Gámez-Pérez, O. O. Santana, and M. L. Maspoch, "Processing of poly(lactic acid): Characterization of chemical structure, thermal stability and mechanical properties," *Polymer Degradation and Stability*, vol. 95, pp. 116-125, 2010.

[100] M. N. Anglès and A. Dufresne, "Plasticized Starch/Tunicin Whiskers Nanocomposites. 1. Structural Analysis," *Macromolecules*, vol. 33, pp. 8344 - 8353, 2000.

[101] Y. P. Khanna and T. J. Taylor, "Comments and recommendations on the use of the Avrami equation for physico-chemical kinetics," *Polymer Engineering and Science* vol. 28, pp. 1042 - 1045, 1988.

[102] L. Petersson and K. Oksman, "Preparation and properties of biopolymer based nanocomposite films using microcrystalline cellulose," in *Cellulose Nanocomposites Processing, Characterization and Properties, ACS Symposium Series 938*, K. Oksman and M. Sain, Eds.: American Chemical Society, 2006, pp. 132 -150.

[103] L. Fambri, A. Pegoretti, R. Fenner, S. D. Incardona, and C. Migliaresi, "Biodegradable fibres of poly(-lactic acid) produced by melt spinning," *Polymer*, vol. 38, pp. 79-85, 1997.

[104] M. S. Huda, A. K. Mohanty, L. T. Drzal, E. Schut, and M. Misra, "“Green” composites from recycled cellulose and poly(lactic acid): Physico-mechanical and morphological properties evaluation," *Journal of Materials Science*, vol. 40, pp. 4221 - 4229, 2005.

[105] J. S. Shelley, P. T. Mather, and K. L. DeVries, "Reinforcement and environmental degradation of nylon-6/clay nanocomposites," *Polymer*, vol. 42, pp. 5849-5858, 2001.

[106] M. D. Sanchez-Garciaa, E. Gimenezb, and M. Lagaron, "Morphology and barrier properties of solvent cast composites of thermoplastic biopolymers and purified cellulose fibers " *Carbohydrate Polymers* vol. 71, pp. 235 - 244, 2008.

[107] B. Braun, J. Dorgan, and D. Knauss, "Reactively compatibilized cellulosic polylactide microcomposites," *Journal of Polymers and the Environment*, vol. 14, pp. 49-58, 2006.

[108] B. Braun and J. R. Dorgan, "Single-step method for the isolation and surface functionalization of cellulosic nanowhiskers," *Biomacromolecules*, vol. 10, pp. 334-341, 2009.

[109] M. Labet, W. Thielemans, and A. Dufresne, "Polymer grafting onto starch nanocrystals," *Biomacromolecules*, vol. 8, pp. 2916-2927, 2007.

[110] M. Hiljanen-Vainio, M. Heino, and J. V. Seppälä, "Reinforcement of biodegradable poly(ester-urethane) with fillers," *Polymer*, vol. 39, pp. 865-872, 1998.

[111] J. N. Coleman, U. Khan, and Y. K. Gun'ko, "Mechanical reinforcement of polymers using carbon nanotubes," *Advanced Materials*, vol. 18, pp. 689 - 706, 2006.

[112] C. G. Robertson, C. J. Lin, M. Rackaitis, and C. M. Roland, "Influence of particle size and polymer-filler coupling on viscoelastic glass transition of particle-reinforced polymers," *Macromolecules*, vol. 41, pp. 2727-2731, 2008.

[113] M. Pluta, M. Murariu, M. Alexandre, A. Galeski, and P. Dubois, "Polylactide compositions. The influence of ageing on the structure, thermal and viscoelastic

properties of PLA/calcium sulfate composites," *Polymer Degradation and Stability*, vol. 93, pp. 925-931, 2008.

[114] B. L. Shah, S. E. Selke, M. B. Walters, and P. A. Heiden, "Effects of wood flour and chitosan on mechanical, chemical, and thermal properties of polylactide," *Polymer Composites*, vol. 29, pp. 655-663, 2008.

[115] R. A. Vaia, T. B. Tolle, G. F. Schmitt, D. Imeson, and R. J. Jones, "Nanoscience and Nanotechnology: Materials Revolution for the 21st Century," *Sampe Journal*, vol. 37, pp. 24-31, 2001.

[116] K. Yano, A. Usuki, and A. Okada, "Synthesis and properties of polyimide-clay hybrid films," *Journal of Polymer Science Part A: Polymer Chemistry*, vol. 35, pp. 2289-2294, 1997.

[117] J. M. Garcés, D. J. Moll, J. Bicerano, R. Fibiger, and D. G. McLeod, "Polymeric Nanocomposites for Automotive Applications," *Advanced Materials*, vol. 12, pp. 1835-1839, 2000.

[118] R. Xu, E. Manias, A. J. Snyder, and J. Runt, "New Biomedical Poly(urethane urea)-Layered Silicate Nanocomposites," *Macromolecules*, vol. 34, pp. 337-339, 2001.

[119] Y. Kojima, A. Usuki, M. Kawasumi, A. Okade, Y. Fukushima, T. Kurauchi, and O. Kamigaito, "Mechanical Properties of Nylon 6-Clay Hybrids," *J. Mater. Res.*, vol. 8, pp. 1185-1189, 1993.

[120] V. Krikorian and D. J. Pochan, "Poly (L-Lactic Acid)/Layered Silicate Nanocomposite: Fabrication, Characterization, and Properties," *Chem. Mater.*, vol. 15, pp. 4317-4324, 2003.

[121] R. A. Vaia and E. P. Giannelis, "Polymer Nanocomposites Status and Opportunities," *MRS Bulletin*, vol. May, pp. 394-401, 2001.

[122] V. Favier, H. Chanzy, and J. Y. Cavaille, "Polymer Nanocomopsites Reinforced by Cellulose Whiskers," *Macromolecules*, vol. 28, pp. 6365 - 6367, 1995.

[123] Y. Pu, J. Zhang, T. Elder, Y. Deng, P. Gatenholm, and A. J. Ragauskas, "Investigation into nanocellulosics versus acacia reinforced acrylic films," *Composites Part B: Engineering*, vol. 38, pp. 360-366, 2007.

[124] W. Helbert, J. Y. Cavaillé, and A. Dufresne, "Thermoplastic nanocomposites filled with wheat straw cellulose whiskers. Part I: Processing and mechanical behavior," *Polymer Composites*, vol. 17, pp. 604-611, 1996.

[125] S.-H. Lee, S. Wang, and Y. Teramoto, "Isothermal crystallization behavior of hybrid biocomposite consisting of regenerated cellulose fiber, clay, and

poly(lactic acid)," *Journal of Applied Polymer Science*, vol. 108, pp. 870-875, 2008.

[126] B. P. Grady, F. Pompeo, R. L. Shambaugh, and D. E. Resasco, "Nucleation of polypropylene crystallization by single-walled carbon nanotubes," *The Journal of Physical Chemistry B*, vol. 106, pp. 5852-5858, 2002.

[127] Z. Su, Y. Liu, W. Guo, Q. Li, and C. Wu, "Crystallization behavior of poly(Lactic acid) filled with modified carbon black," *Journal of Macromolecular Science, Part B: Physics*, vol. 48, pp. 670 - 683, 2009.

[128] M. Sobkowicz, J. Dorgan, K. Gneshin, A. Herring, and J. McKinnon, "Renewable cellulose derived carbon nanospheres as nucleating agents for polylactide and polypropylene," *Journal of Polymers and the Environment*, vol. 16, pp. 131 - 140, 2008.

[129] L. Jiang, E. Morelius, J. W. Zhang, M. Wolcott, and J. Holbery, "Study of the poly(3-hydroxybutyrate-co-3-hydroxyvalerate)/cellulose nanowhisker composites prepared by solution casting and melt processing," *Journal of Composite Materials*, vol. 42, pp. 2629-2645, 2008.

[130] G. Siqueira, J. Bras, and A. Dufresne, "Cellulose whiskers versus microfibrils: influence of the nature of the nanoparticle and its surface functionalization on the thermal and mechanical properties of nanocomposites," *Biomacromolecules*, vol. 10, pp. 425-432, 2009.

[131] E. Manias, H. Chen, R. Krishnamoorti, J. Genzer, E. J. Kramer, and E. P. Giannelis, "Intercalation kinetics of long polymers in 2 nm confinements," *Macromolecules*, vol. 33, pp. 7955-7966, 2000.

[132] M. S. Huda, L. T. Drzal, A. K. Mohanty, and M. Misra, "Chopped glass and recycled newspaper as reinforcement fibers in injection molded poly(lactic acid) composites: A comparative study," *Composites Science and Technology*, vol. 66, pp. 1813 - 1824, 2006.

[133] L. E. Nielsen, *Mechanical Properties of Polymers and Composites* 1ed. New York: Marcel Dekker, Inc 1974.

[134] R. A. Gross and B. Kalra, "Biodegradable Polymers for the Environment," *Science*, vol. 297, pp. 803-807, 2002.

[135] J. M. Schakenraad, M. J. Hardonk, J. Feijen, I. Molenaar, and P. Nieuwenhuis, "Enzymatic activity toward poly(L-lactic acid) implants," *Journal of Biomedical Materials Research*, vol. 24, pp. 529-545, 1990.

[136] A. V. Janorkar, A. T. Metters, and D. E. Hirt, "Modification of Poly(lactic acid) Films: Enhanced Wettability from Surface-Confined Photografting and Increased

Degradation Rate Due to an Artifact of the Photografting Process," *Macromolecules*, vol. 37, pp. 9151-9159, 2004.

[137] S. D. Incardona, L. Fambri, and C. Migliaresi, "Poly-L-lactic acid braided fibres produced by melt spinning: characterization and in vitro degradation," *Journal of Materials Science: Materials in Medicine*, vol. 7, pp. 387 - 391, 1996.

[138] S.-R. Lee, H.-M. Park, H. Lim, T. Kang, X. Li, W.-J. Cho, and C.-S. Ha, "Microstructure, tensile properties, and biodegradability of aliphatic polyester/clay nanocomposites," *Polymer*, vol. 43, pp. 2495-2500, 2002.

[139] F. v. Burkersroda, L. Schedl, and A. Göpferich, "Why degradable polymers undergo surface erosion or bulk erosion," *Biomaterials*, vol. 23, pp. 4221-4231, 2002.

[140] H. Tsuji and H. Muramatsu, "Blends of aliphatic polyesters: V non-enzymatic and enzymatic hydrolysis of blends from hydrophobic poly(-lactide) and hydrophilic poly(vinyl alcohol)," *Polymer Degradation and Stability*, vol. 71, pp. 403-413, 2001.

[141] A. J. Nijenhuis, E. Colstee, D. W. Grijpma, and A. J. Pennings, "High molecular weight poly(-lactide) and poly(ethylene oxide) blends: thermal characterization and physical properties," *Polymer*, vol. 37, pp. 5849-5857, 1996.

[142] A. Belbella, C. Vauthier, H. Fessi, J.-P. Devissaguet, and F. Puisieux, "In vitro degradation of nanospheres from poly(D,L-lactides) of different molecular weights and polydispersities," *International Journal of Pharmaceutics*, vol. 129, pp. 95 - 102, 1996.

[143] G. L. Siparsky, K. J. Voorhees, and F. Miao, "Hydrolysis of polylactic acid (PLA) and polycaprolactone (PCL) in aqueous acetonitrile solutions: autocatalysis," *Journal of Polymers and the Environment*, vol. 6, pp. 31 - 41, 1998.

[144] A. Kulkarni, J. Reiche, and A. Lendlein, "Hydrolytic degradation of poly(rac-lactide) and poly[(rac-lactide)-co-glycolide] at the air-water interface," *Surface and Interface Analysis*, vol. 39, pp. 740-746, 2007.

[145] A. Gopfrerich, "Mechanisms of polymer degradation and elimination," in *Handbook of biodegradable polymers*, vol. 7, *Drug targeting and delivery*, A. J. Domb, J. Kost, and D. M. Wiseman, Eds. Amsterdam: harwood academic publishers, 1997, pp. 451 - 471.

[146] Q. Zhou and M. Xanthos, "Nanoclay and crystallinity effects on the hydrolytic degradation of polylactides," *Polymer Degradation and Stability*, vol. 93, pp. 1450-1459, 2008.

[147] M. Hakkarainen, "Aliphatic Polyesters: Abiotic and Biotic Degradation and Degradation Products," in *Degradable Aliphatic Polyesters*, vol. 157, *Advances in Polymer Science*: Springer Berlin / Heidelberg, 2000.

[148] M. A. Paul, C. Delcourt, M. Alexandre, P. Degée, F. Monteverde, and P. Dubois, "Polylactide/montmorillonite nanocomposites: study of the hydrolytic degradation," *Polymer Degradation and Stability*, vol. 87, pp. 535-542, 2005.

[149] H. Tsuji and S. Miyauchi, "Poly(-lactide): VI Effects of crystallinity on enzymatic hydrolysis of poly(-lactide) without free amorphous region," *Polymer Degradation and Stability*, vol. 71, pp. 415-424, 2001.

[150] H. Tsuji and T. Ishida, "Poly(L-lactide). X. Enhanced surface hydrophilicity and chain-scission mechanisms of poly(L-lactide) film in enzymatic, alkaline, and phosphate-buffered solutions," *Journal of Applied Polymer Science*, vol. 87, pp. 1628-1633, 2003.

[151] S. Wang, W. Cui, and J. Bei, "Bulk and surface modifications of polylactide," *Analytical and Bioanalytical Chemistry*, vol. 381, pp. 547 - 556, 2005.

[152] S. J. de Jong, E. R. Arias, D. T. S. Rijkers, C. F. van Nostrum, J. J. Kettenes-van den Bosch, and W. E. Hennink, "New insights into the hydrolytic degradation of poly(lactic acid): participation of the alcohol terminus," *Polymer*, vol. 42, pp. 2795-2802, 2001.

[153] C. Shih, "Chain-end scission in acid catalyzed hydrolysis of poly (-lactide) in solution," *Journal of Controlled Release*, vol. 34, pp. 9-15, 1995.

[154] Y. Aso, S. Yoshioka, A. Li Wan Po, and T. Terao, "Effect of temperature on mechanisms of drug release and matrix degradation of poly(d,l-lactide) microspheres," *Journal of Controlled Release*, vol. 31, pp. 33-39, 1994.

[155] C. F. van Nostrum, T. F. J. Veldhuis, G. W. Bos, and W. E. Hennink, "Hydrolytic degradation of oligo(lactic acid): a kinetic and mechanistic study," *Polymer*, vol. 45, pp. 6779-6787, 2004.

[156] H. Fukuzaki, M. Yoshida, M. Asano, and M. Kumakura, "Synthesis of copoly(d,l-lactic acid) with relatively low molecular weight and in vitro degradation," *European Polymer Journal*, vol. 25, pp. 1019-1026, 1989.